Earthquake Hazards in the Offshore Environment

U.S. GEOLOGICAL SURVEY BULLETIN 1630

Earthquake Hazards in the Offshore Environment

By ROBERT A. PAGE and PETER W. BASHAM

U.S. GEOLOGICAL SURVEY BULLETIN 1630

DEPARTMENT OF THE INTERIOR

DONALD PAUL HODEL, Secretary

U.S. GEOLOGICAL SURVEY

Dallas L. Peck, Director

UNITED STATES GOVERNMENT PRINTING OFFICE : 1985

For sale by the
Superintendent of Documents
U.S. Government Printing Office
Washington, D.C. 20402

Library of Congress Cataloging-in-Publication Data

Page, Robert Alan, 1938–
Earthquake hazards in the offshore environment.

(U.S. Geological Survey Bulletin 1630)
Bibliography: p. 56–67
Supt. of Docs. no.: I 19.3:1630
1. Earthquakes—United States. 2. Earthquakes—Canada. 3. Earthquake engineering—United States. 4. Earthquake engineering—Canada. 5. Oil-well drilling, submarine—United States. 6. Oil-well drilling, submarine—Canada. I. Basham, P.W. II. Title. III. Series: United States. Geological Survey. Bulletin 1630.

QE75.B9 no. 1630	557.3s	85–600173
[QE535.2.U6]	[363.3'495]	

CONTENTS

FIGURES

TABLES

Earthquake Hazards in the Offshore Environment

By Robert A. Page *and* Peter W. Basham[1]

Abstract

This report discusses earthquake effects and potential hazards in the marine environment, describes and illustrates methods for the evaluation of earthquake hazards, and briefly reviews strategies for mitigating hazards. The report is broadly directed toward engineers, scientists, and others engaged in developing offshore resources.

The continental shelves have become a major frontier in the search for new petroleum resources. Much of the current exploration is in areas of moderate to high earthquake activity. If the resources in these areas are to be developed economically and safely, potential earthquake hazards must be identified and mitigated both in planning and regulating activities and in designing, constructing, and operating facilities.

Geologic earthquake effects that can be hazardous to marine facilities and operations include surface faulting, tectonic uplift and subsidence, seismic shaking, sea-floor failures, turbidity currents, and tsunamis. Seismic shaking typically contributes most to earthquake losses, both directly through vibratory damage and indirectly through triggering of landslides and loss-of-strength failures in sedimentary deposits, which, in turn, may cause local tsunamis and turbidity currents. Examples of damage to ocean-bottom and coastal facilities from sea-floor failures, slide-generated tsunamis, and turbidity currents are numerous. Uplift, subsidence, and tsunamis are likely to be serious hazards only in coastal areas, where large water waves can wreck shoreline facilities and uplift or subsidence can destroy or limit the utility of such facilities. Surface faulting affects only a limited area; it can rupture pipelines and offset or distort foundations, however, and thus cause structures to fail.

Strategies for mitigating earthquake hazards rely on our ability to predict the location and size of future potentially damaging earthquakes, their imminence and frequency of occurrence, and the type, severity, extent, and likelihood of resulting geologic effects. Rather precise estimates of the location and size of future earthquakes can be provided for many seismic zones, principally those with high rates of activity where the causes of earthquakes are relatively well understood, such as along the Pacific margin of the United States and Canada. Although, in such areas, satisfactory estimates of the frequency of earthquake occurrence can commonly be derived, routine prediction of the precise time of future shocks is currently beyond the state of the art. In less seismically active regions, such as the Atlantic and Arctic margins of the United States and Canada, estimates of the location, size, and frequency of future earthquakes are difficult and less precise and reliable because the causes of earthquakes in areas distant from plate boundaries are still poorly understood.

The general absence of detailed documentation and measurement of earthquake effects in the offshore environment seriously constrains our ability to identify and mitigate potential hazards. The hazards posed by some earthquake effects are obvious, and in some places the methods and techniques for evaluating earthquake hazards on land can be applied with little or no modification in the marine environment. For example, experience with surface faulting on land is directly applicable to assessing the potential for and style of surface faulting in offshore earthquakes. For other earthquake effects, differences between the offshore and onshore environment are important and limit the applicability of experience with earthquake effects on land. For strong seismic shaking and sea-floor failure, ignorance of the onsite geotechnical properties of saturated marine sediment and its response to seismic disturbances is a serious impediment. Finally, there are earthquake phenomena peculiar to the marine environment whose origins are poorly understood and whose significance as hazards are neither known nor appreciated.

Mitigation strategies for earthquake hazards include selectively siting facilities and limiting activities in hazardous areas to reduce exposure to hazards, designing and constructing facilities to withstand or accommodate expected earthquake effects, and instituting response plans for earthquake emergencies and for advance warnings of delayed earthquake effects, such as tsunamis. The effectiveness of any particular strategy depends on both the hazard being addressed and the type of facility or activity at risk.

[1]Earth Physics Branch, Canadian Department of Energy, Mines and Resources, Ottawa, Ontario, Canada.

INTRODUCTION

In the last decade offshore petroleum exploration and development have greatly increased. Much of the recent and planned economic activity is in areas of moderate to high earthquake potential. Safe exploration and eventual development of petroleum resources in such areas require that offshore and coastal facilities be designed to resist earthquakes and their geologic and hydrologic effects.

The purpose of this report is to promote an understanding among scientists, engineers, and others engaged in developing offshore resources of earthquakes and their effects, as related to the marine environment, and to provide an introduction to the methods for assessing earthquake potential and for evaluating and mitigating earthquake hazards. Although the techniques for evaluating earthquake potential and associated hazards are relevant to any offshore or coastal site worldwide, the discussion here is illustrated primarily with examples from the United States and Canada. Readers particularly interested in earthquake hazards in the North Sea area are referred to Ritsema and Gürpinar (1983). Because the offshore region is a new frontier, few well-documented examples of earthquake effects in the marine environment are available, and so frequent reference to experience with earthquakes on land is necessary.

The potential for petroleum exists at some scale in essentially all unmetamorphosed sedimentary basins. The geologic history of the Phanerozoic Eon (the past 500-600 m.y.), which has controlled basin formation, is influenced by the major horizontal crustal movements associated with global tectonics. Earthquakes are known to be occurring today in most regions that have undergone orogenic events or reactivation of older geologic structures during the Phanerozoic Eon. Much earthquake activity is occurring at or near continental margins and thus in close proximity to areas of petroleum development.

Acknowledgments.—In addressing the broad subject of earthquake hazards in the offshore environment, we have benefited from informative discussions with numerous colleagues and from their comments on and criticism of the manuscript. In particular, we recognize the contributions of D.M. Boore, M.G. Bonilla, M.A. Hampton, H.J. Lee, D.S. McCulloch, T.L. Youd, and J.I. Ziony of the U.S. Geological Survey, and M.J. Berry and R.D. Hyndman of the Earth Physics Branch of the Canadian Department of Energy, Mines and Resoures.

OFFSHORE EARTHQUAKES OF THE UNITED STATES AND CANADA

Epicenters of the larger historical earthquakes of the United States and Canada are shown in figure 1. West of long 110° W., the earthquakes shown are restricted to magnitudes[2] (M) of at least 6; however, the epicenter patterns are schematic because all significant events cannot be depicted at this scale. East of long 110° W., M=5 earthquakes after 1930 are included to more clearly illustrate the patterns of the lower level of seismicity in the eastern part of the continent. A large number of significant historical earthquakes have occurred on the continental margin (fig. 1), or close enough to that margin to have caused significant effects offshore. The 2,000-m bathymetric contour marks the approximate position of the edge of the continental margin and delimits the potential offshore petroleum-resource areas that have been identified in coastal and offshore unmetamorphosed sedimentary basins (for example, McCrossan and Porter, 1973.)

Pacific margin

The greatest concentration of earthquakes in North America is along the west coast, where several earthquakes of $M \geq 7.7$ have occurred during historical time. These earthquakes reflect brittle deformation occurring in response to contemporary movement between two large lithospheric plates, the Pacific and the North American (fig. 2). The local sense of relative movement between these two plates varies along the length of the boundary. Along the coasts of California, northern British Columbia, and southeastern Alaska, the plates are slipping horizontally past each other; the Pacific plate is moving north-northwestward relative to the North American plate. In contrast, the relative plate motion is convergent along the Alaska Peninsula and the eastern Aleutian Islands.

The style of faulting along the plate boundary changes in response to the local direction of relative plate motion. Right-lateral strike-slip faulting is dominant along the coasts of California, northern British Columbia, and southeastern Alaska. Major strike-slip faults that have generated great earthquakes include the San Andreas fault in California (1857, M=7.9; 1906, M=7.7), the Queen Charlotte fault off British Columbia (1949, M=8.1), and the

---

[2]Magnitude is a measure of the size of an earthquake based on the amplitude of seismic waves. This measure is logarithmic rather than linear; a difference of one unit of magnitude corresponds to approximately a factor of 30 in the energy radiated from the source as seismic waves. Seismologists use several methods, or scales, for calculating magnitudes from instrumental records and for estimating the magnitudes of earthquakes not instrumentally recorded from the effects of ground shaking on structures, people, and natural features. Throughout this report, we use the simple term "magnitude" without indication of the method used for its computation. This usage is adequate for a general discussion of earthquake hazards; however, in applying the methods of hazards assessment and mitigation discussed in this report, it is essential that the practitioner be aware of the differences among various magnitude scales and their implications concerning the source characteristics of earthquakes (see supplementary section below entitled "Intensity, Magnitude, and Seismic Moment"). The magnitude values for specific earthquakes cited in this report refer to the moment-magnitude scale.

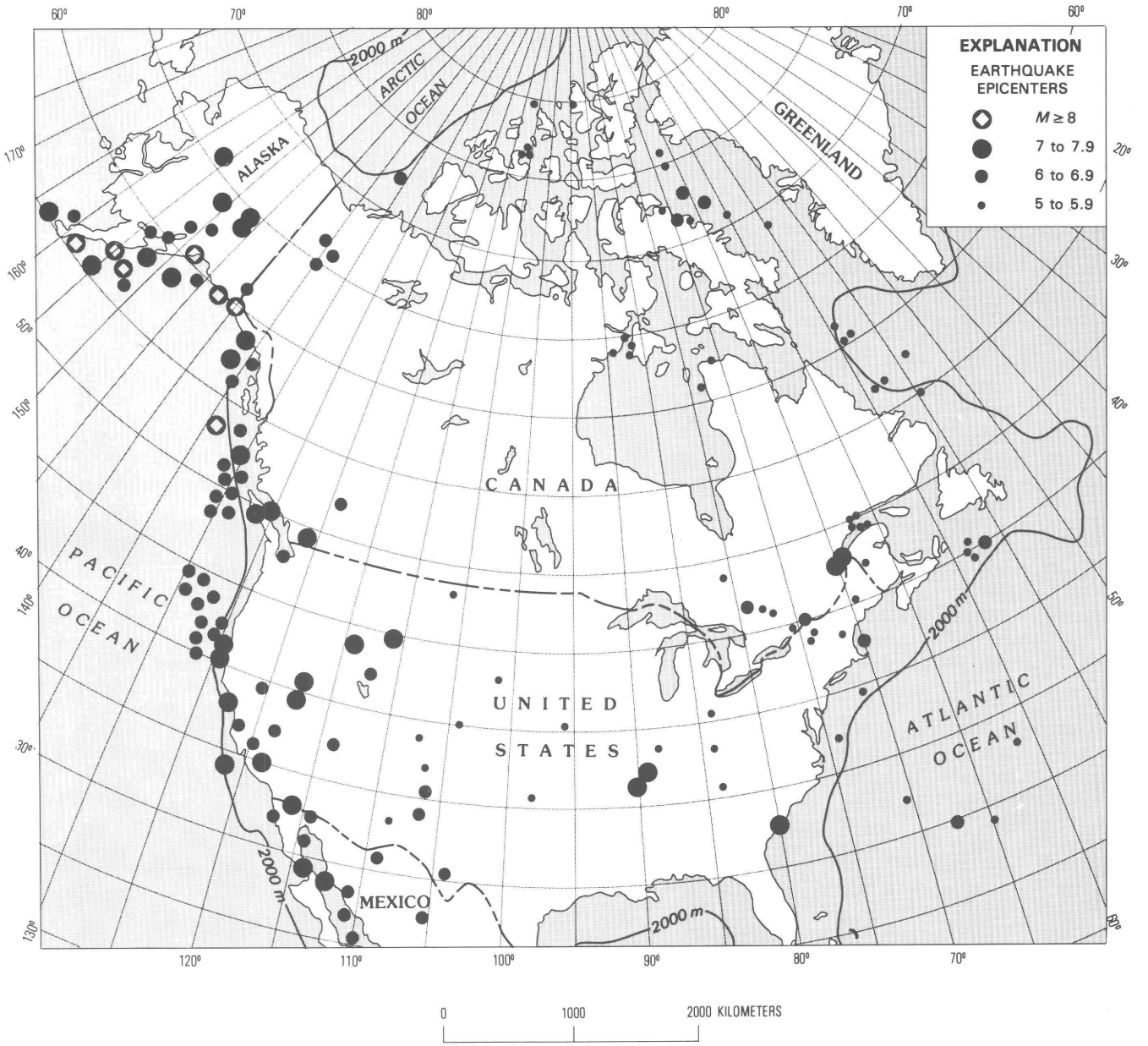

Figure 1. Epicenters of large ($\underline{M} \geq 6$) historical earthquakes in and adjacent to the continental United States and Canada. Larger magnitude symbols obscure numerous historical events of smaller magnitude, particularly along western margin. Historical ($\underline{M}=5$) earthquakes after 1930 are also included for region east of long 110° W. 2,000-m bathymetric contour marks approximate location of edge of continental margin.

Fairweather fault in southeastern Alaska (1958, $\underline{M}=7.7$). Along the Alaska Peninsula and the eastern Aleutian Islands, where the Pacific plate is being subducted beneath the North American plate, dip-slip faulting predominates. The largest earthquakes in North America have occurred along this subduction zone. Most of the Aleutian subduction zone has been ruptured during the past 50 years in a series of four great earthquakes: the Alaska Peninsula (1938, $\underline{M}=8.2$), the Andreanof Islands (1957, $\underline{M}=9.1$), the Prince William Sound (1964, $\underline{M}=9.2$), and the Rat Islands (1965, $\underline{M}=8.7$).

There are many significant complexities in this gross view of the relation between plate tectonics and seismicity along the west coast of North America. Not all the transcurrent motion between the Pacific and North American plates in California is accommodated on the San Andreas fault (fig. 3); part of this motion is distributed among several subparallel faults that define a broad zone of active strike-slip faulting, approximately 100 km wide, which includes the San Andreas (Jennings, 1975). South of San Francisco, where the San Andreas fault is onshore, some of these subparallel faults lie offshore and pose the principal

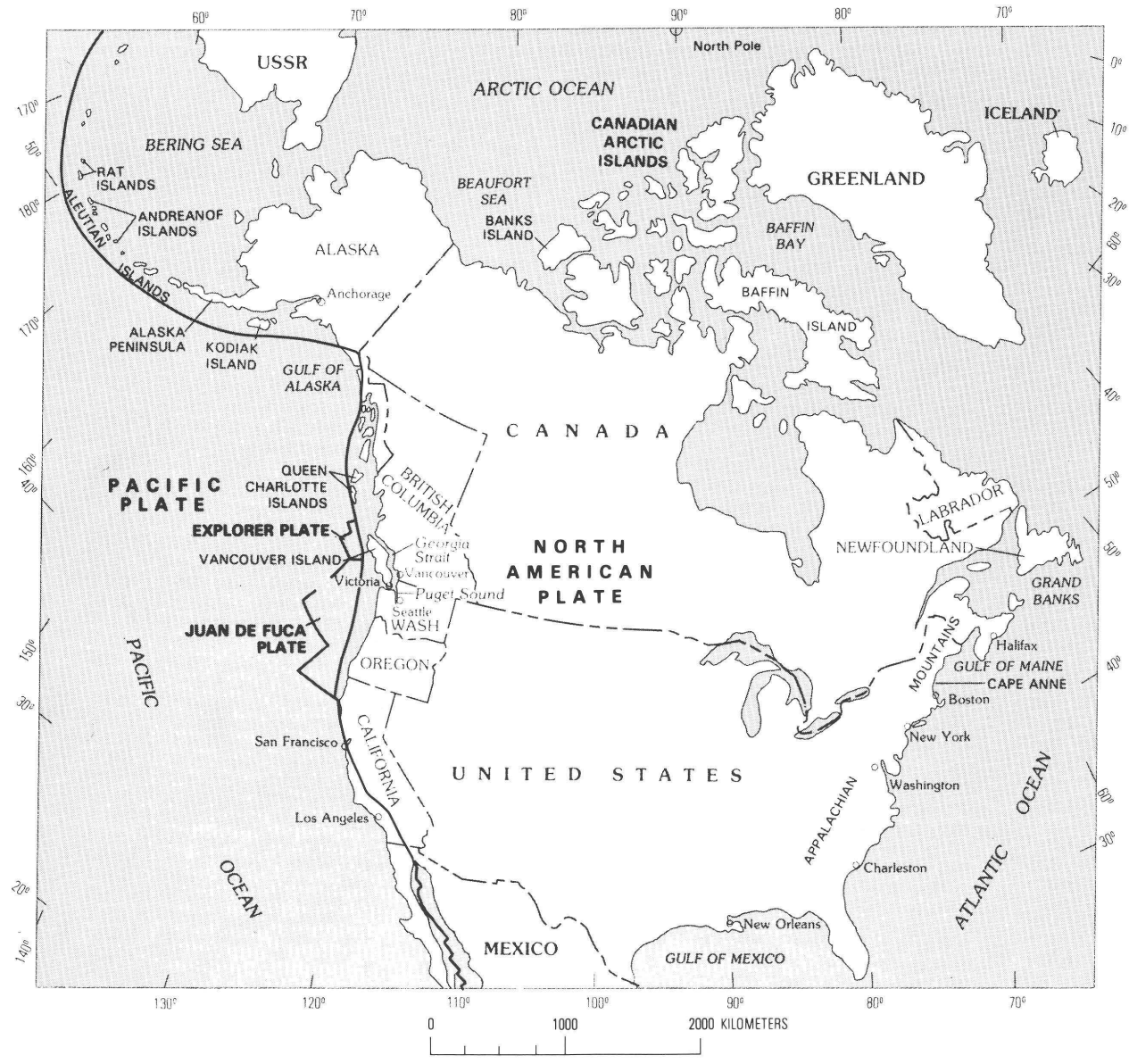

Figure 2. Index map of the United States and Canada, showing tectonic plates, and places and features referred to in text.

earthquake hazard at marine sites. A complexity in southern California is the bend in the San Andreas fault in the Transverse Ranges, north of Los Angeles (fig. 3). This bend is a westward deflection of the northwesterly striking fault and is flanked by a broad east-west zone of compressional tectonics that extends offshore and includes the Santa Barbara Channel (Yerkes and Lee, 1979a). East-west-trending active folds and reverse faults characterize this zone and accommodate north-south shortening of crustal rocks. Active faults off southern California have generated historical earthquakes as large as $\underline{M}$=7.3.

Between Cape Mendocino in northern California and the north end of Vancouver Island, the Pacific and North American plates do not meet along a common boundary; instead, they are separated by smaller plates of oceanic lithosphere—the Juan de Fuca and Explorer plates (fig. 2)—that are being subducted beneath the North American continent (Silver, 1971; Keen and Hyndman, 1979; Smith and Knapp, 1980). The tectonic complexities associated with the intervening plates are only now being resolved. Along the continental margin at these latitudes, earthquake mechanisms indicate brittle deformation between plates, within the oceanic and underthrust segments of the subducting plates, and within the overlying continental lithosphere. The largest historic earthquake along the continental margin is $\underline{M}$=7.3; however, the possibility of a major (possibly as large as $\underline{M}$=8.3) subduction shock along the Juan de Fuca-North American plate boundary has been suggested (Weaver and Smith, 1983; Heaton and Kanamori, 1984). Seaward of the continental margin to distances of about 400 km, earthquakes as large as $\underline{M}$=6.5 delineate the boundary of the Pacific plate,

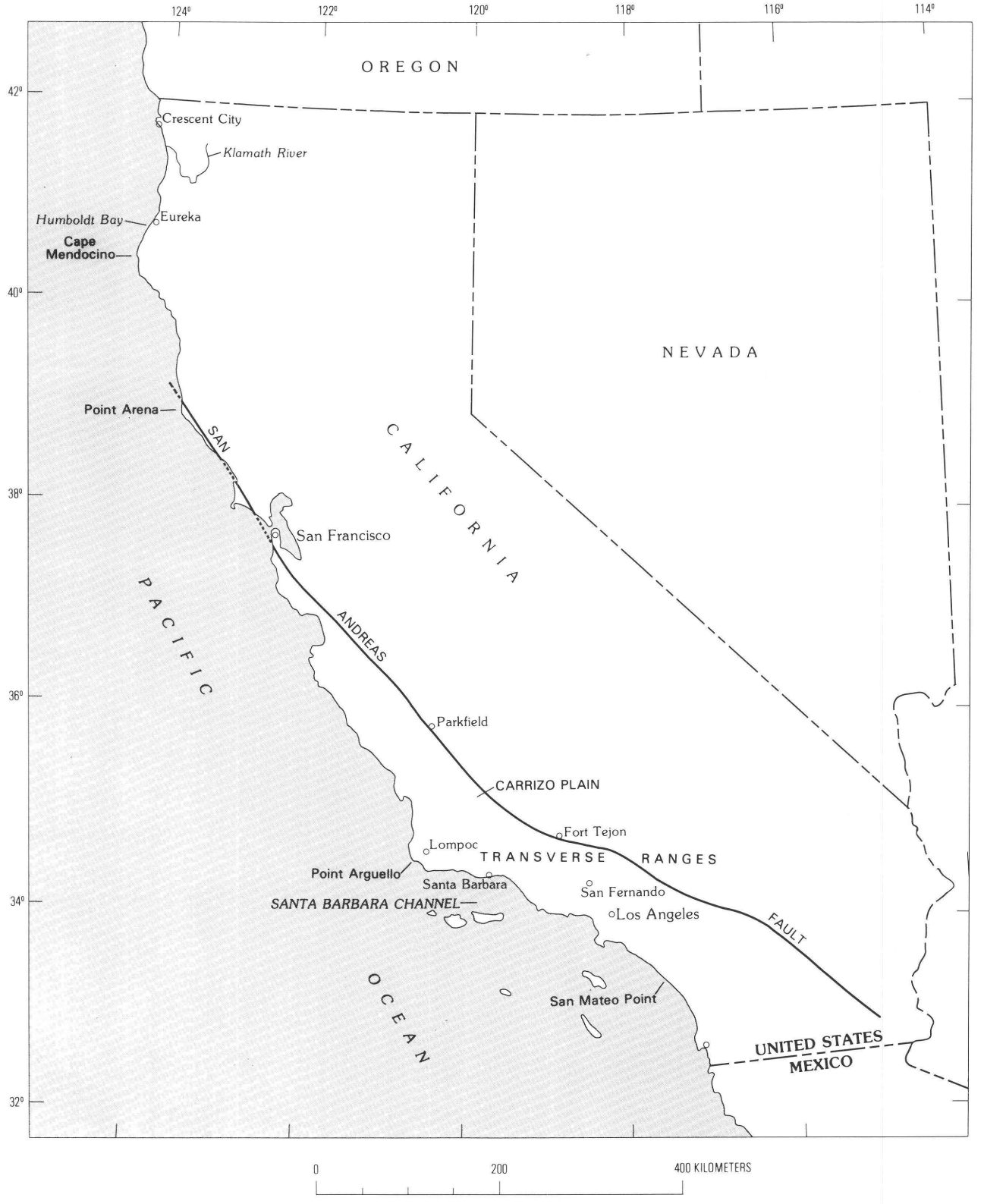

Figure 3. Index map of California, showing places and features referred to in text.

which is composed of a sequence of spreading oceanic ridges and transform fracture zones.

The continental margin along the northeastern Gulf of Alaska between Cross Sound and Prince William Sound (fig. 4) is also characterized by complex tectonics. This is a region of transitional tectonics from transcurrent faulting along the coast of southeastern Alaska and British Columbia to subduction along the Aleutian Island arc. Smaller plates, whose geologic histories and current tectonic significance are only partly understood at this time, separate the Pacific and North American plates and introduce additional boundaries on which tectonic adjustments may occur to generate significant earthquakes (Lahr and Plafker, 1980; Perez and Jacob, 1980). The capability of this segment of the continental margin to generate significant earthquakes was demonstrated by a pair of great ($\underline{M}$=8.1) onshore earthquakes in 1899 that ruptured the coast between Yakutat Bay and Kayak Island.

Atlantic and Arctic margins

Although the continental margins of eastern and Arctic North America (fig. 2) are far less seismically active than the Pacific margin, they have been shaken by several significant earthquakes in historical time. The Atlantic and Arctic margins were formed by rifting and transform (shear) motion between continental masses that separated to form new ocean basins. The evolution of rifted margins includes an early rifting stage, during which the crust is uplifted because of heating and thermal expansion in the mantle, followed by a spreading stage, in which the continents move apart as sea floor is created between them. During the spreading stage, the margin subsides as the lithosphere cools and sediment is deposited on the subsiding basement. The age of the Atlantic margin, defined by its time of the first opening, ranges from Jurassic for the Eastern United States and Maritime Canada, where North America separated from Africa, Iberia, and the British Isles, to Late Cretaceous and Tertiary off Labrador and Baffin Island, where Greenland separated from North America. The Arctic Ocean continental margin was formed during Cretaceous time by the separation of Alaska from the Canadian Arctic islands (Keen and Hyndman, 1979; Sweeney and others, 1978).

The eastern and Arctic margins are passive; the nearest active tectonism currently occurs far to the east at the Mid-Atlantic Ridge or, in the Arctic Ocean, on the Nansen-Gakkel Ridge, which extends from near northeastern Greenland to near the Novasibirskye Islands. Nevertheless, earthquake activity is occurring, albeit at lower rates and with generally smaller magnitudes than on the active margin of western North America. Among the largest historical earthquakes are the following: the Gulf of Maine off Cape Anne, Mass. (1775, estimated $\underline{M}$=5.8-6.1), the Charleston, S.C. (1886, estimated $\underline{M}$=6.9-7.3), the Beaufort Sea off Banks Island (1920, $\underline{M}$=6.2), the Grand Banks (1929, $\underline{M}$=6.5), and the Baffin Bay (1933, $\underline{M}$=6.7). It is generally assumed that most earthquakes along the eastern margin are occurring in the old rifted continental lithosphere. However, too few earthquakes have been accurately located during the era of instrumental seismology to delineate any significant patterns. Furthermore, the geologic features of the margin are too poorly mapped, and the locations of the more significant historical shocks (fig. 1) too uncertain, to support definitive correlations of epicenters with geologic structure.

The origins of these passive-margin earthquakes are not well understood, and several models for their origins have been proposed. One aspect common to many of these models is that the earthquakes are occurring in ancient zones of weakness within the crust that have been reactivated by the current stress regime (Sykes, 1978; Zoback and Zoback, 1981). The notion is that ancient zones of weakness can be the site of modern fault movement if they are suitably oriented in the current stress field and if the shear stress on the fault plane is sufficiently large. For example, Zoback and Zoback (1981) concluded that the Atlantic coast of the United States is under northwestward-oriented compression, on the basis of hydrofracture stress measurements, earthquake focal mechanisms, and late Cenozoic fault offsets. Wentworth and Mergner-Keefer (1981) argued that this compression causes reverse slip on ancient northeast-trending faults and that many of these faults preexisted as normal faults in early Mesozoic time, during the initial rifting to form the Atlantic Ocean. They suggested that reverse faulting, which continues at an average rate of a fraction of a meter per million years, can account for much of the historically observed seismicity along the eastern seaboard, including the 1886 Charleston, S.C., earthquake. Seeber and Armbruster (1981) offered an alternative model for the Charleston earthquake in which another preexisting weakness is reactivated. In their model, the proposed mechanism is backslip on the subhorizontal fault or detachment surface underlying the Appalachian Mountains; this surface was formed in the continental-plate collision that preceded the opening of the present Atlantic Ocean. Other possible mechanisms for the localization of seismicity in the Eastern United States were reviewed by Zoback and Zoback (1981).

Numerous explanations have been offered for the stresses responsible for earthquakes that occur away from plate boundaries. Although numerical models of the driving mechanisms of lithospheric plates seem to explain some of the gross features of stress orientations observed in intraplate regions (Richardson and others, 1979), other geologic processes, such as loading and unloading of the crust, are also important. From a study of the focal mechanisms of earthquakes on the margin of eastern Canada, Stein and others (1979) argued that stresses due to the removal of Pleistocene glaciers are sufficient to reactivate old basement faults parallel to the continental margin. Hasegawa and others (1979) inferred the stress regime of the Canadian Arctic margin along the continental slope in the Beaufort Sea to be a combination of crustal loading from Quaternary sedimentation, remnant tectonic stress associated with the opening of the Arctic Ocean during the Early Cretaceous, and tectonic stress generated currently by ocean spreading at the Nansen-Gakkel Ridge and transmitted across the Arctic Ocean.

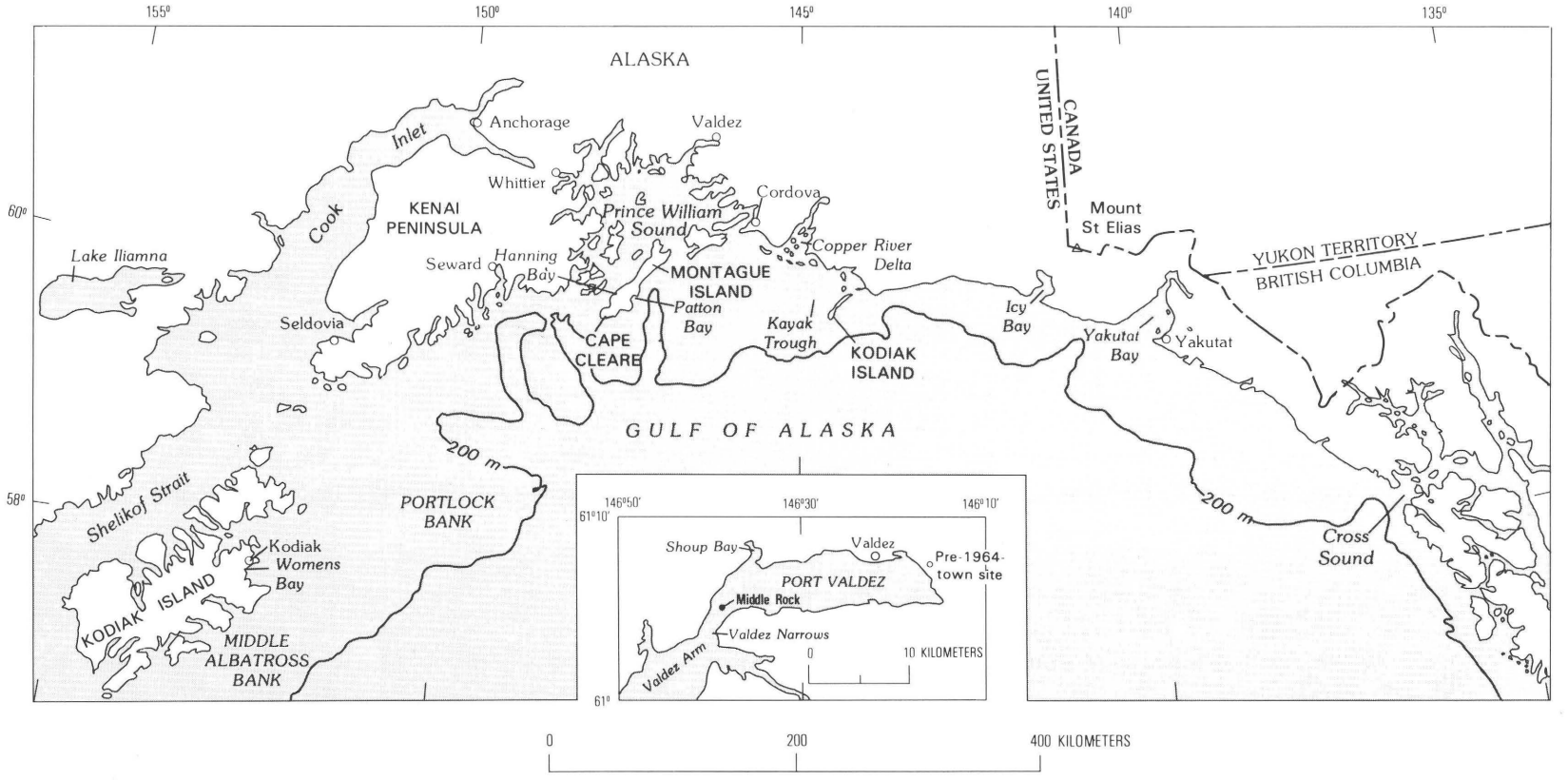

Figure 4. Index map of southern Alaska and the Gulf of Alaska, showing places and features referred to in text. Inset shows Port Valdez region.

Thus, the passive margin of eastern and Arctic North America has undergone significant earthquakes. Unlike the situation for shocks along the Pacific margin, no single unifying tectonic model is recognized that explains the origin of these earthquakes. Different processes, in fact, are probably generating earthquakes in different regions. Uncertainties in regard to the causes of historical shocks limit our ability to predict the location and frequency of future similar-size events in eastern and Arctic North America, and thus present a particular difficulty to the evaluation of earthquake hazards along this margin.

EARTHQUAKE EFFECTS

The various earthquake effects that can pose hazards to offshore facilities range from primary effects, such as tectonic deformation and strong ground shaking, to secondary effects, such as failure of geologic materials, turbidity currents, and tsunamis. Primary effects result directly from the sudden displacement of one rock mass past another along a buried fault, the mechanism that generates an earthquake; secondary effects are those induced by shaking or tectonic deformation.

The ranking of earthquake effects in terms of degree of potential hazard, or in terms of importance to the design engineer, is possible only in a general sense. The order will vary from one earthquake to another, depending on the size and location of the earthquake, and from site to site, depending on distance from the earthquake and on local geologic conditions. Seismic shaking and the resulting geologic effects generally constitute the greatest overall potential earthquake hazards to offshore facilities, including both platforms and pipelines. Tsunamis and tectonic changes in elevation are typically of little consequence to offshore facilities in comparison, for example, with the loads imposed by storm waves. For coastal facilities related to offshore petroleum production, however, tsunamis and uplift or subsidence of the coastline can constitute significant hazards.

Measures to accommodate or mitigate earthquake hazards, if they are to be effective, must be based on recognition of the nature and range of earthquake effects and on an appreciation of the potential consequences of these effects. The purpose of this section is to describe and illustrate the various earthquake effects, beginning with the primary ones. Many earthquake effects have not been well documented in the marine environment; for these effects, examples are drawn from onshore earthquakes.

Tectonic deformation

When opposing rock masses suddenly slip along a buried fault to generate an earthquake, the Earth's surface is deformed over a broad region above the buried fault. For shallow earthquakes, the area of the deformed region is comparable to the area of slip on the buried fault. Such deformation accompanies all earthquakes; however, the amount is generally too small to be significant for earthquakes of $M \lesssim 7$ or with sources deeper than a few tens of kilometers below the Earth's surface. If the buried fault is shallow, displacement on the fault during an earthquake may extend to the surface and cause localized shear offsets and distortions in surficial geologic materials, as well as broadly distributed deformation. Accordingly, two types of tectonic deformation are distinguished—surface faulting and regional deformation.

Surface faulting

Surface faulting is a potential hazard to structures built within or across active fault zones. In large shallow-focus earthquakes of $M \gtrsim 6$, shear displacements at the surface may exceed 1 m over a zone with a width comparable to or less than the amount of the offset. Such displacements may be sufficient to rupture a buried or anchored pipeline or to distort the foundation of a structure to the degree that collapse occurs or the structure must be razed.

The largest surface fault displacements accompanying North American earthquakes have occurred along the Pacific margin. In the 1906 San Francisco M=7.7 earthquake, spectacular strike-slip faulting ruptured the surface over a 430-km-long segment of the San Andreas fault along the north coast of California (Lawson, 1908). About half of this rupture lay offshore. Over the entire length of the rupture, the ground west of the fault was displaced northward relative to that on the east by as much as several meters (fig. 5). The maximum measured horizontal

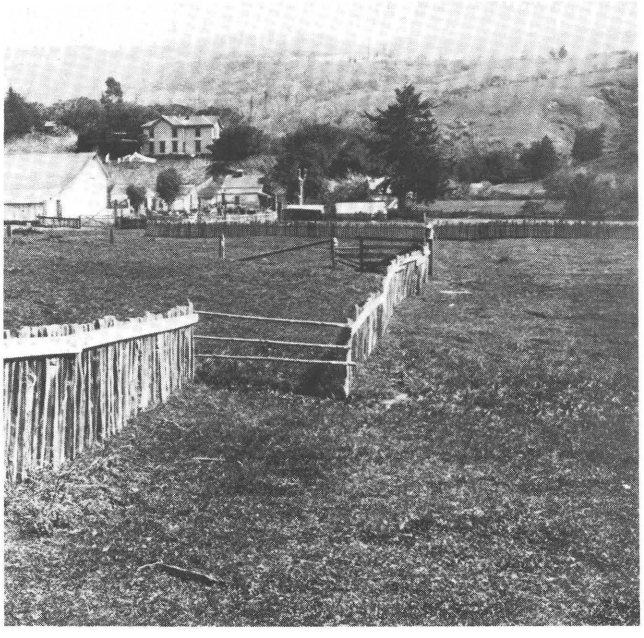

Figure 5. Offset and distortion of fence caused by right-lateral strike-slip fault displacement during the 1906 California earthquake (from Lawson, 1908, pl. 49A). Offset of 2.6 m on main fault trace broke fence (in middle of photograph). Beyond break, which is repaired with poles, fence is distorted by distributed right-lateral shear. Total displacement between straight fence segments on opposite sides of fault is 3.4 m.

offset was about 6 m over a zone 15 to 18 m wide in a road built on marshy ground; however, it may be that ground failure could have contributed to the observed displacement. On competent ground nearby, offsets of about 5 m were measured where the slip was localized in a narrow zone less than 1 or 2 m wide. Larger horizontal displacements have been inferred for earthquakes of comparable magnitude occurring on other segments of the San Andreas fault. Small streamcourses in the Carrizo Plain area in southern California have been offset repeatedly by as much as 9 or 10 m (Wallace, 1968; see subsection below entitled "Geologic Record" and fig. 21).

Dip-slip fault displacement of several meters was documented for the great ($\underline{M}$=9.2) Alaska earthquake of 1964 (Plafker, 1967). This earthquake resulted from northwestward underthrusting of the Pacific plate beneath southern Alaska along a gently dipping fault. Although the primary fault on which the principal slip occurred did not rupture the surface, two reverse faults, possibly branching upward off the primary fault, broke the ground on Montague Island and caused large vertical displacements. Dip slip on the Patton Bay fault caused 6 to 7 m of vertical offset, measured across the full width of the fault zone. A prominent scarp accounted for 2 to 3 m of this offset; the rest was distributed across the downwarped margin of the upthrown block, within 300 m of the scarp. The rupture along the Patton Bay fault was traced for at least 27 km offshore from Montague Island by hydrographic soundings and seismic profiling (Malloy and Merrill, 1969). Surface faulting generated a more spectacular scarp along the Hanning Bay fault. Localization of slip within a shear zone 0.5 m wide created an abrupt 4-m-high scarp in bedrock (fig. 6).

A graphic example of the damage that surface faulting can cause to pipelines and structures is the 1971 San Fernando, Calif., earthquake (Youd and others, 1978b). About 3 km of surface faulting associated with this $\underline{M}$=6.6 earthquake crossed an urban area. Maximum components of cumulative displacement across the principal zone of faulting were 1.9 m of left-lateral slip, 1.4 m of vertical slip, and 0.6 m of horizontal shortening in a direction normal to the trend of the rupture zone (U.S. Geological Survey Staff, 1971). Practically all the lateral slip and horizontal shortening and about half of the vertical slip were concentrated in a narrow band less than 30 m wide. This band sharply defined one boundary of the principal rupture zone and marked the leading edge of the overthrust fault block. Within the overthrust block

Figure 6. Bedrock scarp, about 4 m high, formed by secondary faulting on Montague Island during the 1964 Alaska earthquake (from Plafker, 1967, fig. 31). Fault dips to left about 55°. Slumping and erosion of material from initially overhanging scarp face result in scarp surface that slopes to right. Entire area of photograph was uplifted about 10 m.

away from the leading edge, the balance of the vertical displacement was distributed across numerous small normal (extensional) faults. The number of extensional faults and the displacement on them gradually decreased away from the edge of the overthrust block. Thus, the style of horizontal deformation divided the principal zone of surface faulting into two subzones—a narrow band of lateral shearing and horizontal compression, and a wider, more diffuse band of horizontal extension.

Ruptures within the principal zone of surface faulting in the San Fernando earthquake extended beneath tens of homes and several one- and two-story industrial and commercial buildings. Many of these buildings were damaged beyond repair, although none totally collapsed; nearly all sustained significant structural damage (Youd and others, 1978b). Most pipelines crossing major fault breaks were ruptured, commonly at several nearby locations. Individual pipelines failed in response to both compressional and extensional deformation. A 16-in. welded-steel gas-transmission line, for example, broke in seven places within the principal zone of faulting (compare Southern California Gas Co., 1973, fig. 1, and U.S. Geological Survey Staff, 1971, fig. 2). Near the tip of the overthrust block, one segment of the pipeline was shortened more than 0.1 m (fig. 7), whereas farther from the tip but still within the principal zone, the pipeline failed from horizontal extension of the ground coupled with vertical fault slip. Numerous ruptures in this and other gas-transmission lines occurred within the overthrust block at distances as large as a few kilometers from the principal zone of surface faulting. Although some of these ruptures resulted from slope failures, others probably were related to subsidiary surface faulting.

Figure 7. Shortened section of 16-in. steel gas-transmission line taken from principal zone of surface faulting associated with the 1971 San Fernando, Calif., earthquake (from U.S. Geological Survey staff, 1971, fig. 5). Amount of shortening exceeds 0.1 m.

Subsidence and uplift

Broad-scale vertical deformation of the Earth's surface accompanies large shallow-focus earthquakes generated by dip-slip faulting. Regional deformation, either uplift or subsidence, poses a potential hazard where it results in large permanent changes in water levels along developed shorelines. For offshore platforms, permanent changes in water depth that might accompany large local earthquakes are likely to be small in comparison with the expected heights of storm-generated waves and thus are not a major design consideration. Along a coast, however, permanent changes in water levels may make harbor and pier facilities useless, at least during some tidal stages, and may cause navigational hazards to shipping where the shallow sea floor is uplifted.

Vertical deformation is a first-order effect of dip-slip faulting. Accordingly, tectonic uplift and subsidence are important earthquake effects to consider in coastal areas characterized by either normal or reverse faulting. Along the Pacific margin of North America, for example, potential uplift or subsidence should be a consideration in the siting and design of coastal facilities along the Santa Barbara Channel in southern California and along the south coast of Alaska west of about long 138° W.

The 1964 Alaska earthquake provides a graphic example of regional vertical deformation in a coastal environment. Tectonic uplift and subsidence occurred over two adjacent elongate zones (fig. 8), each approximately 800 km long and 150 to 200 km wide (Plafker, 1969). The maximum measured uplift on land, about 12 m, occurred within a narrow belt, about 3 km wide, between the two reverse faults on Montague Island discussed in the preceding section (fig. 9). Comparable uplift was measured in the adjacent offshore area (Malloy and Merrill, 1969). Most of the uplifted area was offshore, and so the extent of uplift is poorly known. From scattered coastal measurements, an area of at least 10^4 km^2, possibly much greater, is inferred to have risen 3 m. The region of subsidence was largely onshore and thus could be better determined. The maximum measured tectonic subsidence was about 2.5 m.

The extensive vertical deformation that accompanied the 1964 Alaska earthquake caused great damage to harbor and waterfront facilities, both directly through uplift and subsidence of coastlines and indirectly through the generation of destructive tsunamis (see subsection below entitled "Tsunamis") (Eckel, 1967; Arno and McKinney, 1973). Uplift or subsidence affected every coastal community in south-central Alaska from Kodiak to Cordova (fig. 8), although damage from waves and shoreline slides typically far exceeded that directly due to vertical deformation. An exception was the Cordova area, where 2 m of uplift was the greatest cause of earthquake damage. Dock facilities became accessible only at very high tides, so that one cannery had to be abandoned and shallow waterways became unnavigable. No settlements were located in the region of maximum uplift. Subsidence affected more communities and left many waterfront and port facilities subject to flooding by high tides. For example, at Seldovia, where virtually all the damage was caused by

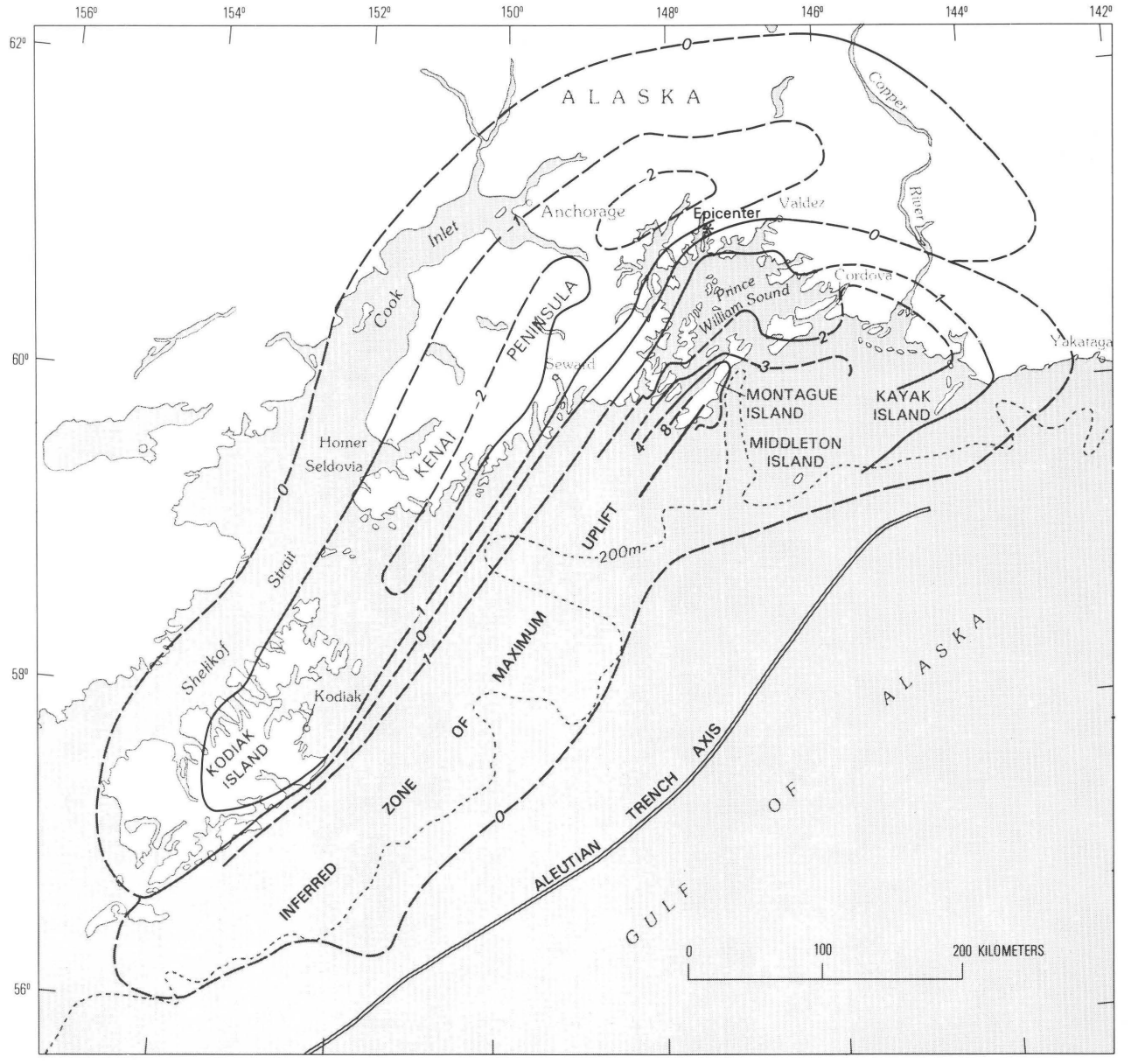

Figure 8. Gulf of Alaska area, showing tectonic uplift and subsidence during the 1964 Alaska earthquake (modified from Plafker, 1965, fig. 2). Heavy contours show displacement (in meters); dashed where approximately located. 200-m isobath (dotted line) marks edge of the Continental Shelf.

tectonic deformation, slightly more than 1 m of subsidence subjected the boardwalk on which the business section of the town was located to flooding at extreme high tides (fig. 10).

Seismic shaking

Seismic shaking typically contributes more to the overall earthquake damage than does any other earthquake effect. Strong shaking contributes to economic and human losses not only directly, through vibratory damage to structures, but also indirectly, through triggering of secondary effects, such as landsliding and loss of shear strength in water-saturated sediment. In contrast to surface faulting, seismic shaking is a pervasive effect that subjects structures throughout a broad area surrounding the earthquake source to significant loading.

Little information is available on the response of bottom-supported offshore structures to earthquakes, especially large events (Hove, 1983). The 1978 Santa Barbara Channel earthquake off southern California provides an example of the shaking effects from a nearby moderate ($\underline{M}$=6.0) shock (Miller and Felszeghy, 1978). A total of $\overline{12}$ offshore platforms were located within 25 km of the buried fault rupture, as inferred from the spatial pattern of aftershocks (Lee and

Figure 9. Former sea floor at Cape Cleare, Montague Island, exposed by tectonic uplift during the 1964 Alaska earthquake (from Plafker, 1969, frontispiece). Wide surf-cut terrace was created at southwest end of the island by 8 m of uplift. Photograph taken at about zero tide stage. View northward.

Figure 10. Flooding of boardwalk and hotel in Seldovia at high tide, caused by about 1.2 m of tectonic subsidence during the 1964 Alaska earthquake. Photograph by U.S. Army Corp of Engineers.

others, 1978); the closest platform was at a distance of about 10 km. Five of these platforms were instrumented with strong-motion accelerographs at the time of the earthquake; however, no records of the earthquake were obtained because of improper setting of the triggering levels of the recorders and inadequate maintenance. Five onshore accelerographs at distances comparable to that of the nearest platform recorded peak horizontal accelerations at ground level of between 0.21 and 0.42 g (Porcella, 1979; Porter and others, 1979); the larger values were recorded on the University of California campus at Santa Barbara in the direction toward which the fault ruptured. The shaking was amplified substantially in the upper levels of multistory buildings. In a three-story reinforced-concrete shear-wall building on the university campus, the peak horizontal acceleration at the roof was 1.04 g, in comparison with 0.42 g at the ground floor (fig. 11). Although significant diagonal cracking occurred in the shear walls of the building, serious structural damage did not occur because the duration of strong shaking was only 2 to 3 s. Mechanical equipment on or near the roofs of multistory buildings on the campus, however, was considerably damaged from building motion, and objects were thrown from shelves. No

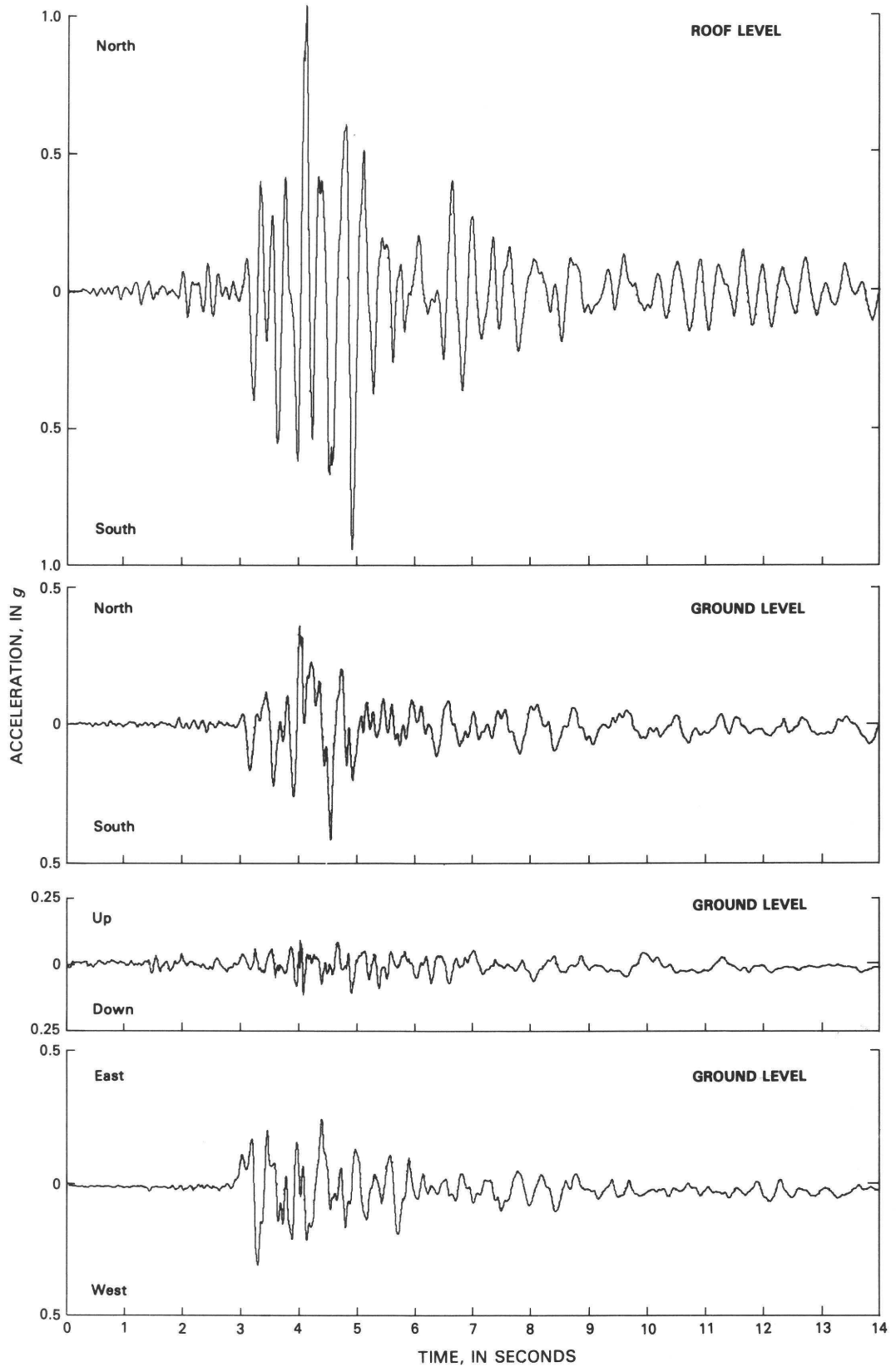

Figure 11. Accelerograms recorded on ground floor and roof of three-story North Hall on the University of California, Santa Barbara, campus during 1978 Santa Barbara M=6.0 earthquake. Amplitude of north-south motion on roof (top trace) was more than twice that at ground level (second trace). Vertical and east-west components of motion were not recorded on roof. Recorder was triggered by vertical P-wave motion sensed at ground level. Time is measured from trigger instant.

damage was reported to any offshore platforms, wells, or oil and gas lines. On the platform closest to where the highest ground motions were recorded on shore, noticeable rocking was reported to have lasted a few seconds. Vibrations were sufficient to automatically shut down compressors on 3 of the 12 platforms.

The ground shaking from a nearby $M \geq 7$ earthquake would be much more significant to offshore platforms than that from the Santa Barbara shock. A larger earthquake would generate more intense motion, especially at periods longer than about 1.5 or 2 s, where the fundamental deformational modes for pile-supported steel and concrete gravity platforms typically lie (Watt and others, 1978; Bea and others, 1979). Because of the greater rupture dimensions, not only would ground-motion spectra for a larger earthquake be richer in long-period energy (Johnson and Traubenik, 1978), but also the duration of motion would be much longer.

Strong ground shaking may pose a hazard not only to the survival of an offshore platform but also to the safety and continuity of operations on the platform. As illustrated above, the motion imposed at the foundation of a structure is amplified at higher levels in the structure. At the top of a structure, it may be sufficient to cause substantial damage to equipment and appurtenances, some of which may be critical for safe operation or shutdown, even though little damage may be done to the structure itself (Kost and Sharpe, 1977). Nonstructural earthquake damage has been documented in considerable detail for the 1971 San Fernando, Calif., and the 1964 Alaska shocks—a nearby moderate event and a distant large shock, respectively (Ayres and Sun, 1973; Ayres and others, 1973).

The direct effects of seismic shaking also constitute a potential hazard to other types of facilities associated with petroleum production. Shaking has caused extensive damage to modern storage tanks and connecting piping (Rinne, 1967; Hanson, 1973; Kennedy and others, 1977; Miles, 1977). By contrast, modern petroleum-transmission pipelines have withstood the direct effects of ground shaking well. Rupture of a buried welded-steel transmission pipeline from shaking alone has not been documented, although such pipelines have failed from the effects of faulting and permanent ground deformation (Kennedy and others, 1977). Modern communication and control systems have been found to be vulnerable to shaking, as was documented in the damage reports for the 1971 San Fernando earthquake (Benfer and Coffman, 1973).

Seismic shaking is a concern not only for marine structures supported on the sea floor but also for floating structures (Hove and others, 1982). The 32,500-ton Norwegian motor tanker Ida Knudsen was located above the source region of an $M=7.8$ earthquake that occurred in 1969 about 450 km west of Gibraltar. Compressional seismic waves from the earthquake violently shook the ship and caused damage so extensive that the ship was classified as a total loss. Hove and others (1982, p. 5) summarized the damage as follows:

> * * * all communication and navigation equipment was destroyed. Instruments mounted on the walls were torn off. Doors were torn off their hinges. Handrailing on stairways were shaken off. Loose equipment and furniture were thrown up into the air. Outriggers on mast were shaken off. Piping was broken. Some equipment was torn loose in way of anchorbolt failure or stretching. Leaden linings in way of machinery mountings were squeezed out. Welded connections and stiffeners had been broken. Bulkheads, hull frames and girders were buckled. Bulkheads were severely torn in one tank. All the wing tanks leaked, however the outer skin was tight except for one tank. In general the bottom plating and also the lower part of the side plating were torn away from the stringers/girders yielding gaps up to 50 mm wide. * * *
>
> After inspection in drydock at Lisnave the ship was condemned as total loss. The hull looked as if it had been subjected to a heavy mine explosion, the inspection report states, which indicates extreme dynamic pressure loadings. * * *

Whether the damage to the Ida Knudsen is typical of what should be expected above the source region of other similar-size earthquakes is not known. Hove and others (1982) presented additional examples of seismic disturbances to ships; none involved comparable levels of damage, but none was near the focus of such a large earthquake. They argued that additional research is needed to determine the extent to which offshore structures, particularly floating structures, are vulnerable to compressional seismic waves transmitted through the water.

Sea-floor failures

Ground failures generated by seismic shaking are a major cause of earthquake damage and casualties on land. Although earthquake effects in the marine environment are relatively poorly documented, there is ample historical and geologic evidence of offshore earthquakes triggering large-scale sea-floor failures. Furthermore, stability analyses indicate that seismic shaking is a likely triggering mechanism for failures on many submarine slopes in earthquake-prone regions (for example, Almagor and Wiseman, 1977; Hampton and others, 1978; Lee and others, 1981). Thus, the potential for seismically induced failure in sea-floor materials is an important consideration for the safe siting and design of offshore facilities in earthquake-prone regions.

As used in this report, the terms "ground failure" and "sea-floor failure" refer to the temporary loss of bearing capacity in surficial geologic materials as well as to their loss of stability and resulting deformation. Accordingly, downslope movement of a slide and loss of foundation support in the liquefaction of granular water-saturated sediment are both classified as failures.

Relatively few seismically induced sea-floor failures have been documented in relation to specific earthquakes. Nearly all these failures involved sliding of relatively steep submarine slopes associated with delta fronts or the continental slope, and have been recognized from the damage to coastal facilities or submarine cables resulting directly from either submarine slides or turbidity currents (see next subsection), or from waves generated by submarine slides

(see subsection below entitled "Tsunamis"). The dearth of documented failures in continental-shelf areas, which are characterized by very gentle slopes (typically, approx 0.1^{o}), undoubtedly reflects inexperience with offshore earthquake phenomena rather than the absence of such failures.

The 1964 Alaska earthquake generated catastrophic submarine slides in the fiords of Prince William Sound and along the south coast of the Kenai Peninsula. In Seward, delta-front failure removed a strip of land about 1.2 km long and as much as 150 m wide from the city waterfront (Lemke, 1967). Harbor, dock, and railroad facilities were lost in the progressive sliding (fig. 12), which began some 30 to 45

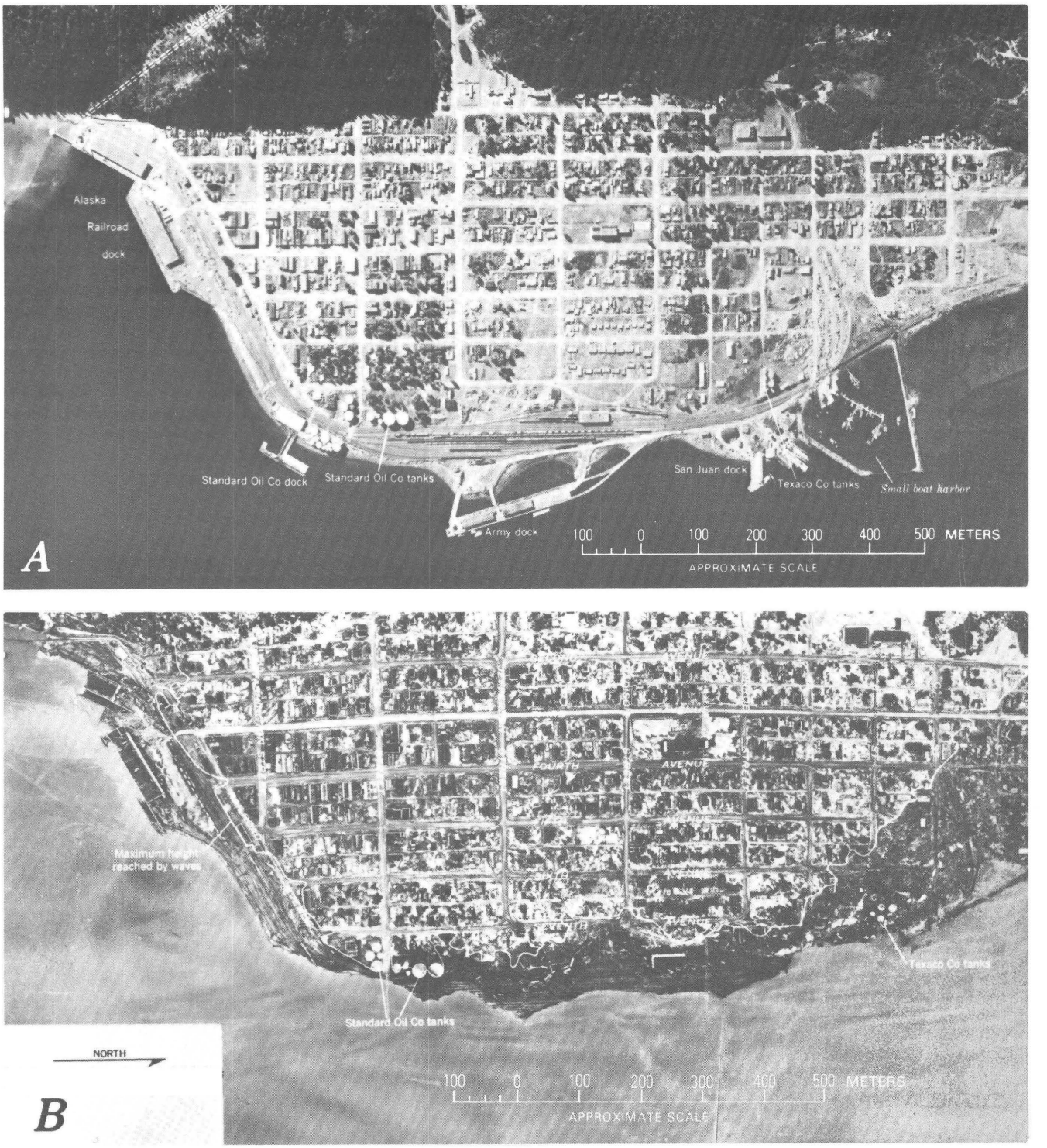

Figure 12. Seward, Alaska, waterfront, before (A) and after (B) the 1964 earthquake (from Lemke, 1967, fig. 2). Note loss of dock, harbor, and railroad facilities from waterfront slides. White line in figure 12B denotes area swept by water waves.

s after violent shaking commenced. When the shaking ceased, the ground behind the landslide scarp was found to be fractured in an incipient-failure condition to distances of more than 250 m from the new shoreline. The submarine sliding generated massive waves that swept the remaining waterfront area, lifted railroad cars and vehicles, and carried burning oil from slide-toppled tanks and ruptured pipelines and valves. Submarine sliding and slide-generated waves also wreaked havoc in Valdez (Coulter and Migliaccio, 1966) and Whittier (Kachadoorian, 1965). These calamitous failures, which were caused by liquefaction of deltaic sediment, occurred on moderately steep slopes, ranging from a few degrees to greater than 20°. There is limited evidence that submarine failures also occurred on gentler slopes (Reimnitz, 1972). Multiple slumps in foreset beds of the Copper River delta are attributed to the 1964 earthquake (fig. 13); the slope of the sea floor there is about 0.5°. These multiple failure surfaces suggest progressive failure of the slope during extended seismic shaking.

The best documented case of earthquake-induced slope failure on the Continental Shelf known to us comes from the M=7.4 earthquake of November 8, 1980, off Eureka, northern California (Field and others, 1982). After this earthquake, local commercial fisherman reported changes of the sea floor in an area previously surveyed by deep-penetration and high-resolution seismic-reflection techniques. Additional seismic profiles were obtained 5 weeks after the shock. Comparison of these postearthquake records with those obtained 1 to 3 years earlier (fig. 14A) reveals an extensive (approx 1 by 20 km) zone of shallow (5 m thick) failure in unconsolidated sediment at a water depth of 60 m on a nearly flat (less than 0.25° slope) bottom. Geomorphic features diagnostic of sediment flow and lateral spreading are visible in side-scan sonar records obtained after the earthquake (fig. 14B). The failure zone is at least 30 km from the closest point of seismic-energy release in the earthquake, as inferred from the distribution of aftershock epicenters.

The potential hazard that submarine slides pose to offshore structures is exemplified by the loss of South Pass 70 Platform B in the Gulf of Mexico (Sterling and Strohbeck, 1973). This platform failed from large-scale downslope movement of sediment to a depth of at least 20 m. The platform was found resting on its side on the bottom, displaced about 25 m in the downslope direction. In this case, the movement was triggered not by seismic shaking but by 20-m-high waves generated by Hurricane Camille.

Pipelines, because of their extended lengths, are particularly susceptible to failure from submarine slides, as is seen by analogy, using experience with communication cables lying on the sea floor. In the 1929 Grand Banks M=6.5 earthquake off the south coast of Newfoundland, submarine sliding ruptured seven cables within an area of about 35,000 km^2 surrounding the epicenter (Heezen and Drake, 1964), and associated turbidity currents broke other cables to distances of 700 km from the epicenter (see next section and fig. 15).

Loss of bearing strength without downslope movement is also a potential hazard to structures situated on or buried in liquefiable sediment in offshore or coastal environments. Earthquake-induced liquefaction can cause structures founded on sediment to settle and tilt, and buried structures to rise by buoyancy through liquefied sediment. Some of the most striking onshore examples of liquefaction effects were associated with the 1964 Niigata, Japan, M=7.6 earthquake (Seed and Idriss, 1967).

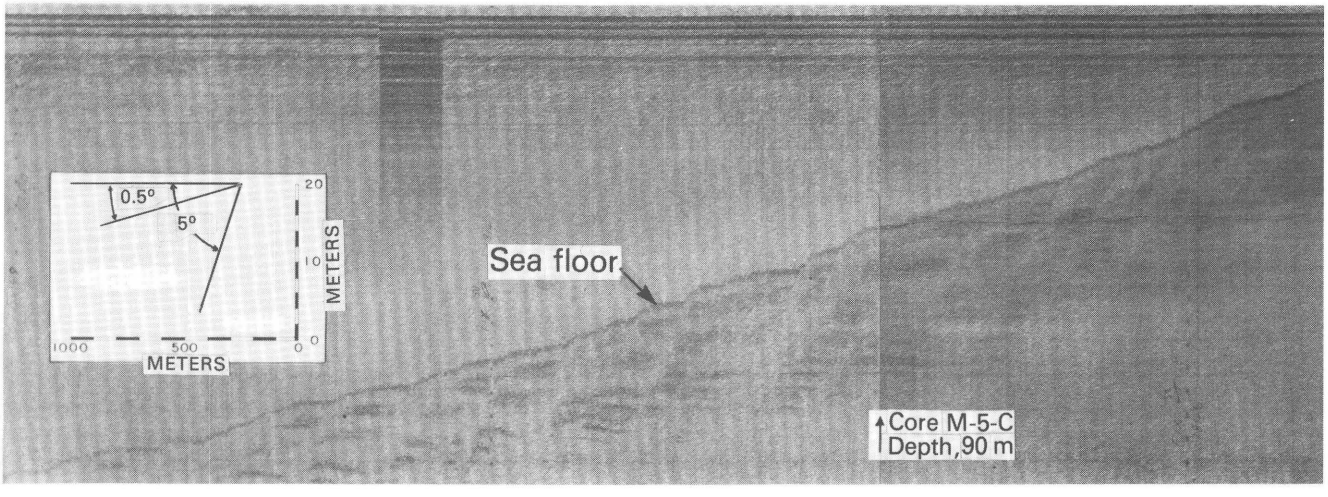

Figure 13. Subbottom seismic-reflection record (vertical section), showing multiple slumps in foreset beds of the Copper River delta, Alaska (from Reimnitz, 1972, fig. 4). Slumps are attributed to progressive slope failure during the 1964 earthquake. Vertical exaggeration, x27.

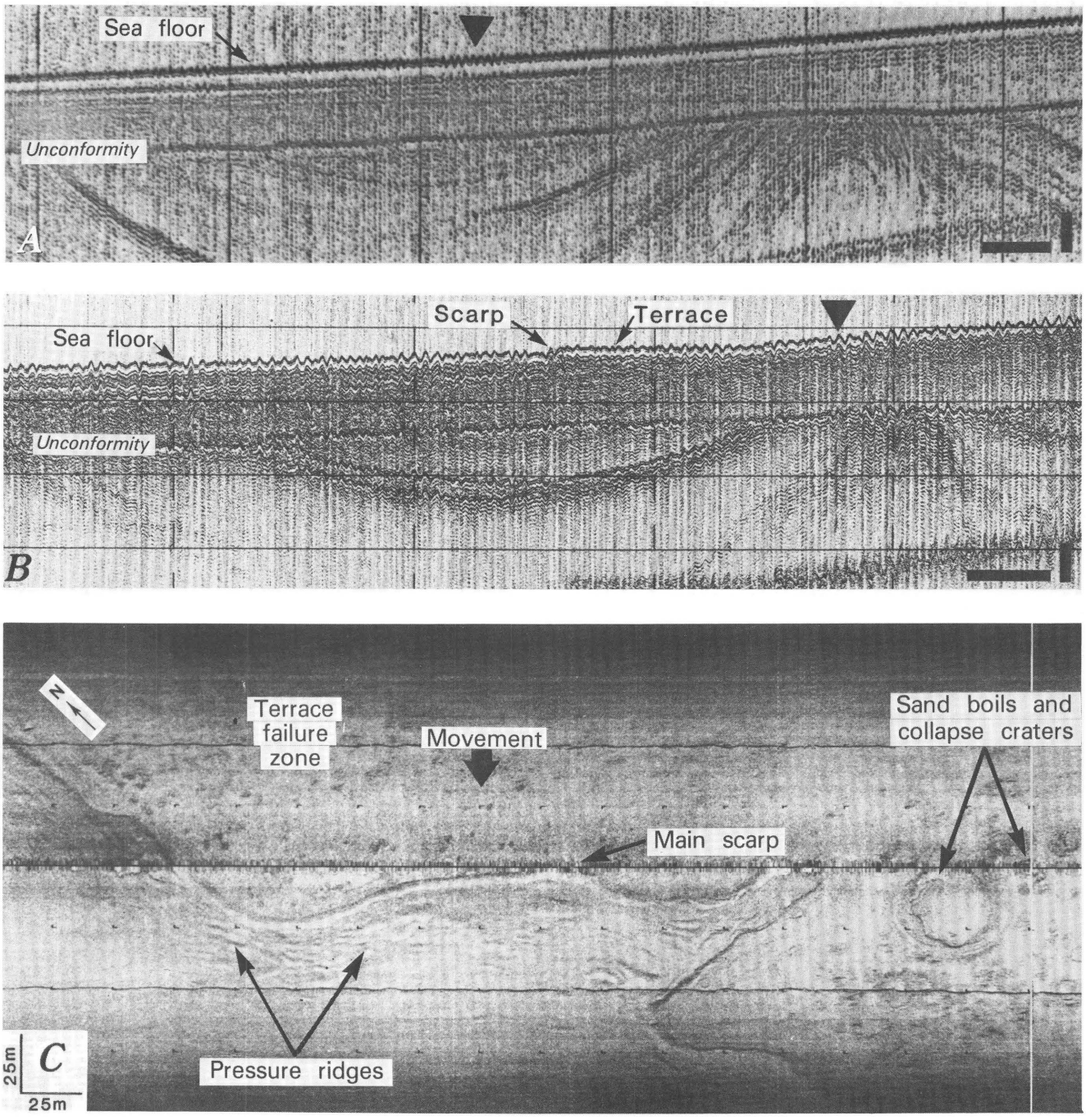

Figure 14. Earthquake-induced sediment failure on the shallow Continental Shelf off mouth of the Klamath River, northern California. High-resolution seismic-reflection (Uniboom) records (vertical sections) along nearly coincident profiles were made before (A, Oct. 1979) and after (B, Dec. 1980) the November 1980 earthquake (from Field and others, 1982, fig. 3). Vertical scale bars, 10 m; horizontal scale bars, 250 m; triangles mark 60-m water depth. Terrace and toe-scarp morphology in figure 14B results from sediment flow and lateral spreading after seismically induced liquefaction. Note smooth, undisturbed sea floor before the earthquake. C, Side-scan-sonar record (plan view) along toe of failure, showing features diagnostic of sediment flow and lateral spreading (from Field and others, 1982, fig. 4). Lateral range is 100 m to either side of ship's trace (centerline). Sinuous 1-m-high main scarp marks termination of flow. Pressure ridges are inferred to be caused by local compression of sediment seaward of advancing flow or spread. Circular features are inferred to be sand-boil vents and collapse craters resulting from ejection of trapped gas or liquefied sediment.

Turbidity currents

Sediment, after slumping, can exhibit a broad range of mobility states, from rigid block motion to turbulent flow. The type of motion after slumping depends on the slope profile, the shape and position of the slip surface, pore-water pressure within the sediment, and the strength and density of the sediment. However, the conditions that must be satisfied for the onset of turbulent flow, or turbidity currents, are not well understood (Plapp and Mitchell, 1960; Morgenstern, 1967; Hampton, 1972).

A turbidity current is a density current in which water containing a large amount of suspended sediment flows downslope under the influence of gravity. After reaching a relatively level section of the bottom, the current may continue to flow for a long distance. The sediment can be put in suspension in several ways, for example, by sedimentation processes at a river mouth, by wave action, or by landslides into or within a body of water. The largest known turbidity currents have been caused by earthquake shaking on a continental slope or shelf that has triggered landslides and slumps. Evidence of the extent of many earthquake-induced turbidity currents has been provided by breakage of cables on the sea floor; for example, the Grand Banks south of Newfoundland (Heezen and Ewing, 1952; Heezen and others, 1954; Heezen and Drake, 1964), the Ionian Sea (Ryan and Heezen, 1965), the western New Britain Trench (Krause and others, 1970), and the Algerian coast (Heezen and Ewing, 1955).

The Grand Banks turbidity current in 1929, caused by the $\underline{M}$=6.5 earthquake on the continental slope south of Newfoundland, has received the most study. The earthquake caused a large gravity slump (fig. 15), the extent of which was inferred from interpretation of a seismic-reflection profile and the locations of cables that failed at the instant of the earthquake (Heezen and Drake, 1964). The slump generated a turbidity current that swept down the slope and onto the abyssal plain. On the basis of the sequence of cable breaks, the velocity of this current was estimated to be approximately 100 km/h near the base of the Continental Shelf. Piston cores, showing a graded layer of sediment, and the locations of the last cable breaks indicated the extent of the current on the abyssal plain (fig. 15). Kuenen (1952) estimated that the thickness of the initial slump was about 50 m and of the resulting turbidity current about 270 m.

Turbidity currents on the continental slope are known to scour submarine canyons and to deposit large volumes of sediment on the sea floor, well out on an abyssal plain. Because of the gentle slopes that characterize the Continental Shelf, however, sea-floor failures on the shelf are unlikely to be transformed into turbidity currents unless they involve steep slopes in an area of rapid sedimentation. Such circumstances exist in Valdez Fiord in southern Alaska, where earthquakes repeatedly have triggered submarine slides that apparently were transformed into turbidity currents (Coulter and Migliaccio, 1966). On five separate occasions, submarine cables have been broken and buried.

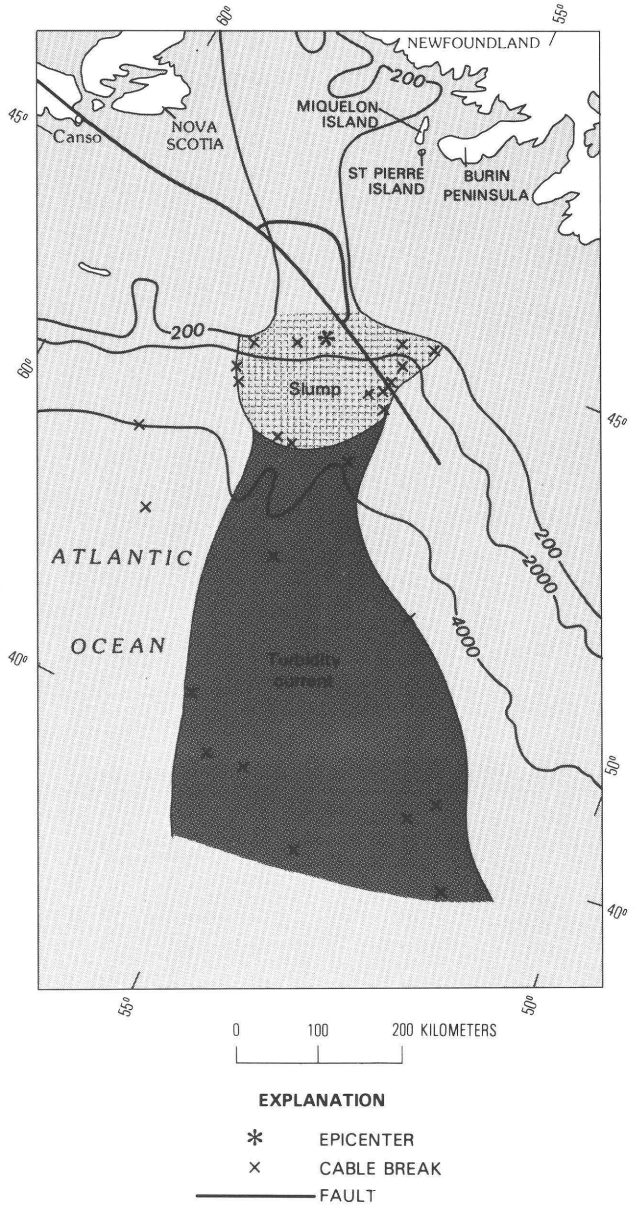

Figure 15. Area of 1929 Grand Banks, Newfoundland, submarine slump and turbidity current, showing epicenter of $\underline{M}$=6.5 earthquake and locations of cable breaks (from Doxsee, 1948) and faults (from King, 1980). Bathymetric contours in meters. Approximate extent of slump and turbidity current from Heezen and others (1954) and Heezen and Drake (1964).

The potential hazards of turbidity currents to offshore facilities arise from the hydrodynamic forces imposed on obstacles in the path of the current and from sediment scour around the foundation of a structure or a buried pipeline. Although the hazard of a turbidity current may not match that of the initiating submarine slide in terms of the potential for concentrated damage within a localized area, the turbidity current will affect a much larger area, extending far downslope from its point of origin.

Tsunamis

A tsunami is a gravitational seawave caused by the sudden displacement of a large volume of water. Tsunamis can be generated by seismic and volcanic activity or by submarine and shoreline landslides. Here, we confine our discussion to earthquake-related tsunamis caused by sudden vertical displacement of the sea floor and by the sliding of subaerial and submarine sediment induced by seismic shaking.

Tsunamis on the open ocean fall under the general classification of long waves, with wavelengths of several hundred kilometers. Their amplitudes over the deeper part of the ocean do not exceed 1 m and thus are difficult to detect from ships or from the air. The wave velocity is proportional to the square root of the water depth and in the deep ocean can be several hundred kilometers per hour. As a tsunami impinges on the Continental Shelf, its velocity decreases, and the wave height increases. A series of waves approaches the coast with periods ranging from about 5 minutes to more than 2 hours. The wave with the greatest height is generally not the first but commonly occurs among the first 10. A tsunami approaching a coastline is subjected to several modifications: energy may be reflected from the continental slope; the Continental Shelf may act as a waveguide tending to trap energy at wavelengths near that of the shelf width; and inlets, harbors, and embayments may cause significant amplification of the waves.

The principal potential hazard from tsunamis is to coastal and shallow-water facilities. Tsunami wave height does not become comparable to that of storm waves until the wave reaches quite shallow water. Under the assumption that no dissipation or reflection of energy occurs as the wave approaches shore, an appreciable proportion of the increase in wave height with shoaling water depth can be accounted for by linear theory (Wiegel, 1970). A 1-m-high wave on the open ocean would increase in height to about 3 m in a water depth of 50 m and to about 5 m in a water depth of 10 m. Therefore, tsunami waves would not subject platforms and other facilities in water depths of tens of meters to loads greater than those generated by storm waves.

Sudden vertical displacement of the nearly horizontal sea floor can displace large volumes of water, whereas horizontal displacement cannot. In the 1964 Alaska earthquake, extensive vertical deformation of the sea floor (fig. 8), caused by low-angle thrust faulting beneath the Continental Shelf, generated several destructive tsunamis, as discussed below in further detail. In contrast, no major tsunami was reported after the 1949 Queen Charlotte $\underline{M}$=8.1 earthquake, which had a strike-slip fault mechanism. All types of earthquakes, however, including strike slip, can generate local destructive tsunamis through vibration-induced submarine slides.

Local tsunamis

For the purposes of discussion, local tsunamis are seawaves impacting near their place of origin. Local tsunamis, which devastated coastal communities during or immediately after the 1964 Alaska earthquake, caused 103 deaths and more than $85 million in damage (Wilson and Torum, 1972a). These waves were generated by two types of mechanisms: the vertical displacement of a large area of the Continental Shelf (fig. 8), which generated trains of long-period waves that first struck the coast about 20 minutes after the earthquake (von Huene and Cox, 1972); and the displacements of large volumes of water by sudden failures of unconsolidated sediment at or below sea level, which generated short-period waves that were largely restricted to a single fiord or strait. Slide-generated waves caused more destruction and loss of life than the tsunami generated by deformation of the Continental Shelf (Weller, 1972).

At Seward, the wave generated by the slide that carried away a 1.2-km length of the waterfront (fig. 12) reached a maximum height of about 10 m. It caused considerable damage to railroad facilities and spread burning oil along the waterfront from tanks that had ruptured (fig. 16). About half an hour later, the first wave from the major tsunami source on the Continental Shelf struck Seward and caused additional extensive damage and spread burning oil farther over the waterfront (Spaeth and Berkman, 1972; Wilson and Torum, 1972a).

Local waves were generated by slides in two separate areas of Port Valdez (fig. 4, inset). Waves caused by submarine slides off the terminal moraine at the mouth of Shoup Bay washed the Middle Rock navigation light in Valdez Narrows off its 10-m-high reinforced-concrete pedestal. The delta-front slide that carried the Valdez dock into the sea generated a violent surging wave that demolished most of the remaining waterfront facilities and completed the wrecking of the fishing fleet (Coulter and Migliaccio, 1966).

Kodiak Island was the only place within the affected area of the Gulf of Alaska for which fairly detailed information on the wave sequence and wave heights is available, owing to a log kept by a naval officer at Womens Bay. A reconstructed marigram shows the water-level fluctuations in Womens Bay (fig. 17). This record is resolvable into three major components: the astronomic tide; a train of modulated waves with periods of about 2-1/2 hours, related to the half-length of the wave generated on the Continental Shelf; and an oscillation of about 80-minute period, representing the second mode of free oscillation of water on the Continental Shelf (Wilson and Torum, 1972a). Waves continued to inundate the shoreline of Kodiak Island with progressively decreasing amplitude until about 12 hours after the earthquake. These waves caused extensive damage to shoreline buildings, fishing vessels, docks, navigation equipment, bridges, and highways. High-velocity currents associated with the repeated ebb and flood of waves resulted in extensive damage through erosion to artificial fills and unconsolidated deposits. Bottom changes offshore from Kodiak Island occurred in water depths of as much as 25 m (Plafker and Kachadoorian, 1966). Waves were also reported on the coast of Kodiak Island before the principal tsunami wave train illustrated in figure 17.

On the Atlantic margin, the 1929 Grand Banks $\underline{M}$=6.5 earthquake generated a tsunami with amplitudes

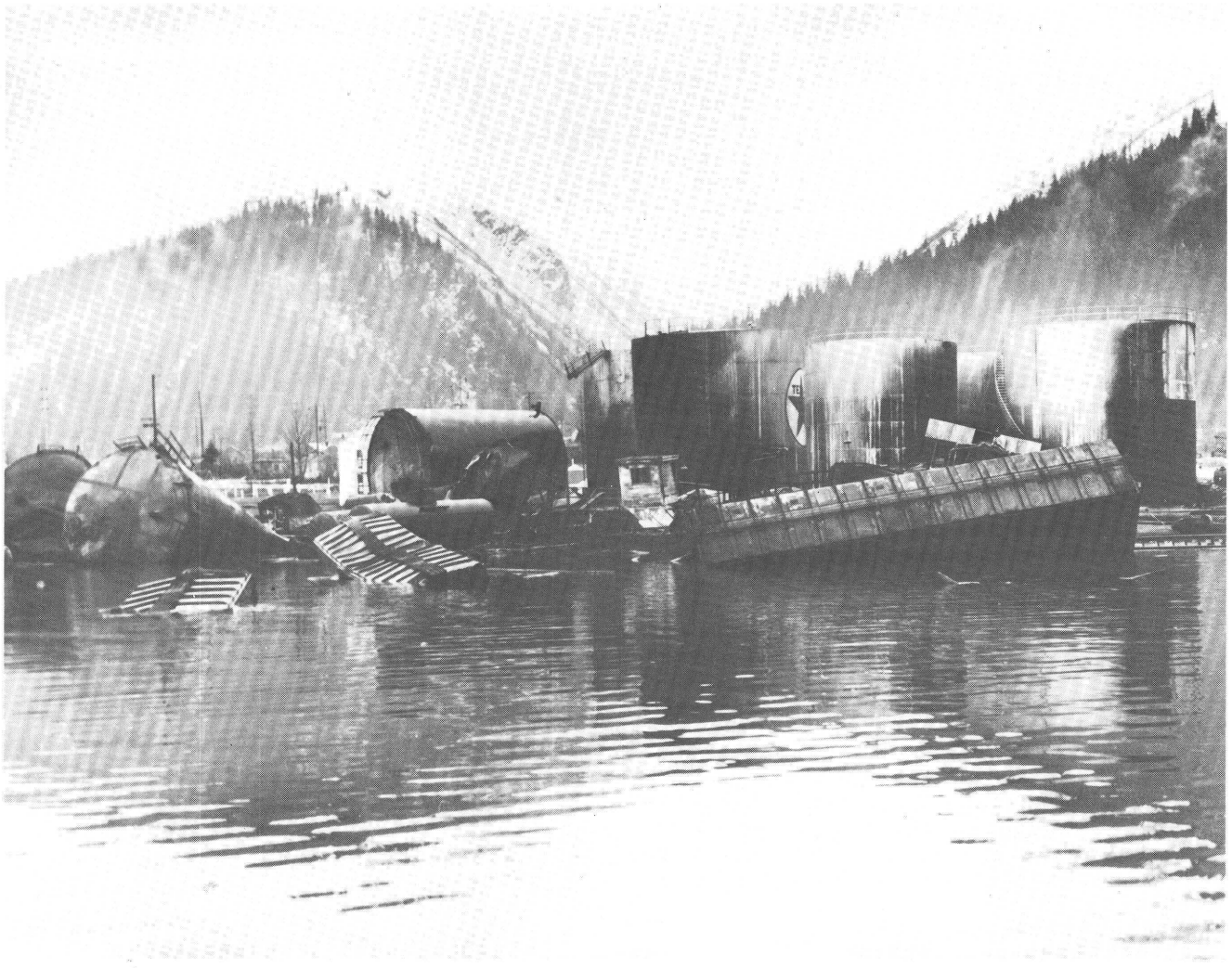

Figure 16. Damage to railroad yard and petroleum-tank farm at Seward, Alaska, caused by waterfront slides, waves, and fire (from Lemke, 1967, fig. 6).

of at least 12 m on the Burin Peninsula on the south coast of Newfoundland (fig. 15). The tsunami, which reached the shore at a time of abnormally high tide and during a heavy gale at sea, caused the loss of 27 lives and extensive damage to homes and fishing equipment (Doxsee, 1948). The traveltime of the tsunami from the epicenter to the Burin Peninsula was approximately 2-1/2 hours (Murty, 1977). There was no warning because no warning system was, or is now, in place along the East Coast. This is the only documented case of tsunami damage on the east coast of North America, although the Caribbean Islands have undergone several tsunamis from local and eastern Atlantic sources (Murty, 1977). It is problematic whether the 1929 tsunami was generated by tectonic deformation of the sea floor related to faulting or by submarine slumping, although slumping seems more likely.

Distant tsunamis

The principal source of the major tsunami generated by the 1964 Alaska earthquake, which swept from the Gulf of Alaska across the length of the Pacific and lapped against Antarctica, was sudden uplift of the Continental Shelf (fig. 8). Extensive studies have been made of the source mechanism, oceanic properties, propagation, coastal modification, runup heights, and associated damage of this tsunami (Berg and others, 1972; Spaeth and Berkman, 1972; Van Dorn, 1972; Van Dorn and Cox, 1972; Wilson and Torum, 1972b).

Along the coast of western Canada, the maximum heights of tsunami waves recorded at most tide stations ranged from 2 to 4 m. An exception was the Alberni Inlet on western Vancouver Island, where amplifying effects generated water levels as much as 9 m above average and caused extensive damage near the head of the inlet (White, 1966). Some of the highest waves occurred along the Washington, Oregon, and northern California coastlines, owing to the coincidence of tsunami waves with high spring tide. Unusually high waves at Crescent City, Calif., have been attributed to dynamic amplification by resonance on the Continental Shelf, as determined by the shape of the coastline and the bathymetry of the shelf (Wilson and Torum, 1972a). Along the coast south of

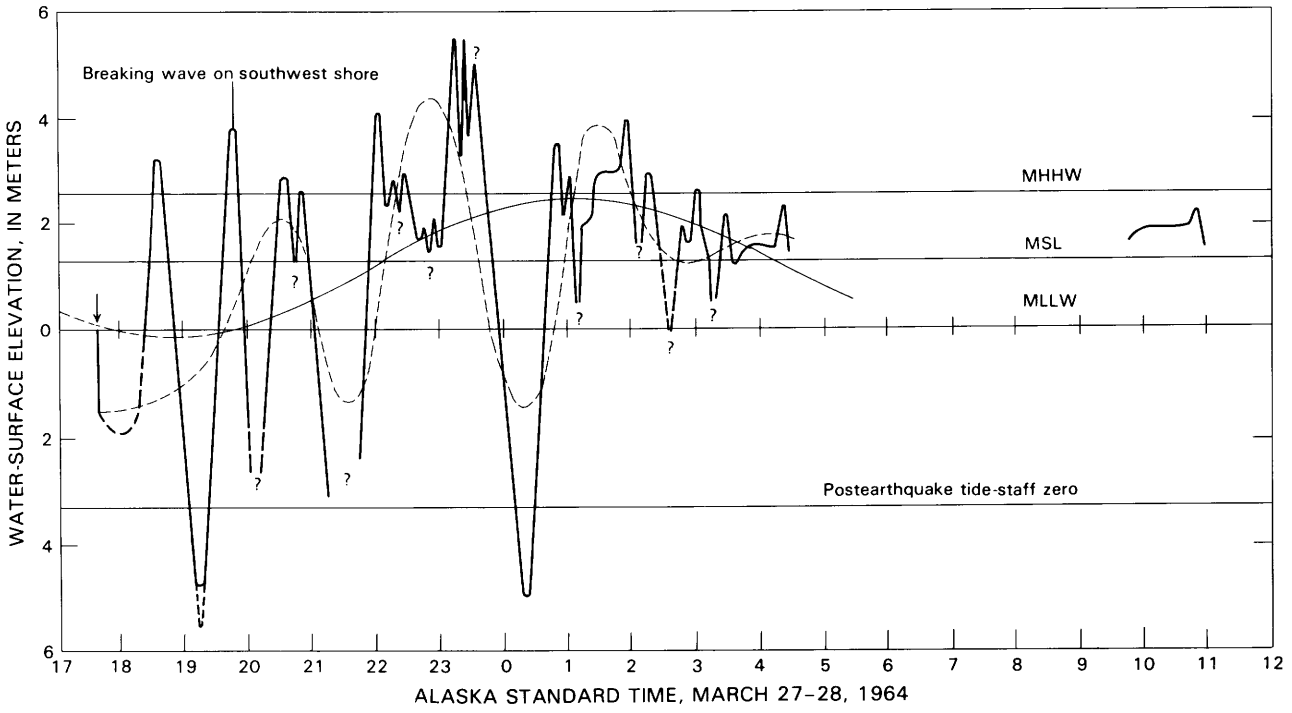

Figure 17. Reconstructed marigram for water-level fluctuations in Womens Bay, Kodiak Island, Alaska, caused by principal tsunami from the 1964 earthquake (from Wilson and Torum, 1972b, fig. 4). Widely fluctuating solid curve, observed water levels; smooth solid curve, astronomic tide; dashed curve, long-period tsunami waves. MHHW, mean higher high water; MLLW, mean lower low water; MSL, mean sea level.

Crescent City, runup was generally much less than that farther north because the tsunami waves arrived 1 to 2 hours after high tide. Elsewhere around the Pacific, runup above ordinary tidal level was about 4 m in Hawaii, 2 m on the coast of Chile, and 0.8 m on the coast of Japan.

The 1929 Grand Banks tsunami did not cause extensive damage in areas other than the south coast of Newfoundland. The islands of St. Pierre and Miquelon, off the tip of the Burin Peninsula (fig. 15), escaped damage. The east coast of Nova Scotia was flooded in several places; fishing wharves and one ship were damaged at Canso. In Bermuda, a dredging vessel broke its mooring chains. The wave was large enough to be noticed in the Azores, but tide gages in the Gulf of St. Lawrence showed no unusual waves (Doxsee, 1948).

The tsunamis from the 1964 Alaska and 1929 Grand Banks earthquakes are two of the many hundred that have been documented in the Pacific, the eastern Atlantic, the Caribbean, and the Mediterranean (Murty, 1977).

ASSESSMENT OF EARTHQUAKE POTENTIAL

There are three strategies for minimizing the potential hazards of earthquakes: avoidance, accommodation, and emergency planning. The success of all three strategies depends on the abilities of earth scientists, first, to assess the potential for earthquakes to occur and, second, to predict their effects. This section discusses the assessment of earthquake potential; prediction, evaluation, and mitigation of earthquake effects are discussed in the next section.

Key considerations in assessing earthquake potential are the location and size of future earthquakes and the frequency and imminence of their occurrence. To assess this potential, the earth scientist must develop a conceptual model incorporating geologic and geophysical information available at various scales to relate the occurrence of earthquakes to ongoing tectonic processes. This model must pertain to a region considerably larger than the site or area of interest because it must encompass all earthquakes that could have a significant effect.

Because of inadequacies and uncertainties in the underlying seismotectonic models, only rarely can earthquake potential be assessed with a high degree of certainty. For example, the historical record of seismicity within a given region typically is short in comparison with the repeat time for the maximum size of earthquake likely to occur in the region. Thus, the historical earthquake record alone does not usually afford reliable estimates of the size and recurrence rate of a maximum earthquake. Although the geologic record may preserve evidence directly related to the size and date of large prehistoric earthquakes, generally the earth scientist has to rely on less direct evidence and exercise considerable judgment in assessing the magnitude and frequency of the largest possible earthquake in a particular region.

Assessments of earthquake potential are likely to be more reliable in seismically active regions than in those of low seismicity. In active areas, where the repeat time for large earthquakes is shorter, the

likelihood is greater that the historical record includes the maximum earthquake that can be generated by specific geologic structures, as well as the cyclic variations in seismicity related to the accumulation and release of strain energy in major earthquakes; moreover, the opportunities to investigate the relations between earthquakes and geologic structures and processes are more numerous. Also, in areas of high seismicity the tectonic processes that cause earthquakes are generally the dominant processes that sculpt the landscape, and so the earthquake-generating processes are more readily deciphered from the recent geologic history. In contrast, the time intervals between earthquakes in relatively inactive areas are longer, and so it is less probable that the maximum possible shock has occurred within historical time. Furthermore, erosional processes are more likely to obliterate or obscure evidence of current seismotectonic processes that might otherwise be clearly preserved in the surficial geology.

Seismotectonic models are developed from information derived from two sources: the historical seismic record and the recent geologic record. The historical record contains relatively detailed and reliable information about earthquake occurrence, but typically it is short in comparison with the repeat time of large earthquakes. The geologic record supplements the historical record by greatly extending the time interval over which information on earthquake occurrence is available; however, the information gleaned is generally far less certain and detailed.

Seismic record

Historical seismicity

Historical seismicity provides an initial estimate of earthquake potential, that is, the location, size, and frequency of future earthquakes in a given region. Seismic history is generally divided into two eras by the point in time when instrumental recording of earthquakes began. Not until about the turn of the 20th century were even larger earthquakes routinely recorded by seismographs. The length of the preinstrumental period is determined by the history of human settlement and record keeping, and varies considerably among the active seismic regions of the globe. For example, useful records date back about 150 years in western North America, 300 years in eastern North America, but about 2,000 to 3,000 years in China and the eastern Mediterranean region.

Coastal settlements provide a record of offshore earthquakes large enough to have been felt on land, but the accuracy with which these events can be located, on the basis of the distribution of damage and other effects, is considerably less than for similar-size earthquakes onshore. For example, reports of felt earthquakes from fishing villages along the Labrador coast date from as early as 1809 (Smith, 1962), and epicenters for these earthquakes were assigned to the locations at which they were felt. No evidence is available, however, from recent instrumental data that significant earthquakes are occurring onshore in this area; the older events most likely occurred offshore in an active zone of seismicity defined by instrumentally determined epicenters of the past 50 years (Basham and Adams, 1982, fig. 2).

The length and value of the instrumental record of seismicity depends on the history of seismograph operations, in particular, the number of stations, their sensitivity, and the methods used to compile data. For example, although it is unlikely that the occurrence of onshore earthquakes of $\underline{M} \geq 7$ in southwestern British Columbia would have been missed after the beginning of regular publication of newspapers, or after about 1860, a similar record for offshore shocks is unavailable before the routine operation of the Victoria seismograph, which began in 1898. Reporting of events as small as $\underline{M}=6$ offshore of British Columbia is incomplete before 1919, when systematic attempts were made by the British in the International Seismological Summary (ISS) to gather seismograph readings and publish a global summary of earthquake locations. There may, however, be significant errors in these results, in part because of the practice of the ISS to locate specifically only the first earthquake from a given region and then to assign subsequent earthquakes from the same region to the first epicenter (Dewey, 1979). At present, the onshore network of seismographs in western Canada is capable of routinely locating only earthquakes of $\underline{M} \gtrsim 4$ in the offshore zones. However, within the southern Georgia Strait and Puget Sound region, monitored by the British Columbia and Washington State networks, the present threshold for complete detection and location is $\underline{M} \sim 2\text{-}1/2$.

Studies of historical seismicity, in addition to revealing the locations and rates of significant earthquakes, provide information on the tectonic component in seismotectonic models. For example, comparison of the directions of fault slip inferred from focal mechanisms of individual earthquakes in the Gulf of Alaska region with those derived from analysis of global plate motions suggests that the Pacific plate is being subducted beneath the continental margin between Icy Bay and Cross Sound, but only at about one-sixth the rate of subduction occurring to the west off the Kenai Peninsula and Kodiak Island (Perez and Jacob, 1980). As a further example, from comparison of slip rates inferred from historical seismicity with those estimated from plate-motion models, in conjunction with sediment deformation along the continental margin and with geodetic measurements, Weichert and Hyndman (1983) have concluded that most of the convergent movement between the Pacific and North American plates in the Puget Sound region is accommodated by aseismic deformation associated with underthrusting and continental compression.

Location of offshore earthquakes

Three reasons for uncertainties or biases in the locations of earthquakes are: (1) poor data, a particularly serious problem for older earthquakes detected on insensitive seismographs with poor timing control; (2) poor distribution of stations about the epicenter; and (3) incorrect velocity models. Attempts (Gawthrop, 1978; Hanks, 1979b) to accurately locate the 1927 $\underline{M}=7.3$ earthquake off Lompoc, Calif., illustrate the difficulties with both early seismograph

recordings and azimuthally biased data from onshore networks. In attempting to locate this significant earthquake, these and other workers have used combinations of: the arrival times of seismic waves from the main shock; the time intervals between the P and S phases for the immediate aftershocks; the distribution of earthquakes, assumed to be aftershocks, that occurred for a few decades after 1934, when epicentral locations began to be routinely reported on the basis of data from an expanded California seismograph network; the distribution of strong shaking in the adjacent coastal region; geodetic-survey data; and the presence of major offshore faults that have been mapped in recent years by seismic-reflection profiling. Considerable uncertainty still exists, however, both in the exact location of the epicenter (uncertainty of tens of kilometers) and in identification of the causative fault.

In addition to uncertainties, serious biases also may exist in the locations of offshore earthquakes determined from data recorded by onshore seismograph networks. Where seismograph stations are unevenly distributed in distance and azimuth relative to the earthquakes being located, the network can resolve hypocentral errors in some directions better than in others, and so, for example, errors in latitude are correlated with errors in longitude. Dewey (1979) presented an example (fig. 18) in which this correlation causes a spurious alinement of epicenters. This apparent alinement was initially interpreted (Vrana, 1971) as evidence for a nascent fracture zone striking northeast toward the California coast north of Point Arguello, in the vicinity of a proposed large nuclear powerplant. More thorough analysis of a larger data set, however, linked the earthquakes to a major northwest-trending fault system (Gawthrop, 1975). The epicenters in figure 18A were determined individually by the International Seismological Centre with P-wave arrivals from 10 or more stations located to the north and east. The trend of these epicenters suggests an active northeast-trending offshore fault zone. Dewey employed a joint-hypocenter procedure to relocate these earthquakes relative to one master event (fig. 18B). The better determined, relocated epicenters indicate a northwestward trend that is statistically significant at the 90-percent-confidence level.

The joint-hypocenter method minimizes the effect on computed hypocenters of unknown errors in the assumed traveltimes from a source region to individual stations. The difference between the observed and computed traveltime, or the traveltime residual, at a given station is postulated to be the same for all earthquakes occurring within a limited source region. To correct for the effect of traveltime errors, or anomalies, the observed traveltimes are adjusted by subtracting station corrections. In the joint-hypocenter method, both station corrections and hypocenters relative to a master event, whose location is assumed to be accurate, are determined simultaneously to minimize the observed traveltime residuals. This procedure yields precise relative locations for a group of earthquakes; however, if the master event is mislocated, the other events will be systematically mislocated in the same way.

Routine location methods based on teleseismic arrivals (that is, data recorded at distances greater than about 2,000 km from the epicenter) assume a spherically or ellipsoidally symmetrical velocity structure for the Earth's interior. Where major lateral variations in structure occur, this assumption can bias the computed hypocenters by tens of kilometers, even

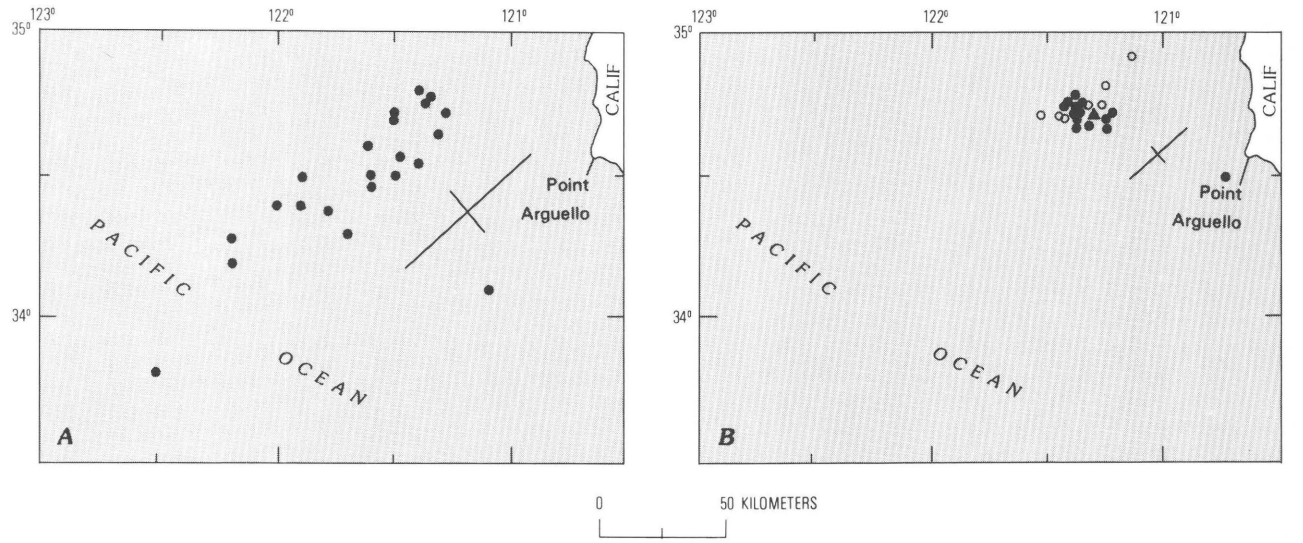

Figure 18. Earthquake epicenters off the coast of central California, determined by various location procedures (from Dewey, 1979, figs. 4, 5). Epicenters in figure 18A determined individually, and those in figure 18B simultaneously by the method of joint hypocenter determination. Principal axes of a typical 90-percent-confidence ellipse for a computed epicenter are plotted to southeast of the group of epicenters in both figures. Dots in figure 18B denote epicenters with semiaxes less than 15 km long, and circles epicenters with larger ellipses. Apparent northeast-southwest alinement of epicenters in figure 18A is spurious and is caused by a correlation of errors in latitude with errors in longitude.

when a relatively uniform azimuthal distribution of arrival-time data is available. Two of the strongest departures from assumed symmetry are the contrast in seismic-wave velocities across the continental margin and the high seismic velocities associated with the downgoing plate at subduction zones. For such departures, the accuracy of hypocenters can be improved if traveltimes are computed by tracing seismic rays through an appropriate Earth model, such as a model for a subduction zone with a dipping high-velocity slab corresponding to the subducted plate (for example, Engdahl and others, 1982). Ray tracing can also improve the location of hypocenters in relation to known near-surface faults if the velocity differences in the region are sufficiently well known (Engdahl and Lee, 1976). In locating regionally or locally recorded earthquakes, various approaches have been followed to account for lateral variations in velocity. For a discussion of this problem and of the theory, practice, and application of microearthquake studies, in general, see the review by Lee and Stewart (1981).

Ocean-bottom seismographs

The deployment of ocean-bottom seismographs (OBS's) can significantly improve both the detection threshold and the location accuracy of offshore seismicity. However, few OBS's have been deployed for long-term earthquake recording because of the costs and logistic and instrumental difficulties. Noteworthy long-term OBS recording efforts, all but one using long cables to transmit data, include: a single station 135 km off Point Arena, northern California, operated from 1966 to 1972 (Sutton and others, 1965; Nowroozi, 1973); a line of four stations deployed in 1978 and extending some 100 km seaward off the Pacific coast of central Honshu, Japan (Meteorological Research Institute, 1980); an array of five stations around the Dos Cuadras oilfield in the Santa Barbara Channel, deployed in 1978 (Henyey and others, 1979); and a single station in the North Sea between Norway and Scotland, deployed in 1980 and linked to the Beryl Alpha production platform via buoy-supported radio telemetry (Turbitt and others, 1983). To date, most OBS's have been deployed for short periods to investigate Earth structure or to accurately locate earthquakes occurring within special study areas during intervals of days to a few months. Prothero (1984) summarized the state-of-the-art in OBS technology.

The potential of OBS's for providing data that help resolve the tectonic processes responsible for offshore seismicity was illustrated in a study of the seismicity of the Juan de Fuca plate off western Canada (Hyndman and Rogers, 1981). The historical seismicity (fig. 19A) shows a broad scatter, about 100 km wide, from the south end of the Queen Charlotte fault to the north end of the Juan de Fuca Ridge. Isolated epicenters extend farther offshore and toward the British Columbia coast. This scatter could represent either location uncertainty or a real distribution reflecting breakup of the lithospheric plates in this area. Rogers (1980) revised the locations of many of these events from previously published values, some by more than 100 km, and reduced the scatter somewhat, but most epicenters have yet to be reassessed in a systematic way.

For comparison, the results from studies utilizing temporary OBS arrays are superimposed on the principal offshore tectonic features (fig. 19B). The microearthquakes are located in a zone 20 to 30 km wide that closely follows the plate boundaries defined from other geophysical and geologic data. The estimated accuracy of the epicenters is better than 5 km for most events within or near the OBS arrays and 10 km or greater for many of the most distant events. The largest event (M=3.8) detected by the OBS arrays, which was located on the Revere-Dellwood Fracture Zone (fig. 19B), was also recorded by permanent land-based seismographs. The routine location of this earthquake by the Earth Physics Branch of the Canadian Department of Energy, Mines and Resources was about 20 km northwest of the epicenter based only on OBS data, and the preliminary routine location by the U.S. Geological Survey was about 50 km northeast (Hyndman and others, 1978).

These results strongly suggest that the historical earthquakes actually occurred on or near the plate boundaries but that significant mislocation scatter and bias were introduced by the poor quality of the historical seismic data and the general difficulties associated with reliably locating earthquakes recorded by an azimuthally limited distribution of stations. The durations of OBS deployments—a maximum of 10 days in any one array configuration—were too short, however, to record a sample of earthquakes including the higher end of the magnitude range and thus to prove that all significant events in the region occur on or near these mapped sea-floor features.

As an alternative to OBS's, buoyed hydrophones, or sonobuoys, can be deployed to investigate offshore seismicity. For example, sonobuoys have been used to study microearthquakes occurring along the Blanco Fracture Zone and the Gorda Ridge off the coast of Oregon (Johnson and Jones, 1978; Jones and Johnson, 1978).

The use of the hypocenter-location (or relocation) techniques, described in the preceding subsection, and, where feasible, the deployment of OBS or sonobuoy arrays can significantly improve our understanding of historical seismicity patterns and the behavior of active fault zones for the purpose of seismotectonic modeling in regions of offshore petroleum development.

Geologic record

The geologic record, where well preserved and decipherable, may disclose evidence of previous earthquake activity and currently active tectonic processes that simply are unknown or unresolvable from historical information. The late Quaternary geologic record (approximately the past several hundred thousand years) and, especially, that of Holocene time (approximately the past 10,000 years) is a critical supplement to the historical seismic record. It affords a glimpse of earthquake activity over a time interval orders of magnitude longer than recorded history and thus provides a framework within which to interpret the long-term significance of historical

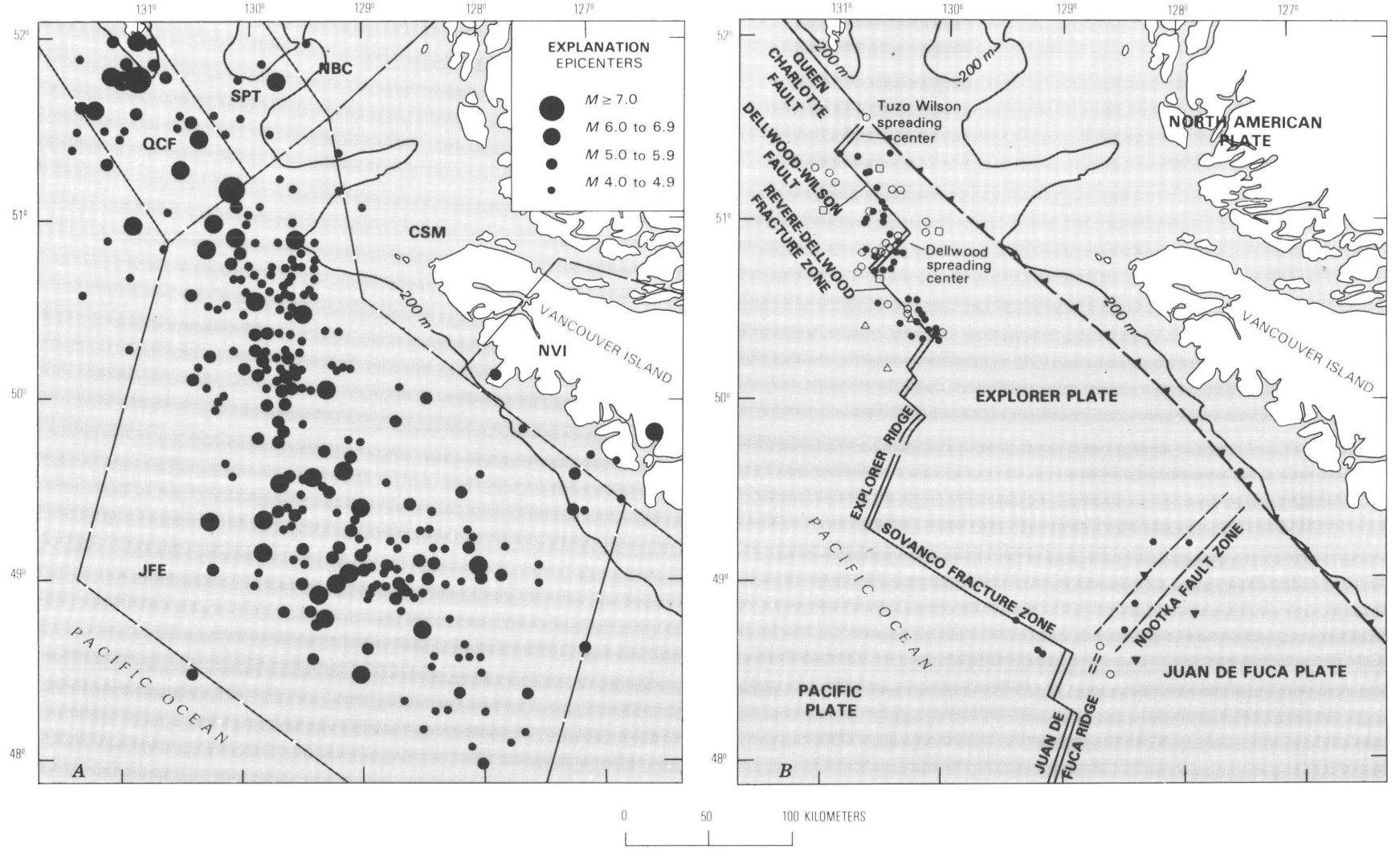

Figure 19. Seismicity off southern British Columbia, Canada, in the region of interaction between the Juan de Fuca, Explorer, and North American plates. 200-m bathymetric contour marks edge of the Continental Shelf. A, Epicenters of historical earthquakes (from Rogers, 1980); dashed polygons are seismic-source zones employed in regional probabilistic-ground-motion mapping (Basham and others, 1982). Earthquake source zones: CSM, Coast Mountains; JFE, Juan de Fuca-Explorer; NBC, Northern British Columbia; NVI, Northern Vancouver Island; QCF, Queen Charlotte fault; SPT, Sandspit. B, Microearthquakes located with data recorded by three separate temporary arrays (squares, open triangles, solid triangles) of ocean-bottom seismographs (from Hyndman and Rogers, 1981, fig. 5). Dots, epicenters with estimated location uncertainties of less than 10 km; circles, epicenters with larger uncertainties. Magnitudes range from 0.2 to 3.8. Arrays operated for about 6 to 10 days. Spreading centers (double lines) and transform fault zones (single lines) separate Pacific plate from Explorer and Juan de Fuca plates. Thrust fault, with sawteeth on upper plate, separates North American plate.

patterns of seismic activity and quiescence (for example, Allen, 1975).

Virtually all earthquakes occur as ruptures on preexisting faults. Accordingly, the identification of faults showing evidence of geologically recent movement is one approach in determining where future earthquakes are likely to occur. Recency and frequency of movement can be used as indicators of the degree of past fault activity and, by extrapolation, of the future behavior of a fault. For example, a fault that has ruptured repeatedly during Holocene time is more likely to generate a significant earthquake during the lifetime of an offshore structure than is one that has not slipped during this time. In many, but not all, circumstances, recency of movement on an individual fault can be determined from the age of the youngest displaced geologic deposit or judged from the geomorphic appearance of the fault, provided that such evidence is preserved.

The identification of faults as potential earthquake sources has been particularly successful in California (for example, Jennings, 1975; Wesson and others, 1975) and in the adjacent offshore area (for example, Greene and others, 1973; Ziony and others, 1974; Buchanan-Banks and others, 1978; Yerkes and Lee, 1979b). Contributing to this success are the following factors: the earthquakes are typically shallower than 15 or 20 km; surface faulting has been observed, when searched for, for most onshore earthquakes $M>6.0$ and many of $M=5.0$-5.9; and the rates of movement for many faults exceed the rates at which natural geomorphic processes obscure surficial evidence of faulting. Mapping of active offshore faults has also been successfully pursued elsewhere off the west coast of the United States and Canada (for example, Hyndman and others, 1979; Carlson and others, 1985).

The methods and tools for fault mapping in the marine environment (Sieck and Self, 1977; Ploessel, 1978) differ from those employed on land (Sherard and others, 1974; Slemmons, 1977). High-resolution seismic (acoustic)-reflection profiling is the most widely used technique for the identification of active offshore faults. The utility of the technique is illustrated by a seismic-reflection profile (fig. 20) across the Nootka fault zone, the seismically active strike-slip boundary between the Explorer and Juan de Fuca plates off Vancouver Island. This zone consists of a central core of active faults that offset the ocean floor, flanked by buried faults that are no longer active (fig. 20B). A recently developed tool of great potential is digitally rectified side-scan sonar, which provides undistorted, detailed plan-view images of the sea floor comparable in quality and utility to aerial photographs of the land (Clifford and others, 1979).

Information pertaining to the frequency and maximum size of earthquakes within a particular region or on an individual fault can also be extracted from the recent geologic record in some circumstances. For example, detailed geologic investigations of active onshore faults in the Western United States have yielded approximate dates and, in some places, amounts of fault displacement for large prehistoric earthquakes on faults within several tectonic provinces (for example, Bonilla, 1973; Machette, 1978; Sieh, 1978a; Swan and others, 1980). Estimates of the size of prehistoric earthquakes have been derived from measured prehistoric fault displacements, using the empirical relations between magnitude and displacement derived for different types of faults (for example, Slemmons, 1977; Bonilla and others, 1984) or from comparison of the geologic effects preserved from a prehistoric event with those from a documented, historical shock (for example, Sieh, 1978a).

An example illustrating the value of the geologic record is the San Andreas fault in central California (Wallace, 1968). On the Carrizo Plain, a series of four small stream channels (A-D, fig. 21) are offset right laterally 8 to 12 m along a 200-m length of the fault. These offsets are attributed to slip associated with the 1857 earthquake, which had an estimated magnitude of 7.9. One of the channels (D, fig. 21) also exhibits two earlier comparable offsets (D', D''), features suggesting the recurrence of earthquakes of $M \sim 8$ on this segment of fault. The dates of these pre-1857 offsets are not known, however, an average recurrence interval of 240 to 450 years has been determined for major earthquakes on this segment of the San Andreas fault from knowledge of the average slip rate on the fault and the amount of slip in prehistoric earthquakes (Sieh and Jahns, 1984). A second example, from the zone of surface rupture of the 1971 San Fernando, Calif., earthquake (Bonilla, 1973), illustrates geologic evidence of a prehistoric episode of dip-slip faulting (fig. 22). The earlier faulting was determined to have occurred about 200 years ago, by radiocarbon dating of a piece of wood buried in the debris that accumulated at the base of the scarp formed by prehistoric faulting. It is inferred that an earthquake larger than the $M=6.6$ shock in 1971 was associated with this earlier faulting because the prehistoric vertical displacement exceeds that observed in 1971.

In the United States and Canada, where the written history practically nowhere encompasses the complete cycle of stress buildup and release associated with a large earthquake, the geologic record has provided most of what is known about the repeat time and size of large earthquakes on onshore faults. In contrast, marine geologic evidence pertaining to the date and size of offshore earthquakes has yet to be recovered and applied. In coastal regions of rapid plate convergence, episodes of vertical crustal deformation accompanying large earthquakes may be preserved in the coastal geology, for example, in a sequence of elevated marine terraces (Plafker, 1969). Although it might be hoped that the geologic record would permit inferences about the frequency and maximum size of large coastal shocks related to dip-slip faulting, such inferences are difficult not only because an adequate Quaternary geologic record is rarely preserved but also because the patterns of deformation witnessed in historical earthquakes are complex and variable.

The imprint in the geologic record from a single earthquake typically is relatively small and difficult to resolve. Thus, detailed fault investigations more commonly yield rates of cumulative fault displacement derived from a series of several shocks (for example, Sharp, 1981), rather than time intervals between successive large shocks. From cumulative displacement rates, the average rate of earthquake occurrence

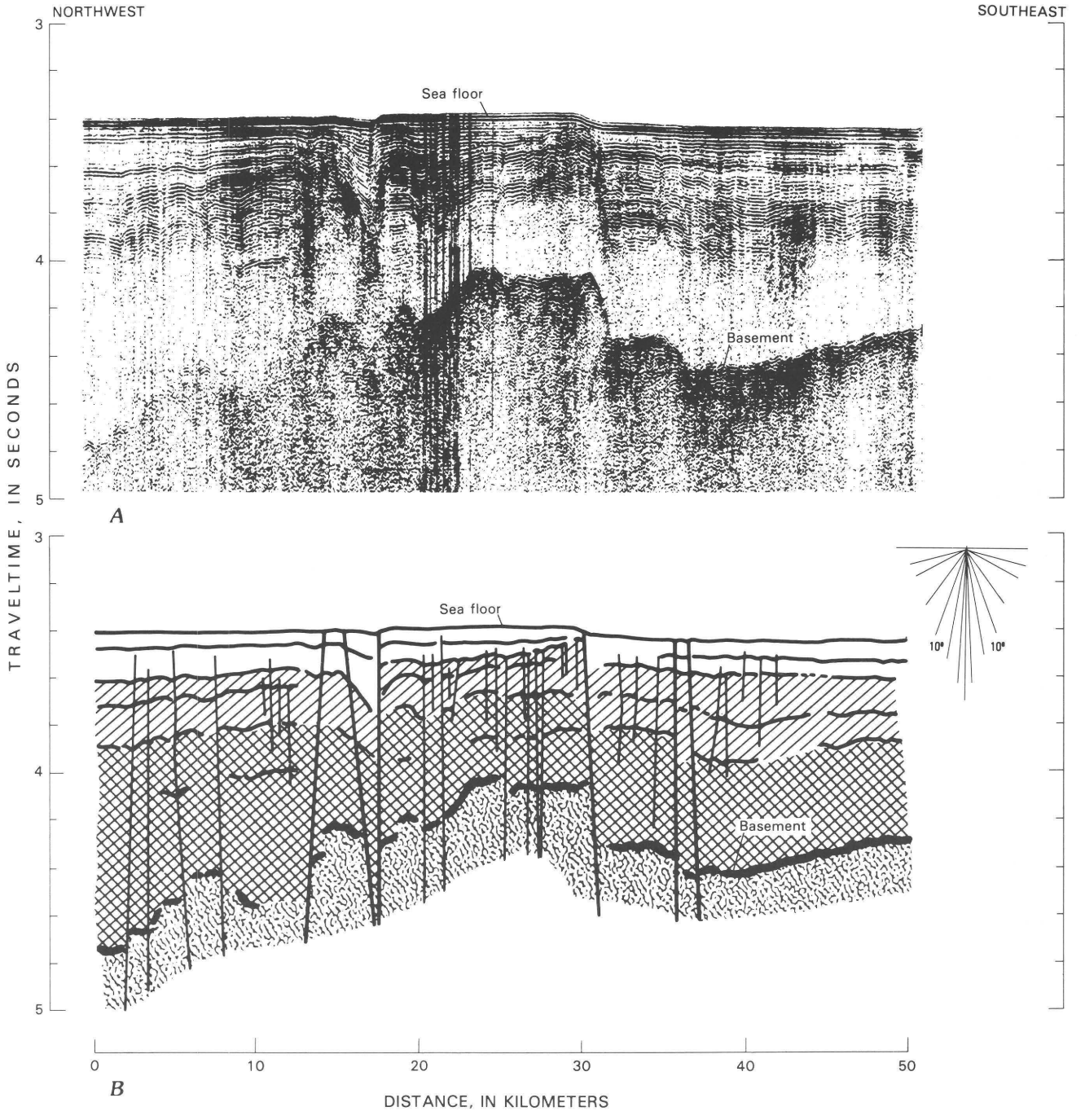

Figure 20. Seismic-reflection profile (vertical section) across the Nootka fault zone off Vancouver Island (from Hyndman and others, 1979, figs. 7, 8). A, Reflection profile showing basement uplift of several hundred meters, active faults offsetting the sea floor, and formerly active faults offsetting buried, older geologic horizons. B, Interpretation of reflection profile. Vertical scale is two-way traveltime for reflected seismic waves. In the sedimentary column, 1 s of traveltime corresponds to a distance of about 1 to 2 km. Vertical exaggeration, x16.

can be estimated by relating earthquake magnitude to fault offset through seismic moment (Anderson, 1979). Like magnitude, seismic moment is a measure of earthquake size; but unlike magnitude, it can be determined from geologic data, namely, the slipped area and average displacement on the fault, as well as from seismograms (see supplementary section below entitled "Intensity, Magnitude, and Seismic Moment"). Estimates of occurrence rates require assumptions with regard to the maximum size of earthquakes and the fraction of displacement that occurs aseismically, that is, without association with earthquakes, as in creep movement (Wallace, 1970). Similarly, on a larger scale, estimates of occurrence

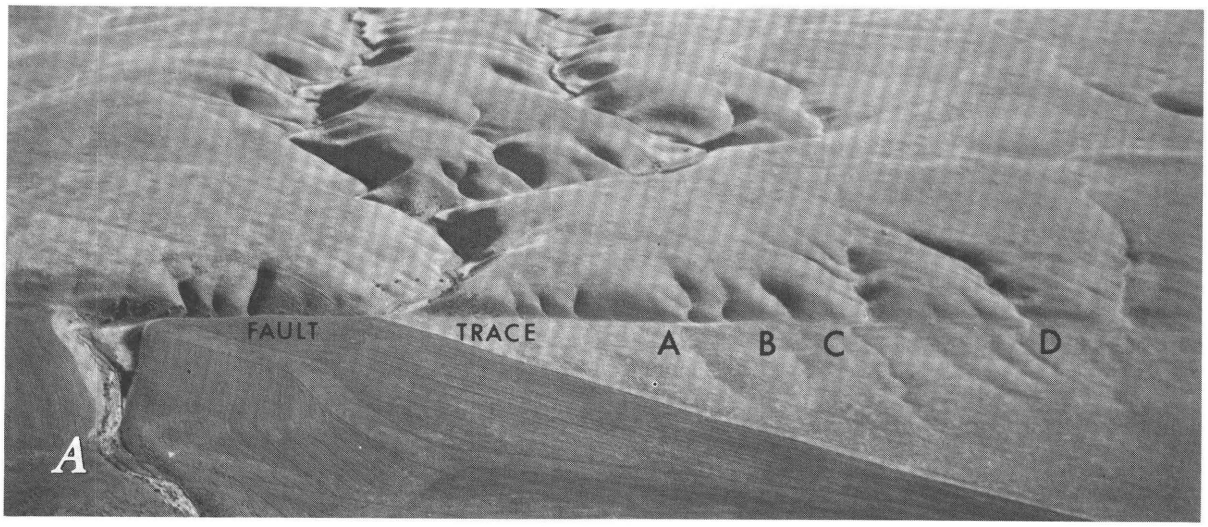

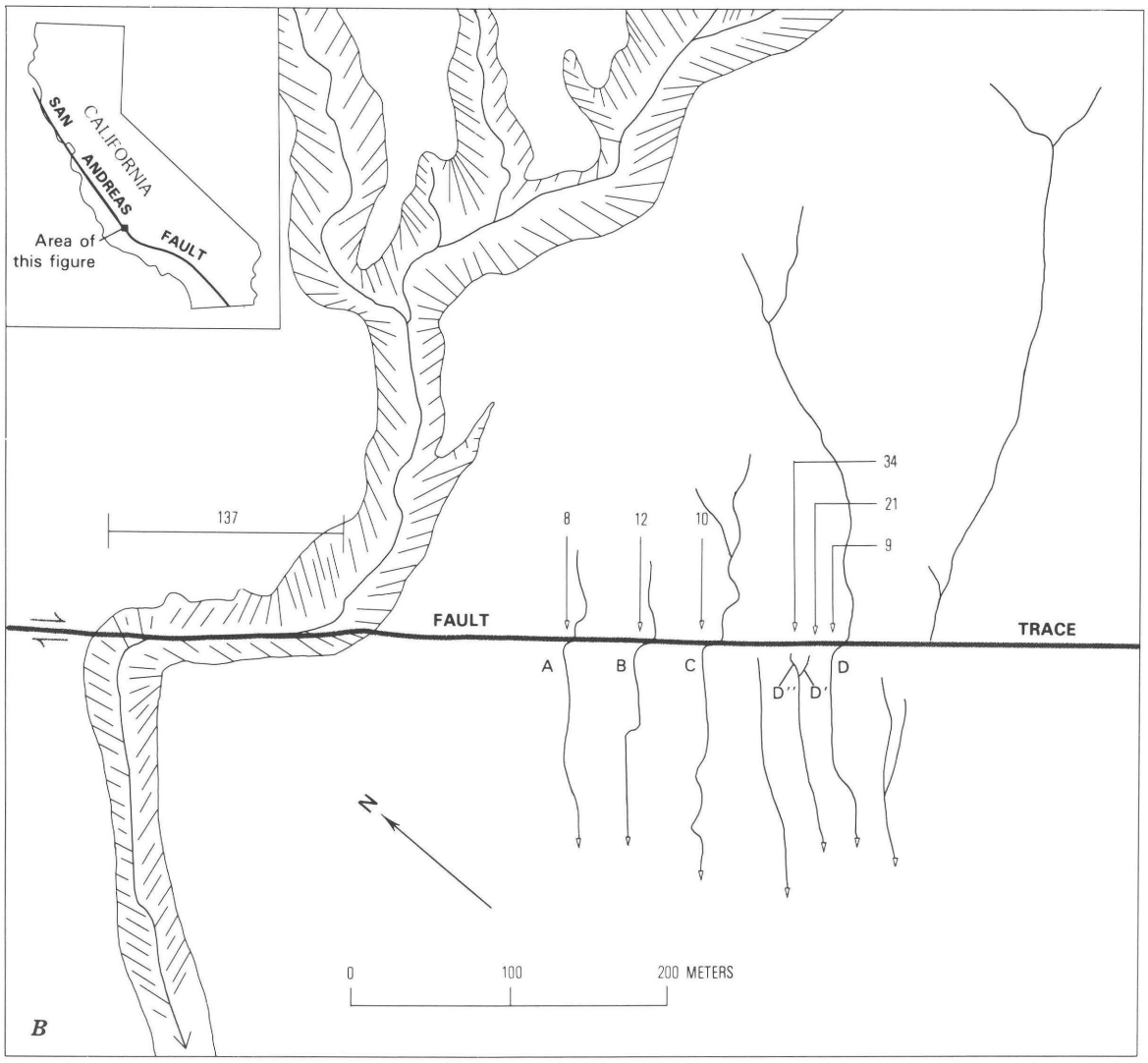

Figure 21. Stream channels offset by right-lateral strike-slip displacement on the San Andreas fault, Carrizo Plain area, Calif. A, Photograph by R.E. Wallace, U.S. Geological Survey. B, Sketch map of foreground of figure 21A, showing amounts of offsets (in meters) for channels of various ages (from Wallace, 1968, fig. 8). Youngest, least incised channels record amounts of offset from individual prehistoric earthquakes. Offset channels A-D attributed to slip from 1857 earthquake; D' and D" indicate offsets from previous earthquakes. Pair of arrows indicate direction of relative movement along fault.

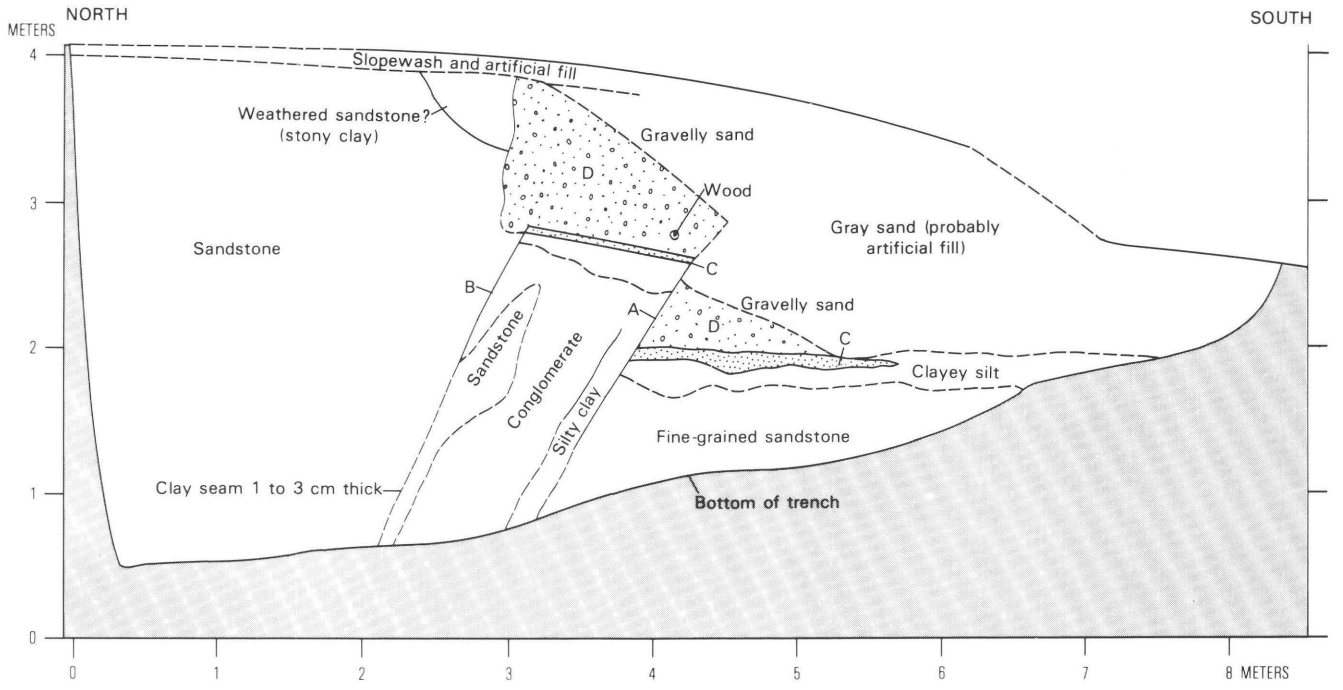

Figure 22. Geologic section of wall of trench excavated across fault that slipped during the 1971 San Fernando, Calif., earthquake (from Bonilla, 1973, fig. 10). 1971 rupture offset sand bed (C) and overlying wedge of gravelly sand (D) along fault A. Earlier episode of reverse slip greater than 1 m along fault B is inferred from absence of sand bed north of fault B. Wedge of gravelly sand is interpreted as colluvium and collapsed bedrock deposited against scarp formed by earlier episode of slip on fault B. Age of materials near base of wedge is known to be 100 to 300 years from radiocarbon dating of a buried piece of wood.

rates for earthquakes occurring on faults constituting major plate boundaries can be derived from long-term rates of relative plate motion.

There are various approaches to estimating the size of the maximum possible earthquake in a region, all of which have limitations and problems that lend uncertainty to the estimates. For recognized faults, the most common approach deduces maximum possible magnitude from the mapped fault length or some fraction (commonly one-half) of that length, using empirical relations between magnitude and length of faulting for various styles of faulting (for example, Slemmons, 1977; Bonilla and others, 1984). The use of fault area in place of fault length has also been advocated (Wyss, 1979; Singh and others, 1980). Empirical relations between dimensions of faulting and earthquake magnitude are founded both on field measurements of surface faulting and on seismologic and geodetic inferences concerning the extent of subsurface rupturing. In the absence of recognized faults, estimates of the maximum possible earthquake within a region are generally based on one or more of the following considerations: historical seismicity of the region, tectonic deformation of young geologic units within the region, geologic and tectonic relations of the region to the surrounding area, and analogs with regions having similar geologic and tectonic characteristics. By considering as many of the above factors as is possible, the most reliable estimate is sought.

Finally, the geologic record provides a framework for assessing the significance of apparent seismic quiescence in a region with a short recorded history. The historical absence of seismicity need not imply future quiescence unless some other evidence indicates the absence of tectonic deformation during Holocene or late Quaternary time. For example, historical quiescence in the vicinity of a fault that clearly exhibits repeated Holocene displacement is evidently a transient feature; significant earthquakes are likely to occur in the future, possibly even the near future.

Seismotectonic models

A seismotectonic model describes the earthquake-generation processes and structures within a given region and projects the spatial, temporal, and magnitude distribution of future earthquakes in that region. The accuracy or reliability of the model depends directly on the degree of knowledge concerning processes and structures, as gained from investigations of the type described previously. A seismotectonic model may be quite accurate, at least to the degree required for the evaluation of earthquake hazards pertinent to engineering design. For example, a fault zone may have well-documented historical and current seismicity; its spatial extent may be clearly defined; and the average rate of significant earthquakes may be estimable from historical seismicity and geologic evidence. For such a zone, the model may also specify additional characteristics, such as the typical dimensions and attitudes of fault breaks, and various source parameters of expected earthquakes, such as maximum magnitude or seismic moment, which is directly proportional to the product of the slipped area on the fault and the average displacement over the slipped area, (see supplementary

section below entitled "Intensity, Magnitude, and Seismic Moment").

Conversely, a seismotectonic model may be uncertain or tentative. The earthquake-source zone may be delineated by only a diffuse pattern of historical and recent earthquakes, with little documented evidence for their association with geologic features or with little knowledge of the causative tectonic forces. In addition, the available data may be insufficient to estimate the average recurrence rate of significant earthquakes or the magnitude of the largest possible earthquake. Nevertheless, such earthquakes must be accounted for in assessments of earthquake potential and associated effects, and the seismologist may have little choice but to draw an approximate boundary around the source zone and to assume that similar earthquakes will occur in the future, either randomly throughout the zone or at the estimated epicenters of the more significant historical events.

Seismotectonic models may be formulated in various ways, depending on the purpose of the hazard assessment in which they are to be used. Different levels of knowledge concerning geologic hazards are needed at different stages and by different parties in the development of offshore petroleum resources. In deciding whether to hold a lease sale, a governmental body may want a national or broad regional overview of the relative geologic hazards among various proposed lease areas. For selecting tracts to be offered in a lease sale and for bidding on tracts in the sale, more detailed knowledge is required to identify the potential hazards associated with individual tracts. Finally, for the siting and design of offshore production facilities and for the governmental regulation of operations, highly detailed knowledge of the specific hazards affecting a given site is needed.

The seismotectonic model prepared for a large region generally does not have the same degree of information and specificity needed for detailed application to a specific site or small area. For example, evaluation of the relative ground-shaking hazard for a continental shelf requires ground-motion estimates to be derived on a gross regional basis, so as to provide information applicable to typical sites throughout the entire shelf region. For such a broad-scale evaluation, not all potential earthquake sources that may affect any site throughout the region can be investigated in the same degree of detail that is required for assessing hazards to a critical facility at a specific site. Thus, for regional evaluations, seismotectonic models will be generalized, as a rule.

In the following subsections, we illustrate these concepts with discussion of seismotectonic models for parts of the active west and passive east margins of North America.

Active western margin

The seismicity of western Canada has recently been modeled to derive new probabilistic-ground-motion maps of Canada (Basham and others, 1982). For this application, broad earthquake source zones were defined. The Queen Charlotte transform fault and the system of spreading-ridge and transform-fault segments constituting the boundary between the Pacific plate and the Juan de Fuca and Explorer plates are selected for illustration (fig. 19A).

The Queen Charlotte fault zone defines the continental boundary along the west coast of the Queen Charlotte Islands. This area has virtually no continental shelf; instead, an almost continuous, but irregular, slope extends from the 1-km-high mountains on the islands to the 3-km-deep sea floor. A 25-km-wide terrace, bounded by parallel fault scarps, interrupts the continental slope at a depth of 2 km and represents the fault zone. This zone is the probable origin of most historical earthquakes along the west coast of the Queen Charlotte Islands; low-magnitude events, occurring beneath the continental edge of the terrace, suggest that the landward fault is currently the main active element of the fault zone (Hyndman and Ellis, 1981). The Queen Charlotte fault is modeled as a long narrow source zone (QCF), the south end of which is shown in figure 19A.

The JFE source zone (fig. 19A) encloses the main cluster of historical earthquakes associated with the interaction of the Juan de Fuca and Explorer plates with the Pacific plate. Although most of these earthquakes probably occurred on the spreading ridges and fracture zones shown to be active by the OBS experiments discussed in the subsection above entitled "Ocean-Bottom Seismographs" (Hyndman and Rogers, 1981), gross characterization of this zone is adequate for the purpose of constructing a national map depicting probabilistic ground motion, which will be used primarily for earthquake-resistant design of common structures, principally onshore.

The rates of earthquakes in the QCF and JFE source zones are given by cumulative magnitude-recurrence curves (fig. 23). The best-fit line was computed by using a maximum-likelihood method (Weichert, 1980) that has been developed to account for estimates of earthquake rates for unequal observation periods and for various magnitudes. Upper limits to possible magnitudes are assumed for the two zones; this assumption leads to the downward curvature to zero rate at large magnitudes.

A maximum magnitude of 8.5 is assumed for the QCF source zone, which would be generated by rupture of most of the length of the fault zone. The largest known earthquake was of M=8.1, which occurred in 1949 with an epicenter west of the Queen Charlotte Islands. In the JFE source zone, the seismicity data alone may provide some indication of the maximum magnitude. Although the estimated rate for $M \geq 6.5$ earthquakes is about one every 10 years, in fact, there have been no earthquakes of $M>6.5$ in the estimated period of complete reporting starting in 1917. The faults in the JFE source zone have a maximum length of about 100 km and could have a vertical extent of about 10 km; thus, the maximum fault area is about 1,000 km^2. Relations between magnitude and fault area (Kanamori and Anderson, 1975; Singh and others, 1980) suggest that the maximum possible earthquake is of $M \sim 7.0$, consistent with the historical data.

For estimating the probability of ground shaking on a regional scale (see next section), earthquakes within a seismic-source zone are typically assumed to occur randomly over time unless the historical or geologic record indicates nonrandom occurrence. A

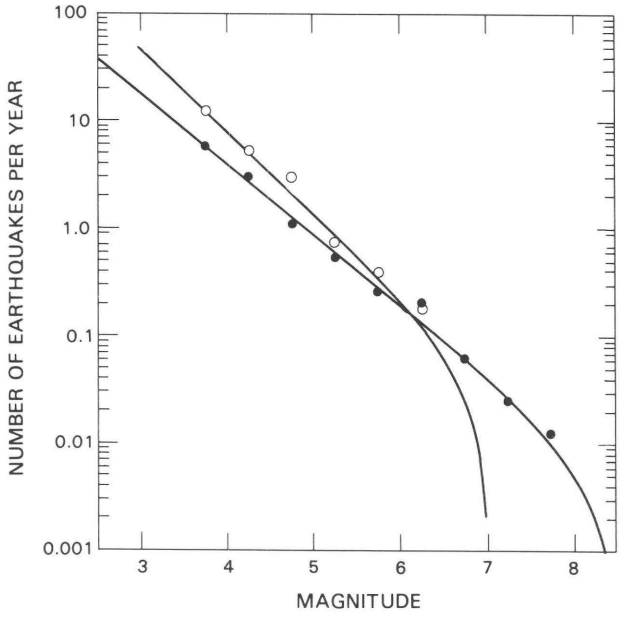

Figure 23. Cumulative magnitude-recurrence relations for the Queen Charlotte fault (QCF, dots) and Juan de Fuca-Explorer (JFE, circles) earthquake-source zones of figure 19A (from Basham and others, 1982, figs. 15, 17). Data points are for observed number of earthquakes per year larger than a given magnitude. Curves are fitted to data by assuming upper-bound magnitudes of 8.5 and 7.0, respectively.

nonrandom component can be incorporated into the seismotectonic model for a seismic gap, that is, a region in which repeated large earthquakes have occurred in the past but not recently, and thus in which a large shock may be expected in the near future. An example is the Gulf of Alaska region (fig. 24).

Sykes (1971) identified a seismic gap between the aftershock zones of the 1964 Prince William Sound and the 1958 Fairweather fault earthquakes. No major earthquake has occurred in this gap since two M=8.1 earthquakes ruptured the gap in 1899 (McCann and others, 1980). Lahr and others (1980) demonstrated that this gap was only partly filled by the 1979 St. Elias earthquake (M=7.6). Lahr and Plafker (1980) concluded that the gap-filling rupture(s) in a future major earthquake(s) would most likely occur on the main north-dipping thrust faults between Kayak Island and Icy Bay. If the Pacific and North American plates have been converging at the rate of 5 cm/yr since the 1899 sequence and if movement between these two plates has not been accommodated in plastic deformation, enough elastic strain has already accumulated to cause a potential slip of 4 m. If this amount of slip occurred in a single earthquake, it would generate an event as large as M=8 that would likely fill the remainder of the gap.

Thus, a seismotectonic model of the Gulf of Alaska region must account for the fact that the next great earthquake is more likely to occur in this gap than at any other point on the border of the northern gulf. This possibility, however, should not be considered to the exclusion of the fact that significant earthquakes will continue to occur on other major tectonic features bordering the gulf.

Passive eastern margin

The continental margin south of Newfoundland provides a good example of the difficulties in constructing reliable seismotectonic models to describe future earthquake occurrence along the passive eastern and Arctic margins of North America (Basham and Adams, 1982).

The seismicity of Newfoundland and the adjacent shelf (fig. 25) is probably incomplete at the M=5 level before the mid-1950's, and at the M=4 level before 1965. With the present seismograph network, few earthquakes of $M<4$ can be located in the offshore areas of figure 25.

The most significant earthquake in this region was the 1919 Grand Banks M=6.5 event near the edge of the continental slope at the mouth of the Laurentian Channel (see also fig. 15). This earthquake had aftershocks as large as M=6.0. $M\sim5$ earthquakes occurred also at the mouth of the Laurentian Channel in 1951, 1954 (two events), and 1975, and northeast of Newfoundland in 1922 (the location of this last event is uncertain by at least 100 km). The M=4 earthquakes, and the few smaller events that have been located, are scattered throughout the shelf area.

Although the epicenters at the mouth of the Laurentian Channel (fig. 25) are uncertain by tens of kilometers, the observed scatter is not simply the result of random errors in locating shocks, originating at a common point, on the basis of arrival times of seismic waves recorded at distant seismographs. Instead, seismologic evidence indicates that these events are occurring within an extended source zone, which for purposes of probabilistic calculations of ground motion (see subsection below entitled "Areal Evaluation") is modeled as the quadrilateral shown in figure 25. Although this source-zone model is currently favored, several key questions still remain to be answered. Can further seismologic studies of these earthquakes and other geologic and geophysical studies of the region lead to an understanding of the tectonic processes and active faults that generated the 1929 earthquake? Do similar geologic features exist in other areas of the shelf that could cause similar earthquakes? Do small earthquakes scattered throughout the shelf provide evidence for the existence of these features? Is there evidence in the unconsolidated sediment that could reveal the recurrence period of such events in Holocene time? A speculative source-zone model that assumes large earthquakes occur uniformly along the eastern Canadian margin over long periods of time has been studied by Basham and others (1983).

Gravity, aeromagnetic, and seismic-reflection data have been used to delimit the faulting mapped in figure 25. King and MacLean (1970) and King (1980) associated the 1929 and other earthquakes with the fault system that intersects the Laurentian Channel and extends eastward, possibly linking with the Newfoundland Fracture Zone. Various studies (for example, Sykes, 1978; Stewart and Helmberger, 1981)

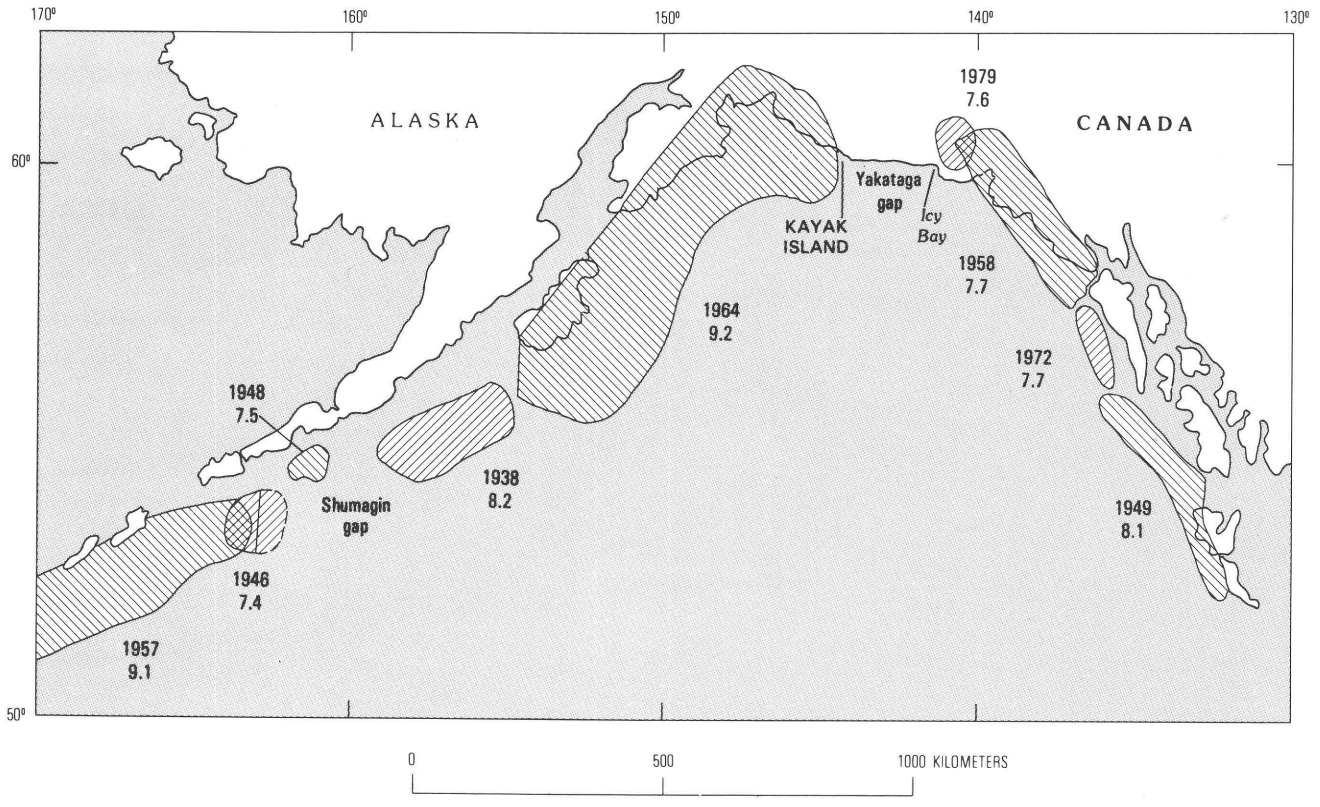

Figure 24. Aftershock zones of $\underline{M}$>7.3 earthquakes since 1938 in the Gulf of Alaska, showing the Yakataga and Shumagin seismic gaps (modified from Sykes, 1971, fig. 4, and Lahr and others, 1980, fig. 1). 1979 St. Elias earthquake sequence, which occurred on east edge of the Yakataga gap, only partly filled gap between 1958 and 1964 rupture zones.

have suggested that the seismicity of the Atlantic continental margin is related to such linear features as fracture zones and seamount chains which are nearly normal to the margin. Stein and others (1979) suggested that the stresses due to glacial unloading are sufficient to reactivate old faults parallel to the margin. The available seismic profiling has not shown clear evidence of recent offsets in the sea-floor faulting within this region; high-resolution seismic profiling of the uppermost 20 m of sediment would be required to investigate youthful faulting at these sites.

The recurrence rate of 1929-size earthquakes in the Laurentian Channel source zone (fig. 25) is problematic. On the one hand, the historical frequency of shocks suggests the occurrence of an earthquake as large as that in 1929 about once in 300 years (Basham and others, 1982, 1983). On the other hand, a recurrence interval of at least 100,000 years has been inferred from marine geologic investigations (Piper and Normark, 1982). This inference is based on the assumption that an earlier shock of comparable magnitude would have caused widespread sea-floor failure, similar to that which occurred in 1929 (fig. 15). High-resolution seismic-reflection profiling and bottom coring reveal no such disturbance in sediment at least 100,000 years old.

Similar problems exist in constructing accurate seismotectonic models for elsewhere along the passive eastern and Arctic margins of North America. These problems may be most tractable in regions that have undergone a large historical earthquake, such as Charleston, S.C. (1886, estimated $\underline{M}$=6.9-7.3), Baffin Bay (1933, $\underline{M}$=6.7), and the Beaufort Sea (1920, $\underline{M}$=6.2); however, only a single large shock has occurred in each of these regions. In contrast to the western margin, where numerous large historical events delineate active tectonic features, a single large earthquake in each of these eastern regions represents a very limited data base on which to found a seismotectonic model. Although detailed geologic and geophysical investigations may possibly reveal the geologic features responsible for such individual earthquakes, similar seismogenic features elsewhere along the margin may go unnoticed because they have not generated a large earthquake during historical time and thus have not become a candidate for detailed investigations. The origin of the 1886 Charleston earthquake has been studied intensively (Gohn, 1983; Hays, 1983, but neither the tectonic structure on which this shock occurred nor the implication of this shock for similar events elsewhere along the Atlantic margin has yet been clearly resolved.

Induced seismicity

An additional consideration in assessing earthquake potential is the possibility that the activities

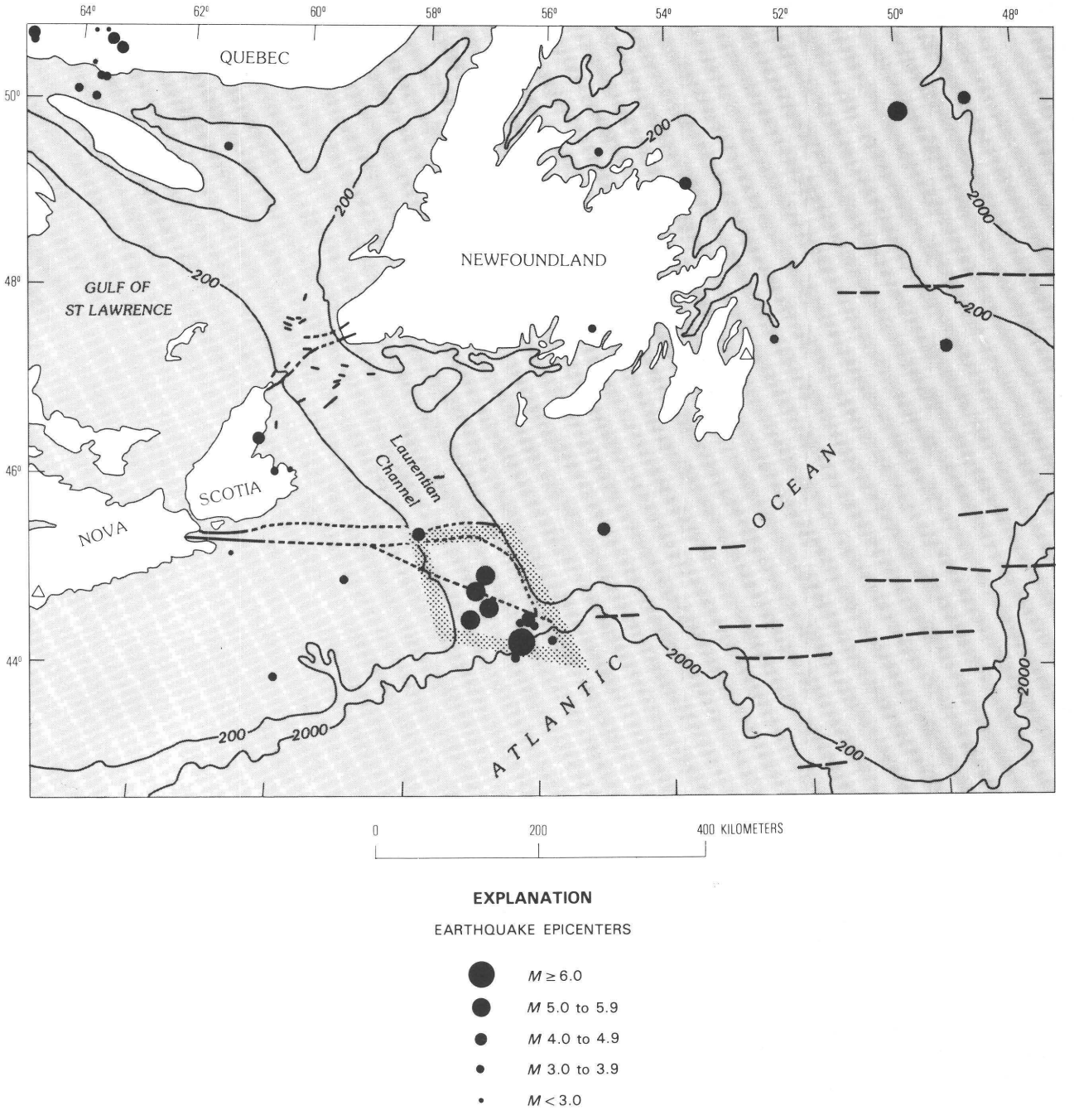

Figure 25. Continental Shelf south of Newfoundland, showing earthquake epicenters from 1929 to 1980, 200- and 2,000-m isobaths, seismograph stations (triangles), and offshore basement faults (dashed where uncertain) (from Basham and Adams, 1982, fig. 3). Short-dashed fault traces west of long 55.5° W. were observed on seismic-reflection profiles (King and MacLean, 1970); long-dashed traces east of long 55.5° W. were inferred from magnetic and gravity studies (Lefort and Haworth, 1978). Quadrilateral at mouth of the Laurentian Channel is earthquake-source zone used in regional probabilistic ground-motion mapping.

associated with petroleum recovery may significantly alter the natural rate of earthquake activity in the vicinity of a critical offshore facility. A common technique for stimulating secondary recovery of oil involves injection of fluids into the reservoir under high pressure. Evidence from various geologic and tectonic settings indicates that if the injection wells bottom in the proximity of existing faults, significant seismic activity can be triggered, even if earthquakes were previously rare or even unknown.

A graphic example of seismicity induced by fluid injection was the earthquake sequence near Denver,

Colo., during the 1960's (Healy and others, 1968; Hsieh and Bredehoeft, 1981). Injection of waste fluids into a 3.7-km deep well bottoming in fractured Precambrian crystalline rocks triggered earthquakes as large as $\underline{M}$=4.8. This sequence of earthquakes appears to have no parallels in the local seismic history. The earthquake hypocenters migrated away from the well over time and extended horizontally to a distance of about 7 km by 1967, 5 years after injection started. Focal mechanisms indicate right-lateral slip within a buried fault zone parallel to the trend of the earthquake hypocenters. The mechanism offered to explain the triggering is the reduction of frictional resistance on preexisting faults that allows seismic slip to occur in response to ambient tectonic stresses. The injected fluid partially offsets the normal stress locking the fault, by an amount equal to the pressure of the fluid, and thus lowers the frictional resistance to sliding.

After the Denver study, a classic experiment to examine more closely the role of fluid pressure in the triggering of earthquakes was undertaken in the Rangely oil field in Colorado, where waterflooding operations in the reservoir were triggering earthquakes (Raleigh and others, 1976). By the injection and backflow of fluid in four 2-km-deep injection wells straddling a subsurface fault in the reservoir rock, pore pressures in the vicinity of the fault were controlled, and the earthquake activity sequentially was turned off, on, and off again. During the first year of this experiment, fluid was injected, and earthquakes occurring within 1 km of the bottom of wells were recorded at the average rate of 28 per month (fig. 26). In November 1970, injection was stopped, and withdrawal of fluid caused the earthquake activity to decrease to about one event per month. Injection was resumed in May 1971; however, the probabilistic bottom-hole pressure did not substantially exceed the critical pressure predicted for earthquake triggering until November 1972, when the rate increased to about 20 events per month. In May 1973, injection terminated, the wells were backflowed, and earthquakes within 1 km of the wells abruptly terminated. The largest earthquakes recorded during the experiment were of $\underline{M} \sim 3.0$. The earthquakes occurred on a minor fault, not expressed in the surface geology—one that would have gone undetected were it not within an oil field. Focal-mechanism solutions for the earthquakes indicate strike slip.

Other places where earthquake activity may have been related to hydrocarbon production include Alberta (Milne, 1970; Wetmiller, 1985) and Oklahoma and Texas (Rogers and Malkiel, 1979). Induced seismicity has also been linked to high-pressure fluid injection in the vicinity of a fault in association with the hydraulic mining of salt in western New York (Fletcher and Sykes, 1977). Thus, evidence to date documents that significant earthquakes, at least approaching $\underline{M}$=5, can be triggered on existing faults by fluid injection. There is no reason to believe that an earthquake of $\underline{M}$>5 could not be triggered inadvertently on a sufficiently large fault favorably oriented to the regional tectonic stress field.

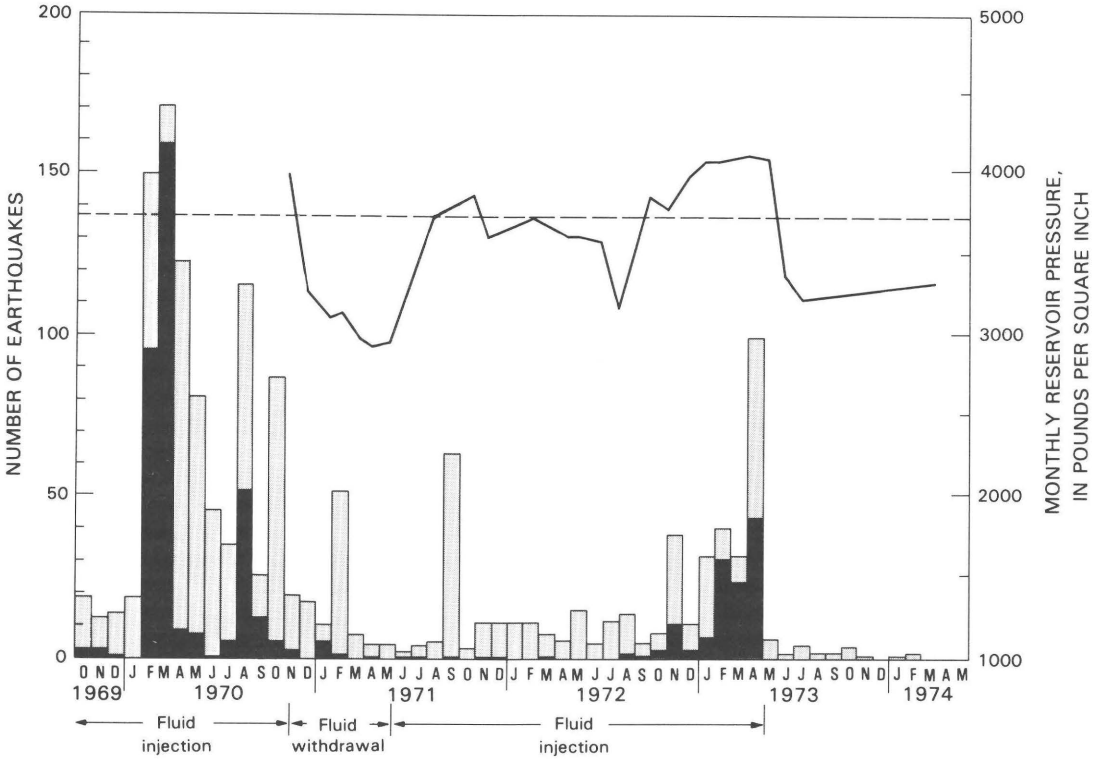

Figure 26. Monthly number of earthquakes (bars) and monthly reservoir pressure (curve) at the Rangely, Colo., oil field during earthquake-control experiment (from Raleigh and others, 1976, fig. 7). Solid bars indicate earthquake activity within 1 km of bottom of experimental wells; open bars show number of shocks occurring elsewhere in the field. Dashed line shows predicted critical fluid pressure required to trigger earthquakes.

EVALUATION AND MITIGATION OF EARTHQUAKE HAZARDS

The evaluation of earthquake hazards involves the prediction of effects from earthquakes whose potential for occurrence is defined in a seismotectonic model. Should these estimated effects appear to be potentially hazardous, mitigation measures can be invoked. Effective mitigation strategies include avoidance, accommodation, and emergency planning. First, structures can be sited to avoid or limit exposure to hazardous earthquake phenomena. Second, structures can be designed and built to accommodate the estimated effects of earthquakes. Third, response planning for an earthquake emergency can minimize the adverse consequences of failure in a structure or system and can promote rapid recovery.

Which of these three strategies would be most effective in a particular situation depends on the specific type of hazard. For example, avoidance may be a feasible and effective measure for mitigating the hazards associated with surface faulting or seismically induced sea-floor failures, whereas accommodation would likely be chosen as the preferred strategy for minimizing potential damage from strong shaking. Emergency response planning is an effective mitigation measure when advance warning of a potential hazard can be provided, as is done now for tsunamis. With advance warning, people can vacate dangerous localities and structures, hazardous operations can be shut down, and facilities can be protected. Were reliable methods of predicting earthquakes available today, the importance of emergency planning as a mitigation measure would be greatly increased over what it is now.

As discussed in the preceding sections, earthquake potential rarely can be assessed with a high degree of certainty. Likewise, earthquake effects are rarely predictable with the level of precision and certainty that engineers and planners desire. Accordingly, the mitigation of earthquake hazards requires judgments: scientific judgments in estimating effects, engineering judgments in adopting mitigative measures, and socioeconomic judgments in deciding on acceptable risk.

Surface faulting

There are two effective strategies for mitigating potential hazards from surface faulting. First, structures of limited dimension can be sited selectively to avoid active fault zones where surface rupture is likely. Second, in circumstances where a structure must cross a zone of potential surface rupture, either because of the extended size of the structure or because of some critical siting constraint, the structure can be designed to accommodate the effects of surface faulting. For example, where it crosses an active fault, a pipeline can be oriented to minimize the strains induced by fault movement, and the mode of pipeline burial or anchoring in the vicinity of the fault can be chosen to distribute the strains induced by fault movement over a length of the pipeline greater than the width of the shear zone in the ground (Kennedy and others, 1977). In addition, automatic shutoff valves can be installed to stop the flow and limit discharge from a ruptured pipeline. The strategy of avoidance requires the ability to identify active surface faults. The principles and methods for identifying active faults were discussed in the preceding subsection entitled "Geologic Record." The strategy of accommodation requires not only that active surface faults be identified but also that the style of future faulting be predicted.

Surface faulting is a complex phenomenon, important aspects of which are poorly documented and physically not well understood. Numerous observations of the patterns and amounts of surface fault displacements have been made after historical earthquakes. These observations provide an empirical basis for estimating the amount and type of displacements in future earthquakes. However, few well-documented eyewitness accounts and no instrumental records of faulting have been obtained during an earthquake that reveal, for example, when surface ruptures develop in relation to the time of strong shaking or how the displacement at one point on a fault increases over time. Two parties witnessed normal faulting on a secondary fault during the 1983 Borah Peak, Idaho, M=6.9 earthquake. Both parties reported the scarp formed within an interval of a few seconds and after the onset of shaking; however, one stated the formation of the scarp coincided with the onset of the violent phase of shaking (Pelton, 1984), while the other claimed it followed (Wallace, 1984). Bonilla (1970) and Slemmons (1977) summarized much of what is currently known about the phenomenon of surface faulting and provided empirical relations between earthquake magnitude, type of fault, and various parameters of surface faulting, such as the length and width of surface rupture and maximum fault displacement.

Not all the surface displacement on seismically active faults accompanies earthquakes. Some earthquake-generating faults exhibit aseismic slip or creep behavior, in which surface slip accumulates slowly, commonly not in obvious association with earthquakes (fig. 27). Fault creep may occur in discrete episodes, characterized by as much as 1 to 2 cm of slip within an interval of hours or days, or as nearly uniform motion at rates as high as 2 to 3 cm/yr (Burford and others, 1978). The most notable example of creep behavior is

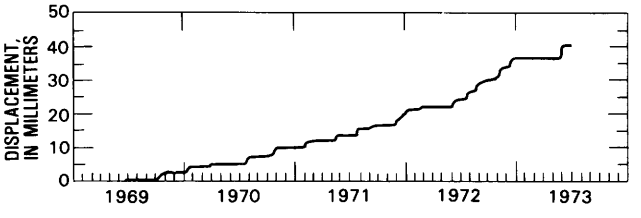

Figure 27. Fault-creep displacement measured on central section of the San Andreas fault 14 km southeast of San Juan Bautista, central California (from Nason, 1973, fig. 5). Most creep occurs in discrete episodes, typically with 1 to 3 mm of slip. Although some episodes correlate with the occurrence of nearby earthquakes, many do not.

on the San Andreas fault in central California, where creep accounts for as much as 3.2 cm/yr of right-lateral slip and locally accommodates all the motion between the crustal blocks on either side of the fault (Burford and Harsh, 1980). Tectonic creep has also been documented on several other faults, including normal and reverse faults.

Most measurements of the surface fault displacements associated with large shallow-focus earthquakes have been made hours, days, or even weeks after the earthquake. In interpreting such observations, it is commonly assumed that all the measured displacement occurred at the time of the earthquake. This assumption has been proved appropriate in some events, most conclusively for the 1971 San Fernando, Calif., earthquake (Savage and others, 1975), but incorrect in several other events in which repetitive measurements conducted over several weeks or months, starting within a few days after the earthquake, have documented continuing fault slip. Such continuing movement is referred to as afterslip. Afterslip may occur in the form of both aseismic slip and coseismic slip associated with the aftershocks that normally follow large shallow-focus earthquakes. A spectacular example of afterslip was associated with the 1966 Parkfield earthquake on the San Andreas fault in central California. In the year after the $\underline{M}$=6.2 main shock, at least 20 cm of afterslip occurred at a site near the midpoint of the rupture, far exceeding the surface displacement occurring at the time of the main shock (Smith and Wyss, 1968). The rate of displacement decreased approximately logarithmically over time from about 10 mm/d a few days after the earthquake to about 5 mm/mo at the end of a year. Substantial afterslip has also been measured after several other earthquakes (for example, fig. 28); many, though not all, of these have been associated with strike-slip faulting. There is also evidence, though much more limited, that surface slip may occasionally precede earthquakes. It is doubtful, however, that foreslip either occurs so frequently or contributes so much to the total displacement as does afterslip.

Until the presence or absence of creep, foreslip, and afterslip has been documented in many more events incorporating a wide range of fault type, tectonic and geologic environment, and earthquake size, the contributions of these modes of slip relative to the coseismic displacement accompanying a large earthquake cannot be confidently predicted.

The pattern of surface ruptures accompanying a large earthquake is typically complex. This pattern is generally simplest for earthquakes on steeply dipping strike-slip faults and most complex for gently dipping reverse faults. Even for strike-slip faults, however, the complexities can be numerous (fig. 29). For example, in the $\underline{M}$=6.5 Imperial Valley, Calif., earthquake of 1979, displacement on the 30-km-long main fault was predominantly strike slip, with a maximum strike-slip component of 55 to 60 cm measured during the first day after the earthquake and a maximum dip-slip component of about 10 cm (Sharp and others, 1982). Significant afterslip was observed over most of the zone of surface rupture, and by 160 days after the main shock the maximum amount of

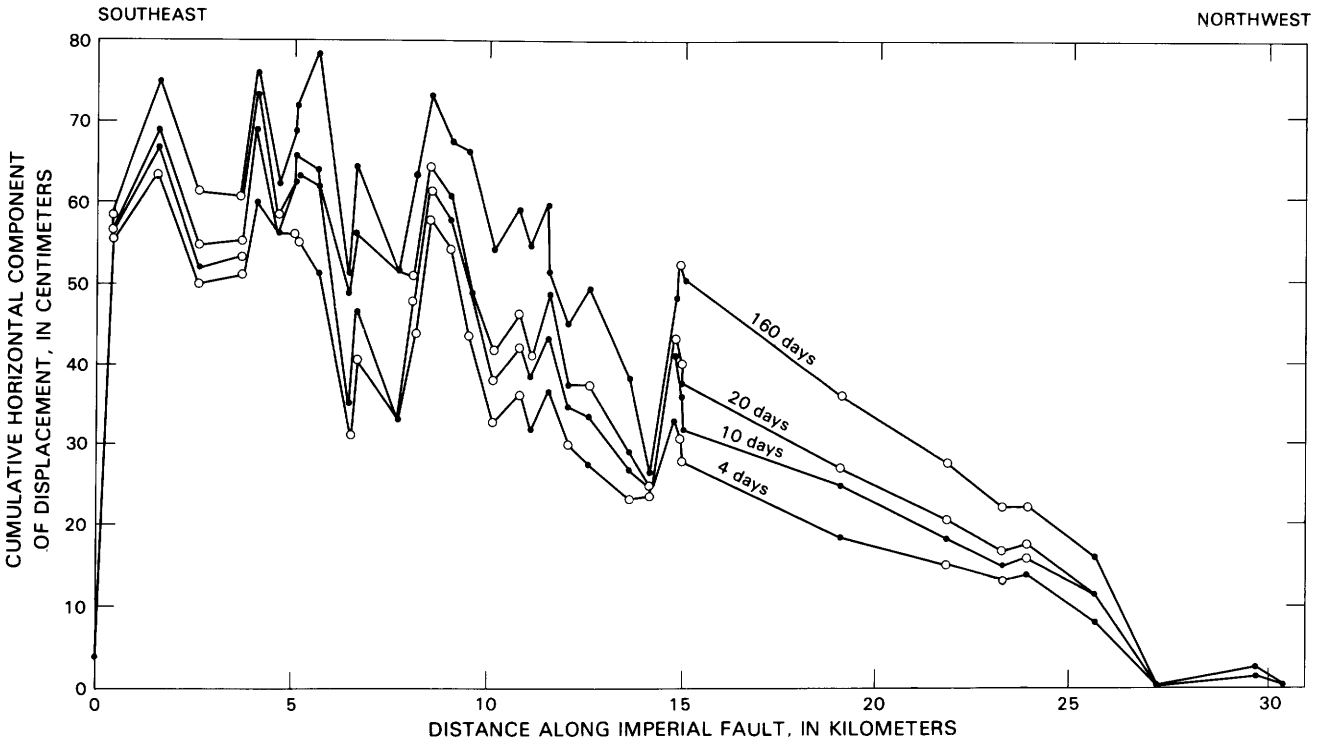

Figure 28. Horizontal component of fault displacement as a function of position along the Imperial fault, determined for times of 4, 10, 20, and 160 days after the 1979 Imperial Valley earthquake (from Sharp and others, 1982, fig. 101). Dots, measured values; circles, interpolated or extrapolated values.

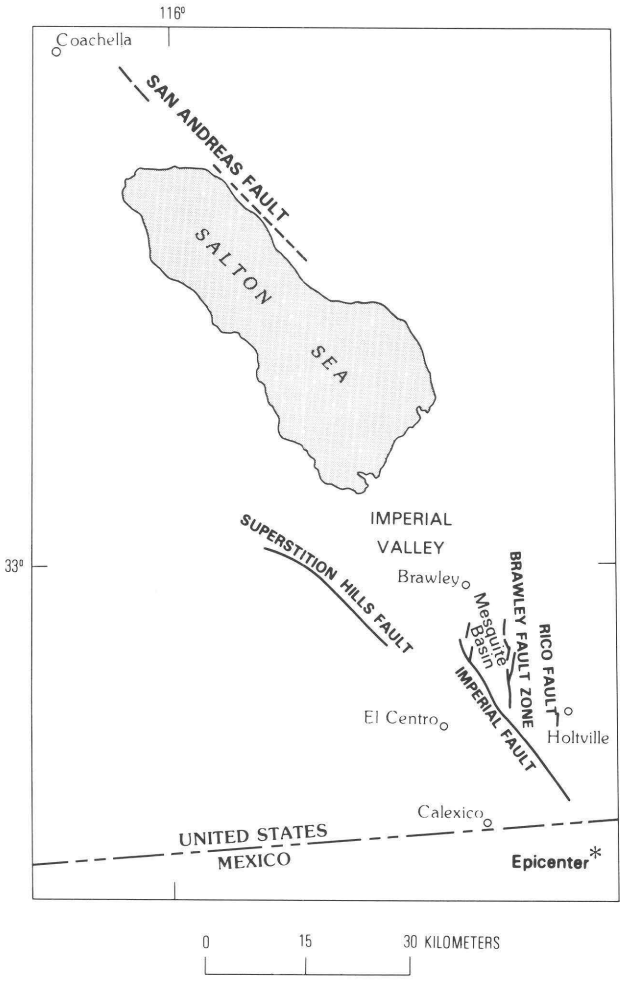

Figure 29. Imperial Valley area, southern California, showing surface fault ruptures accompanying the 1979 Imperial Valley earthquake. Primary displacement occurred on the Imperial fault, and subsidiary movement on branch faults, most notably those composing the Brawley fault zone. Minor displacements were triggered on the Superstition Hills and San Andreas faults, which lie well outside the zone of seismic-energy release (from Sharp and others, 1982, fig. 84).

strike slip had grown to nearly 80 cm (fig. 28). On a 13-km-long subsidiary fault branching off the main trace, the type of slip was different, predominantly normal rather than strike slip. The maximum displacement on a single break along this subsidiary fault was 12 cm of oblique slip. Small surface displacements were also documented on distant faults, not directly connected to the segment of the Imperial fault on which the primary rupture occurred. As much as 1 cm of strike slip was measured on the San Andreas fault (Sieh, 1982) and 2.2 cm on the Superstition Hills fault (Fuis, 1982) at distances of about 60 and 25 km, respectively, from the north end of the Imperial fault. These displacements on the San Andreas and Superstition Hills faults appeared to be aseismic slip triggered by the earthquake on the Imperial fault.

Bonilla (1970) summarized measurements of the surface displacement on branch and secondary faults as a function of distance from the main fault zone, and measurements of the width of the main fault zone and the maximum distance to branch and secondary faults from the main fault zone as a function of earthquake magnitude.

Although the observational evidence is limited, important regularities seem to exist in the patterns of faulting between successive earthquakes on the same fault system. For example, surface offsets occur on preexisting traces of faulting with few exceptions, although in many places preexisting traces have been recognized only after a new episode of faulting. In addition, the sense of dip-slip and strike-slip components at individual points along a fault generally is the same from one large earthquake to another, even if the rupture zones for the two shocks only partly coincide. The ratio between dip-slip and strike-slip components, however, appears to vary more (Sharp, 1982). Thus, despite the complexities in the spatial patterns of faulting, important characteristics of faulting seem to be predictable on the basis of past fault history.

Empirical correlations of maximum surface fault displacement with earthquake magnitude provide a basis for predicting the maximum surface displacements for earthquakes of a postulated magnitude. Relations between maximum surface displacement and earthquake magnitude for strike-slip, reverse-slip, and normal-slip faults show that maximum displacement increases with magnitude (fig. 30). The considerable scatter in the data, however, indicates that considerable uncertainty is attached to such estimates of maximum displacement.

In selecting a design value of fault displacement for a structure that must cross an active fault, we are generally interested in knowing the most probable surface fault displacement for a postulated earthquake in addition to the maximum displacement. The amount of fault displacement may vary considerably as a function of position along the fault trace. The maximum displacement may occur near the center of the rupture zone, near one of the ends where the displacement decreases to zero (fig. 28), or at some other intermediate point. Points where the initial slip is low may also be sites of relatively high rates of afterslip, as was observed after the 1979 Imperial Valley earthquake (fig. 28).

Subsidence and uplift

Dip-slip faulting in a large shallow-focus earthquake causes uplift and subsidence over a broad region with dimensions approximating those of the buried fault rupture. In spite of its extent, such deformation is of serious consequence to relatively few facilities, namely, those offshore and coastal facilities whose function or safety would be compromised by a permanent change in elevation of the sea floor or coastline referenced to sea level. The most effective strategy for mitigating these potential adverse consequences is accommodation of the effects of uplift and subsidence in the design of facilities. Rarely is it

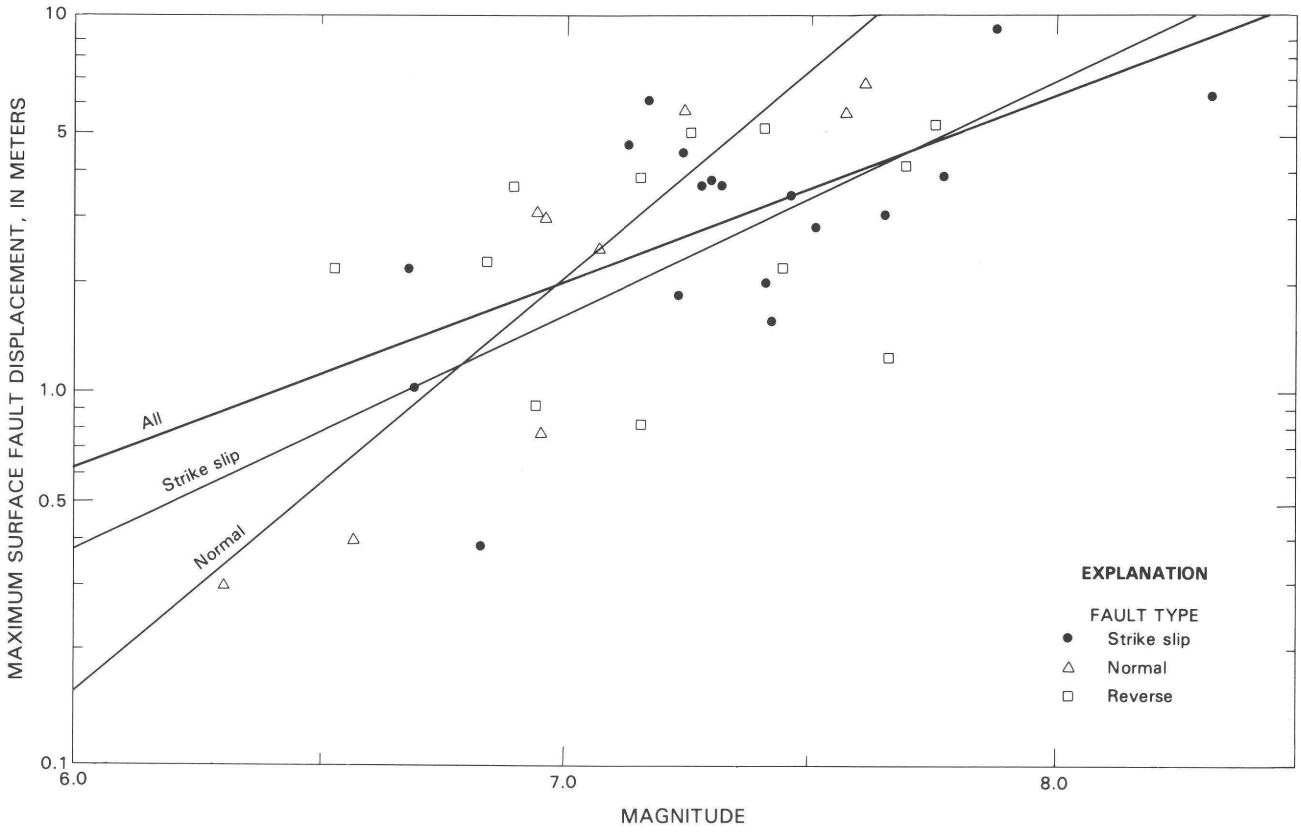

Figure 30. Maximum surface fault displacement as a function of surface-wave magnitude for strike-slip, reverse-slip, and normal-slip faults (modified from Bonilla and others, 1984). Curves are weighted least-squares regressions of logarithm of displacement upon magnitude. No curve is shown for reverse-fault data alone because of the large scatter in that data set.

possible to avoid this problem by selective siting, because, unlike surface faulting, the phenomenon is not localized. Moreover, the location of an offshore or coastal facility generally is severely constrained by geographic, geologic, and hydrographic requirements, and so suitable alternative sites that would be free from uplift or subsidence commonly are not available.

Broad-scale vertical deformation is likely to be a significant design consideration only for shallow-focus earthquakes of $M \gtrsim 7.0$ with a major component of dip-slip faulting. Because coastal and marine facilities must be designed to accommodate tides and storm waves, a permanent change in elevation of the shoreline or in depth of water offshore of less than a meter is probably of little consequence in most places. To a first approximation, the maximum uplift or subsidence may approach half the amount of dip-slip displacement on the buried fault. From observations of surface faulting and inferences from seismologic and geodetic investigations, 2 m is a representative value for fault displacement for an $M=7$ reverse- or normal-fault earthquake (fig. 30). The potential consequences of vertical deformation increase markedly with earthquake size because both the amount of uplift and subsidence and the size of the affected area increase with earthquake magnitude.

The seismotectonic model for a given region incorporates judgments on the size, focal depth, and sense of faulting of future earthquakes and thus provides a preliminary basis for determining whether vertical deformation is a potentially significant earthquake problem. In coastal regions, more direct evidence of the potential for vertical deformation may be preserved in the late Quaternary history of ancient shorelines. For example, along the Santa Barbara Channel in southern California, a series of emergent marine terraces indicate average tectonic-uplift rates as high as 10 mm/yr for the past few tens of thousands of years (Lajoie and others, 1982). This area is characterized by active folds and reverse faults and abundant seismicity. Since 1912, three $M=6$ shocks have occurred offshore in the channel, and larger reverse-slip earthquakes are thought to be possible in the future (Lee and others, 1979). The uplift rates along the Santa Barbara Channel are an order of magnitude greater than those calculated from displacements of dated shoreline features farther south along the California coast between San Diego and Los Angeles, a region of comparable seismicity dominated by strike-slip faulting. Although there have been no large historical earthquakes accompanied by significant coastal uplift along the Santa Barbara Channel, it may be prudent to interpret much of the observed deformation as the cumulative effect of many episodes of uplift associated with shocks of $M \geq 7.0$.

Elsewhere along convergent plate boundaries, such as in southern Alaska and along the Aleutian Islands, where vertical deformation is more rapid and

thus more clearly expressed in the geologic record, the late Quaternary history of deformed shorelines can be especially useful in assessing uplift potential (for example, Plafker, 1969; Plafker and Rubin, 1978).

The pattern of uplift and subsidence accompanying a postulated earthquake is predictable from elastic-dislocation theory, assuming the geometry of the causative fault and the distribution of slip on the fault (Savage and Hastie, 1966). The accuracy of this prediction is limited by the validity of assumptions about the fault and the distribution of slip. Experience with modeling the deformation in historical earthquakes (Savage and Hastie, 1966; Hastie and Savage, 1970; Jungels and Frazier, 1973) indicates that gross patterns of uplift and subsidence are satisfactorily predictable. Experience also suggests, however, that significant detailed features in the deformation associated with future earthquakes may not be predictable because of ignorance concerning the complexities in subsurface fault geometries and the distribution of slip on primary and subsidiary faults. The widespread occurrence of thick layers of soft sediment beneath the sea floor further complicates these predictions in the offshore environment.

Seismic shaking

Seismic shaking affects a large area around the earthquake source. Because of its pervasiveness, this hazard typically cannot be avoided or significantly reduced by shifting the site for a facility by a few kilometers. Although the location of offshore facilities seldom can be governed by considerations of seismic shaking, such considerations may preclude certain structural configurations in particular areas and may guide the selection of pipeline routes (Patwardhan, 1978).

The primary strategy for mitigating shaking hazard is accommodation by designing and constructing facilities to withstand earthquake shaking with limited damage. Relative to other mitigation strategies, the practice of earthquake-resistant design and construction is quite advanced. Years of experience with structures on land are relevant to marine structures founded on the sea floor. Sophisticated modeling and analysis techniques have been developed and applied in the earthquake-resistant design of costly critical onshore structures, such as high-rise buildings, bridges, pipelines (Ariman and Muleski, 1981), and nuclear powerplants. With some modifications, these techniques are also applicable to the design of sea-floor-supported offshore platforms (Delflache and others, 1977; Nair, 1978; Watt and others, 1978; Bea and others, 1979) and to the associated piping, equipment, and appurtenances essential to safety and operations (Kost and Sharpe, 1977). McGavin (1981) addressed the problem of designing essential building equipment to remain operational after a major earthquake; though directed toward buildings, much of his discussion is also relevant to the aseismic design of essential equipment on an offshore platform.

For many facilities, the consequences of damage or failure can be limited if safety procedures are implemented promptly when a large earthquake strikes. Earthquake-alarm systems can be designed to initiate emergency procedures in the advent of strong shaking. For example, an alarm system has been installed on the Maui A Platform in the Tasman Sea off New Zealand (Tyler and Beck, 1983). This system indicates when horizontal motions of the platform reach half the seismic-design levels. To avoid false alarms related to the noisy vibrational environment on the platform, motion is monitored only in the frequency band of the six lowest vibrational modes of the platform, and ground motion is simultaneously monitored at an adjacent onshore site 37 km away, so that the seismic origin of an alarm signal can be confirmed.

In regard to floating offshore structures, seismic shaking has received little attention, either as a potential hazard or as a design consideration (Hove and others, 1982).

The seismic waves from an earthquake can be approximately grouped in two classes: body waves, which radiate in all directions from the earthquake source; and surface waves, which propagate along the boundary separating two mediums of contrasting seismic velocity, such as the sea floor or the Earth's surface. The energy in body waves propagates in all directions, whereas that in surface waves is trapped within a boundary layer. Thus, body waves attenuate more rapidly with distance than do surface waves, and at large distances surface waves may be the dominant type of seismic wave.

Surface waves generally have much longer periods than do body waves and travel at lower velocities. The periods of surface waves are characteristically longer than 1 s, in the range containing the fundamental natural periods of common bottom-supported offshore platforms (Bea and others, 1979). In comparison, the dominant periods of body waves are characteristically less than 1 s, in the range within which the resonant periods of ships and floating platforms typically lie (Hove and others, 1982). A further difference between these two wave types is the dispersion of surface waves. Because seismic velocities vary with depth within the Earth, surface waves of different period, or wavelength, propagate at different speeds and thus cause an extended wave train to be observed at distances from the source. In contrast, body waves are nondispersive and appear as short relatively high-frequency pulses, apart from the complication of refractions and reflections and the extended source dimensions of large earthquakes. Thus, strong ground shaking initiates with high-frequency body waves, followed by an extended train of low-frequency surface waves.

The two types of body waves are (1) compressional (P) waves, for which the motions of particles in the medium parallel the direction of propagation, as with sound waves in air, and (2) shear (S) waves, which travel more slowly than P waves and for which the motions are perpendicular to the direction of propagation, as with waves on a vibrating string. In nearly all geologic situations, P- and S-wave velocities increase with depth beneath the surface.

This behavior causes body waves to refract upward and propagate nearly vertically as they approach the surface. Accordingly, at the ground surface, S waves excite predominantly horizontal motion, and P waves vertical motion. On land, structures are designed to withstand vertical loads greater than gravity, but horizontal design loads are typically much less than gravity. Shaking damage to onshore structures is largely attributable to nearly vertically propagating shear waves, which excite structures in their weaker, horizontal directions. Offshore structures founded on the sea floor are subject to both P and S motions; however, floating structures are isolated from shear waves, which cannot propagate in a fluid. Nonetheless, floating structures are vulnerable to shaking damage; compressional waves alone can carry enough energy to cause serious damage, at least in the source region of a major earthquake (Hove and others, 1982).

The damage potential of seismic shaking is determined by several properties of seismic waves: amplitude, duration, frequency content, and pulse sequence. Damage potential increases with the amplitude of shaking; however, the relation is complex because of the nonlinear inelastic response of sedimentary deposits and structures to damaging levels of motion. Structures and, in some places, sedimentary deposits respond to shaking in a resonant manner, whereby relatively large deformations and stresses result if the shaking includes several cycles of motion with frequencies close to the resonant frequencies of the structure or deposit. Duration and pulse sequence are important factors because failure mechanisms in both structures and geologic materials depend on the number of stress-strain cycles greater than some amplitude as well as on the sequence in which cycles of different amplitudes occur. Thus, no single parameter can adequately portray the damage potential of seismic shaking.

The principal source of quantitative information on ground shaking is the set of onshore instrumental records of strong ground motion collected from past earthquakes. Summaries of significant strong-motion records obtained in the United States since recording began in 1932 are contained in the annual publication "United States Earthquakes," published by the U.S. Department of Commerce and U.S. Geological Survey. In addition, records collected since 1976 in California under the California Strong Motion Instrumentation Program are cataloged in the Special Report Series of the California Division of Mines and Geology. The small number of recordings available from Canada were compiled by Weichert and Milne (1980) and Weichert and others (1982). Information from nearly 1,000 digitized strong-motion records from 16 countries, including Japan and Italy, was compiled by Crouse and others (1980).

Three factors limit the reliability of predictions of seismic shaking at offshore sites. First, no instrumental data are available against which to test predictions. Although ocean-bottom strong-motion seismographs have been deployed in recent experiments (Reece and others, 1981; Steinmetz and others, 1981), to date no sea-floor recordings have been obtained close to the source of earthquakes large enough to be of engineering importance. In regard to sea-surface recordings of compressional waves from a submarine earthquake, we are not aware of any records obtained close to the source region where damage has been reported. Second, strong shaking at offshore sites can be predicted by using theory to extrapolate from empirical data obtained on land, although onshore studies do not encompass the range of sedimentologic and hydrologic conditions that are commonly encountered in the marine environment. Few onshore data concern the dynamic response of soft, saturated sediment to intense seismic shaking. A further complication in the marine environment is the common presence of gas trapped in the sediment. Third, the onshore data base is deficient in recordings of damaging levels of shaking obtained close to the source of large earthquakes. For example, only few records have been obtained within 40 km of an M=7 earthquake, and none exists from within 75 km of an M=8 shock. Thus, prediction of seismic shaking offshore is very much an extrapolation beyond evidence obtained on land.

The seismic motion recorded at a particular site from a given earthquake is the result of three processes: radiation of seismic energy at the earthquake source, propagation of the radiated seismic waves through heterogeneous Earth structure, and modulation of the seismic waves near the site by local geologic structure and surficial materials. Each of these processes is complex, and their effect on the recorded motion is difficult to predict because either the physics of the process is poorly understood or the shallow structure of the Earth is not known in sufficient detail, or for both reasons. Thus, reliable estimates of seismic shaking, with the precision that engineers desire, are largely impossible at this time. Recent advances, however, both in understanding of the component processes and in modeling of these processes by sophisticated computational methods enable us to limit the problem and to provide estimates of seismic shaking in terms of ranges of expected values.

A comprehensive review of standard practices and methods for estimating strong ground motion on land was provided by Hays (1980). Aki (1982) briefly summarized, from a seismologic perspective, the state of the art in predicting strong ground motion from a basic understanding of fault mechanics and seismic-wave propagation. However, a comprehensive discussion of the application of such state-of-the-art techniques to engineering situations has yet to be written. Boore (1983) has reviewed progress in strong-motion seismology from 1979 through 1982, with particular emphasis on the prediction of strong ground motion; an extensive bibliography is included.

In the following discussion, we focus on the problem of predicting strong ground motion and address two aspects of this problem: prediction of motion from postulated earthquakes at specific sites, and probabilistic estimation of shaking on an areal basis. The problem of predicting compressional-wave disturbances at the sea surface has received little attention (Hove and others, 1982) and is not discussed further here; it is amenable to theoretical analysis and deserves investigation.

Site-specific evaluation

Detailed, quantitative estimation of site-specific ground motion requires sophisticated computational techniques for modeling the generation, propagation, and local modulation of seismic waves. Because of the large number of variables and the complexity of physical processes entering into the problem, seldom can these methods provide a reliable, precise estimate of the amplitude, frequency, duration, and pulse-sequence characteristics of strong ground shaking. Many engineering applications, therefore, rely on simplified quantitative representations of ground motion, such as average response spectra, representing ensemble averages of spectra over a range of magnitude, distance, and site situations, or on representative time histories of ground motion derived from recorded or simulated strong motions. For a particular earthquake and site situation, these engineering representations of seismic ground motion are generally normalized on the basis of some predicted gross measure of ground motion, such as peak acceleration, velocity, or displacement and duration (Newmark and Hall, 1969; Newmark and others, 1973; Watt and others, 1978; Bea, 1979; Bea and others, 1979).

Numerous statistical correlations of peak-ground-motion parameters with magnitude, distance from the earthquake source, and site geology have been derived from instrumental strong-motion records (Idriss, 1978; Boore and Joyner, 1982). Such correlations are useful in estimating ground motions for design purposes, though with some limitations. Attenuation curves (fig. 31) of Joyner and Boore (1981) show mean and 84th-percentile values of peak horizontal acceleration and velocity, based on earthquakes in western North America, primarily California. The acceleration curves are well constrained by data at distances beyond 3 km for the magnitude range 5.0-6.6 and beyond 30 km for the magnitude range 7.4-7.7; the velocity curves are reasonably constrained only for the magnitude range 5.8-6.6.

The data from which these curves are derived exhibit considerable scatter as can be seen in the residual data for peak acceleration (fig. 31B). The standard deviation of the log-normally distributed acceleration data is a factor of 1.8, about equal to the change in acceleration expected for a unit change in magnitude (fig. 31A). The scatter in the velocity data is comparable to that in the acceleration data, but velocity is a more sensitive function of magnitude and varies by a factor of about 3 for a unit change in magnitude (fig. 31C). Peak velocities recorded on soils more than a few meters thick are generally amplified about 50 percent above those recorded on rock (fig. 31C), whereas peak accelerations appear to be relatively insensitive to site geology. Such empirical attenuation relations are utilized in the probabilistic mapping of ground shaking, as discussed in the next subsection.

Caution must be exercised in estimating design ground motions from empirical attenuation relations. Within the ranges of distance and magnitude for which instrumental data are currently sparse or absent, estimates from empirical relations are model-dependent extrapolations, and estimates based on different models are commonly discordant (for example, compare Joyner and Boore, 1981, and Campbell, 1981). Furthermore, such estimates are subject to change upon the acquisition of new instrumental data that would better constrain the model. The data base is most deficient close to the sources of earthquakes of $M \geq 7.0$, where damage is most likely. On the other hand, for distances and magnitudes for which data are more numerous, attenuation relations based on different model assumptions, analysis techniques, and data sets commonly predict similar motions (Boore and Joyner, 1982). A further complication is the unexplained variation in the data, which undoubtedly reflects processes not accounted for in a simplified empirical model, such as azimuthal dependence in the radiation of seismic waves or localized amplification or attentuation of seismic waves due to geologic structure at or near the recording site.

In the absence of empirical data, we must look to theoretical methods to estimate peak ground motions. A simple, two-parameter model of the earthquake source (Brune, 1970) provides a basis for estimating both long- and short-period levels of motion. For long periods, Hanks (1976) demonstrated that this model satisfactorily predicts the relative amplitudes of long-period motion excited by the 1952 Kern County (M=7.5) and 1971 San Fernando (M=6.6) earthquakes, and has applied the model to estimating the level of long-period ground motion in the Los Angeles basin arising from a repeat of the 1857 Fort Tejon earthquake (M=7.9) along the southern section of the San Andreas fault, considered to be the maximum earthquake likely to affect the Los Angeles area. For short periods, Hanks (1979a) showed that the root-mean-square ground acceleration measured over the duration of faulting can be estimated from the source model, and McGuire and Hanks (1980) documented that measured values of peak and root-mean-square acceleration correlate well. These theoretical models, based on a simplified source model, hold much promise, but additional studies are needed to verify their accuracy and their applicability to a large number and wide variety of earthquakes.

Peak-ground-motion parameters provide only limited information on the properties of strong shaking—namely, the amplitude of motions within limited frequency bands—and they convey no information about the duration of shaking or the sequence of seismic-wave amplitudes of different periods. Over the past decade, however, methods have been developed and demonstrated for calculating synthetic seismograms that closely approximate many of the important characteristics of actual strong-motion recordings. This advance became possible with improved understanding of fault mechanics and seismic-wave propagation, and with powerful new computational techniques. Currently, representative strong-motion seismograms, limited to periods longer than about 1 s, can be readily calculated. For example, long-period seismograms in the Los Angeles area have been estimated for a major earthquake on the southern section of the San Andreas fault from both a theoretical (Bouchon and Aki, 1980) and a semiempirical (Kanamori, 1979) approach.

Seismogram-modeling techniques are an important tool for investigating strong shaking on the

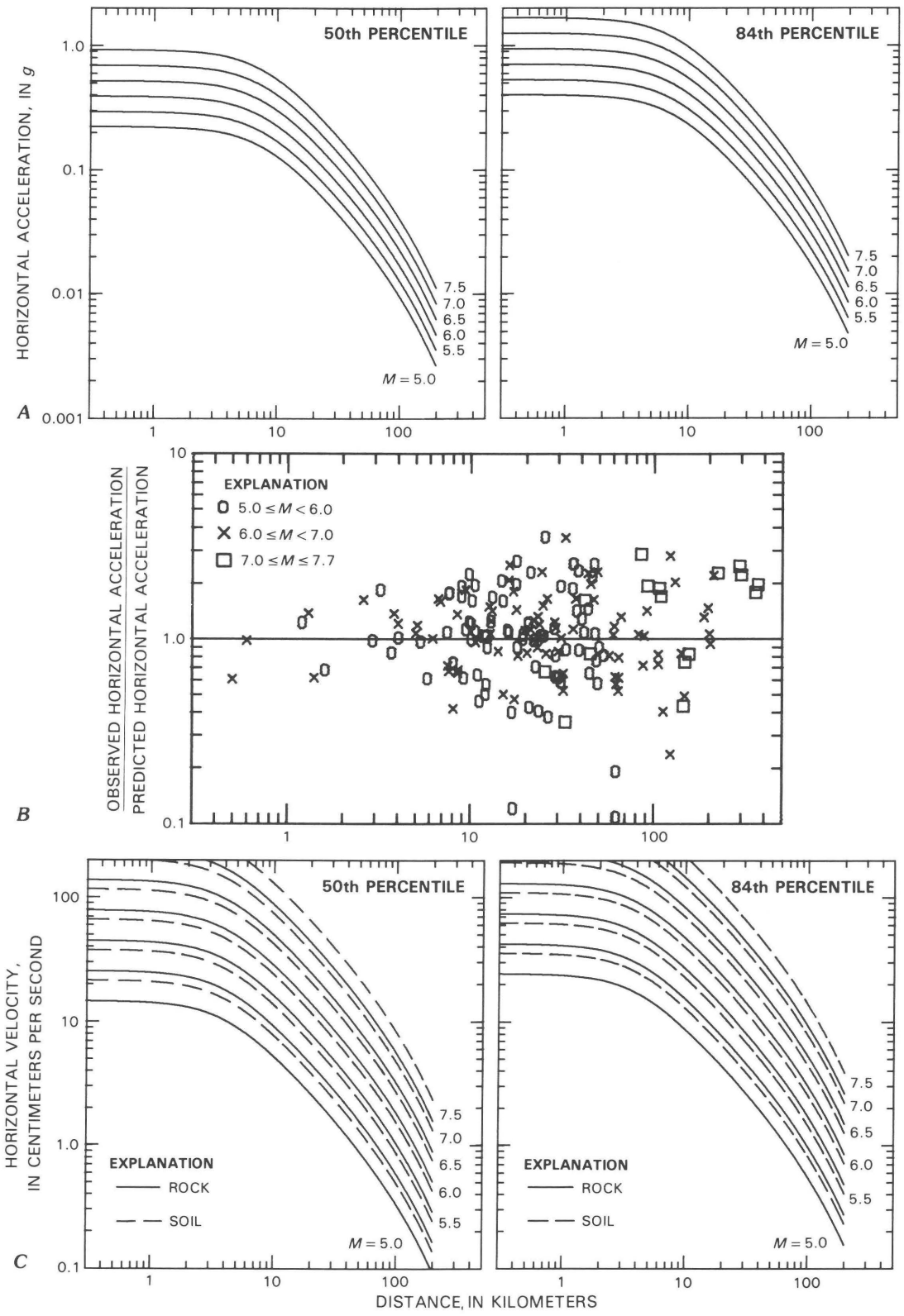

Figure 31. Peak horizontal ground acceleration and velocity versus shortest distance to surface projection of fault rupture, as a function of moment magnitude. A, Attenuation curves for 50th- (mean) and 84th-percentile peak accelerations (from Joyner and Boore, 1981, fig. 4). Shape of curve is assumed to be independent of magnitude. B, Residuals of logarithm of peak acceleration with respect to mean acceleration curves plotted in figure 31A (left), as a function of distance and magnitude (from Joyner and Boore, 1981, fig. 5). C, Attenuation curves for 50th- (mean) and 84th-percentile peak velocities as a function of local geology at the site (from Joyner and Boore, 1981, fig. 9).

sea floor. Swanger and Boore (1978a) used the modal superposition of surface waves to model long-period ground motion in sedimentary basins at several tens of kilometers from shallow earthquakes. They showed that flat-lying deep sediment forms a waveguide that enhances the surface-wave component of the ground motion. Swanger and Boore (1978b) extended this method to predict long-period motion on the Continental Shelf. For Love-type surface waves from an M=7.5 earthquake propagating 50 and 100 km across a typical shelf consisting of 100 m of soft soils overlying 8 km of consolidated sediment, the longer period motion is amplified by a factor of 3 or 4 relative to that for a typical onshore path in hard rock. The pseudorelative-velocity-response spectra at 5-percent damping for surface-wave motions are shown in figure 32. Swanger and Boore (1978b) also demonstrated that a strong velocity contrast at depth can cause resonance within a narrow period band that may be important in the nonlinear response of offshore structures.

Using a different computational method, Spudich and Orcutt (1982) calculated synthetic sea-floor seismograms for a velocity model typical of the Continental Shelf, except for the important absence of the water layer. They assumed a shallow oblique-thrust earthquake and computed vertical and radial seismograms over a broad distance range. The synthetic seismograms (fig. 33) show an extended train of low-frequency surface waves following the high-frequency body waves. For this case, the horizontal motions (radial component) are about 3 times larger than the vertical motions and continue about twice as long. Spudich and Orcutt separately considered the effect of a 1.5-km-thick layer of water on vertical sea-floor motions and found that the water overburden decreases high-frequency motions significantly and alters the dispersion characteristics substantially, so that the surface waves persist much longer. The effect of water overburden would be less significant for water depths typical of continental-shelf areas, that is, for depths less than 200 m.

Although the complete source-propagation-site problem cannot be modeled satisfactorily at shorter periods, the problem of local modulation of seismic shaking at the site is tractable. The dynamic response of surficial sediment can be computed by using vertically propagating body waves incident at the base of the sediment. A strong-motion record from a rock site is selected that is typical of the earthquake magnitude and distance under consideration. This selected record is then used as input motion at the sediment-rock interface, and the dynamic response of the sediment is computed to provide an estimate of the surface motion. The accuracy of this computation is limited by the extent to which the dynamic stress-strain relations of the sediment are known. The response of surficial geologic materials to nondamaging levels of motion, for which the stress-strain relation remains linear, can be predicted with considerable accuracy (Joyner and others, 1976; Johnson and Silva, 1981).

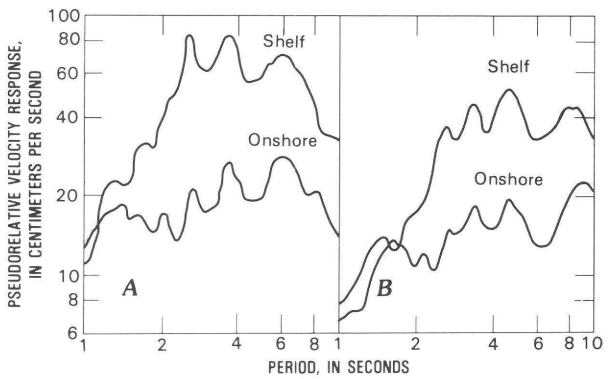

Figure 32. Pseudorelative-velocity-response spectra at 5-percent damping, computed for surface-wave (Love) motions for representative onshore and continental-shelf sites at distances of 50 km (A) and 100 km (B) from an M=7.5 earthquake (from Swanger and Boore, 1978b, fig. 3).

Estimates have been made of the response of surficial sediment to damaging levels of input motion in the underlying bedrock, that is, of the high-strain, nonlinear response that might occur in the nearfield of a large earthquake. However, no empirical data are available for testing and calibrating such estimates. Joyner and Chen (1975) computed the nonlinear response of a 200-m-thick section of water-saturated, firm alluvium excited at its base by horizontal shaking with a peak acceleration of 0.7 g and a peak velocity of 67 cm/s. Relative to a site with exposed rock, motion at the surface of the alluvium is amplified for periods longer than 1.5 s by a factor of as much as 2 and is somewhat reduced for short periods. Moriwaki and Doyle (1978) analyzed the response of three postulated offshore sites characterized at the surface by rock, by 65 m of stiff clay, and by 65 m of soft clay. They found that the stiff clay amplified moderate input motion (peak acceleration, 0.3 g) and generally attenuated intense motion (peak acceleration, 0.6 g); whereas the soft clay greatly attenuated short-period components and amplified long-period components of both moderate and intense input motions. For moderate motion, the soft clay attenuated (by a factor of at least 2 or 3) spectral components with periods shorter than about 1 s and amplified components with periods longer than about 3 s; the attentuation of short-period components was greater for intense motion. For weaker input motion (peak acceleration, 0.05 g), soft cohesive soils can amplify motion at periods less than 1 s (Martin and others, 1979).

Thus, methods are available, some involving state-of-the-art mathematical modeling, to estimate ground-shaking characteristics for site-specific situations. The rigor with which these methods should be pursued to determine the shaking potential should depend on the earthquake exposure of the site, the type of structures or facilities being designed, and the possible consequences of damage or failure.

Areal evaluation

The types of ground-shaking evaluation described in this and the preceding subsection cannot be completely separated. A site-specific study may be extended to a small area, such as a petroleum reservoir or lease area, to assess the implications of

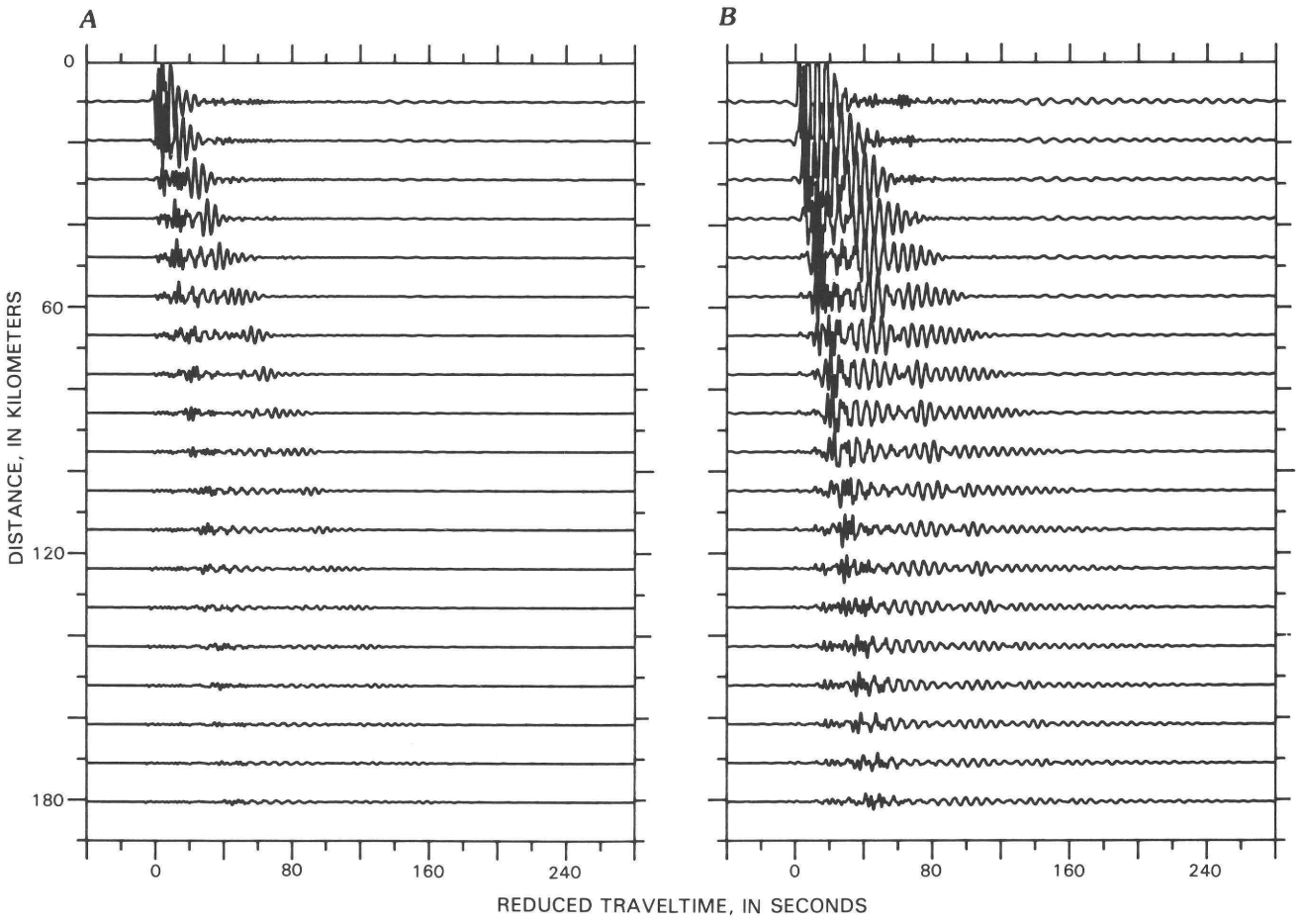

Figure 33. Theoretical sea-floor seismograms as a function of distance for a representative velocity model of the Continental Shelf (modified from Spudich and Orcutt, 1982, figs. 2, 3). A, Vertical motion. B, Radial motion. Amplitudes indicate relative ground velocities at the various distances. Traveltime is reduced by time required for a 5-km/s wave to propagate to the site, or approximately by the P-wave traveltime. At increasing distance, seismograms are dominated by extended trains of late-arriving low-frequency surface waves.

varying thicknesses of sediment or of varying locations of sites relative to known active faults.

Site-specific evaluations are generally undertaken for critical facilities in earthquake-prone regions, and commonly for less critical structures as well, when maps of predicted strong ground motion are not available, are too small in scale, are not sufficiently conservative (that is, display values of ground motion that are too likely to be exceeded), or do not depict ground motion in the frequency band of interest.

Ground-shaking maps are important for offshore development. They provide information on the spatial variations in shaking severity that can be factored into decisions on priorities of areas to be leased and on strategies for safe and economic exploitation of offshore resources. They also provide ground-motion parameters for design of less critical facilities. We contend, however, that the information portrayed in ground-shaking maps derived by uniform application of present techniques to a large area is generally insufficiently precise and reliable to serve as a basis for the design of a critical facility in a region of moderate or high earthquake potential.

Construction of probabilistic ground-shaking maps

Most recent ground-shaking maps provide probabilistic estimates of potential shaking, which are based not only on the recorded history of damaging earthquakes but also on geologic evidence of active tectonism that suggests the likelihood of future earthquakes in areas devoid of historical seismicity. Such maps can serve as a reference source for the levels of ground motion to be accommodated in the earthquake-resistant design of common or noncritical structures (for example, Applied Technology Council, 1978). Probabilistic shaking maps have recently been published for Canada and its continental margins (Basham and others, 1982, 1984), the contiguous United States (Algermissen and others, 1982), coastal California and the adjacent Continental Shelf (Thenhaus and others, 1980), the Pacific Northwest and the adjacent shelf (Perkins and others, 1980), the East Coast and the adjacent shelf (Perkins and others, 1979), Alaska and the adjacent shelf (Thenhaus and others, 1985), and individual lease areas on the Alaskan

Continental Shelf (Woodward-Clyde Consultants, 1978).

Probabilistic ground-shaking maps have four basic elements in their construction: a set of seismic-source zones developed from a seismotectonic model of the study region; magnitude-recurrence relations for each of these zones; functional relations for the magnitude and distance dependence of the strong-ground-motion parameters being mapped; and an analytical technique for computation of the ground-motion parameters at selected points throughout the region at desired probabilities of exceedence (fig. 34).

The principal difference between the source zones delineated for areal analysis of shaking potential and those developed for a site-specific study is one of scale and detail of knowledge. The level of geologic and geophysical investigation that can be pursued to define an earthquake source near a specific site commonly is not feasible for broad-scale analysis of a large area. There is a limit to the rigor of earthquake-source investigations, imposed by the requirement to depict strong ground shaking with comparable accuracy at all points on the map. Thus, the degree of confidence in the ground-motion estimate at an arbitrary point is less than that for a site-specific evaluation. Examples of seismic-source zones developed for areal evaluation of shaking potential are illustrated in figures 19 and 25; further illustrations were presented by Patwardhan and others (1981), Thenhaus (1983), and Basham and others (1982).

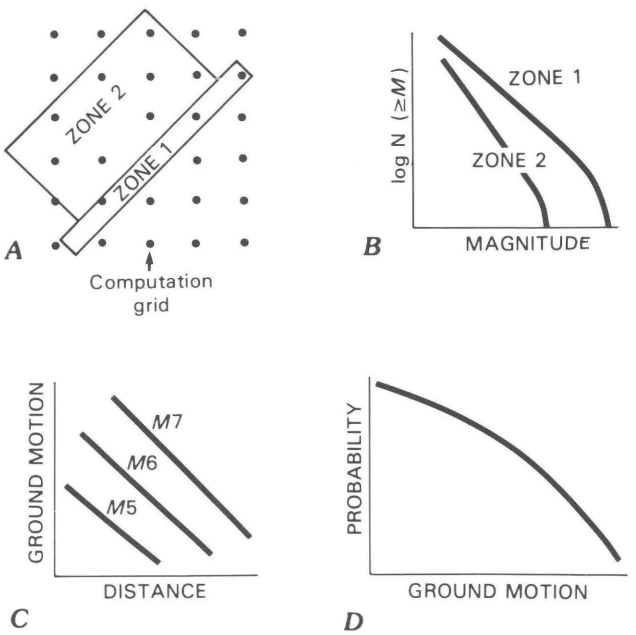

Figure 34. Schematic illustration of steps in method for determining probabilistic estimates of seismic ground motion (from Basham and others, 1981, fig. 4). A, Earthquake-source zones and computation grid. B, Magnitude-recurrence relations, terminating at an upper-bound magnitude. C, Ground-motion attenuation. D, Calculated probability distribution of ground-motion parameters at a gridpoint.

Magnitude-recurrence relations establishing the frequency of shocks as a function of magnitude are required for each of the source zones. In some zones the historical and recent seismicity provides a reliable estimate of the rates of significant earthquakes (see fig. 23). In other zones it does not, and judgment is required to assign magnitude-recurrence relations based on available information (for example, Perkins and others, 1980; Basham and others, 1982).

Magnitude-recurrence relations are terminated by some selected upper-bound magnitude. Though straightforward in zones that have undergone great ($M \geq 7.5$) historical earthquakes, the selection of upper-bound magnitudes is generally difficult in less active seismic zones. If the cause of the earthquakes is poorly understood, as, for example, on the eastern and Arctic margins of the United States and Canada, then the dimensions of potentially active faults, the magnitudes of associated upper-bound earthquakes, and the frequency of shocks are not known. Although great earthquakes occur principally in regions of major plate interactions, earthquakes approaching $M=7$ have also occurred on the passive Atlantic margin of the United States and Canada during historical time. The influence of the choice of upper-bound magnitudes on mapped values of shaking can be determined as part of a sensitivity analysis. For example, if an upper-bound magnitude has an estimated average recurrence rate of 0.001 event/yr, it will not contribute heavily to ground motions computed at an annual exceedence probability of 0.01.

Attenuation relations, which relate the strong-motion parameters being mapped to magnitude and distance, are also required, even though available data to define these relations for the region in question may be scarce or absent. Extrapolations are sometimes possible from a region for which data are available to a region of similar geologic and tectonic environment that lacks data, for example, from the western conterminous United States to western Canada (Hasegawa and others, 1981). Even though the regions are dissimilar, the almost complete absence of relevant strong-motion recordings in eastern North America has promoted extrapolations of data from the Western United States based on empirical comparisons of the attenuation of modified Mercalli intensities (for example, Nuttli, 1979; Hasegawa and others, 1981).

Two important limitations of attenuation relations are the absence of controlling instrumental data in the nearfield of large earthquakes and the substantial scatter in the limited data that do exist. Most compilations of ground-motion-amplitude data show the standard deviation for an individual observation to be a factor of about 2 about the average regression value (for example fig. 31). This scatter can be accounted for in estimating ground motion by including a stochastic term in the attenuation relation. Although the effect of this term on estimated ground-motion values with a small probability of being exceeded is to increase these values relative to the case in which there is no scatter in the data (Weichert and Milne, 1979), the amount of this increase will depend on the assumed standard deviation and on the slope of the magnitude-recurrence relation (see Algermissen and others, 1982).

Most recent probabilistic ground-shaking maps are based on the computational method developed by Cornell (1968). This method treats earthquakes as occurring randomly in space and time throughout planar source zones at rates specified by the magnitude-recurrence relations. For each gridpoint on a map, a distribution function for the probability of exceedence is computed by numerically integrating contributions to the ground-motion parameter from all relevant source zones (fig. 34). The results for all gridpoints can be displayed as contours of the ground-motion parameter at a fixed probability of exceedence, or of the probability of exceedence at a fixed level of ground motion. Computer programs have been developed to treat earthquakes as either point or linear sources (McGuire, 1976, 1978), and to allow for the nonrandom occurrence of earthquakes (Patwardhan, 1978).

Maps depicting shaking at very low probabilities of exceedence should be used with caution. The choice of a very low level of probability yields extreme values of ground motion in the nearfield of large earthquakes. In the commentary accompanying the recent national ground-shaking maps of Canada, the user is cautioned to undertake additional investigations in areas of high earthquake potential (Heidebrecht and others, 1983).

Western Canada

Probabilistic ground-shaking maps of western British Columbia, southeastern Alaska, and the adjacent offshore region are shown in figure 35. The seismotectonic model (fig. 19A) and magnitude-recurrence relations (fig. 23) for part of this region were described above. These maps display, for sites underlain by firm soil, values of peak horizontal acceleration and velocity with probabilities of exceedence of 10 percent in 50 years. In other words, there is a 90-percent probability that the mapped values will not be exceeded over a 50-year interval.

The active Queen Charlotte and Fairweather faults, which are the dominant earthquake sources in western Canada and southeastern Alaska, respectively, account for the belt of high-amplitude motion along the coast (fig. 35). Because of the stronger dependence of peak velocity on magnitude and the slower attenuation of peak velocity with distance, the influence of the major coastal faults is larger and more pervasive for velocity than for acceleration.

These maps depict probabilistic ground shaking within two dominant frequency bands—acceleration in a band around 5 Hz, and velocity in a band around 1 Hz—and thus provide information on relative levels of expected shaking, respectively, for ordinary rigid structures and for larger, more flexible structures with lower resonant frequencies, such as offshore platforms.

Gulf of Alaska

Two probabilistic peak-acceleration maps for the northeastern Gulf of Alaska region (fig. 36) enable the user to compare estimates of acceleration derived by different investigators using somewhat different approaches.

Thenhaus and others (1985) published a series of maps depicting probabilistic estimates of acceleration on rock at varying return periods[3] for Alaska and the adjacent offshore region. These maps are revisions of maps prepared earlier for Federal agencies responsible for leasing Outer Continental Shelf oil and gas resources and supervising exploration and production. The Gulf of Alaska part of the 100-year-return-period[4] map is shown in figure 36A. For this study, the entire State and adjacent shelf area were partitioned into 24 seismic-source zones. Some zones are well controlled by knowledge of historical or Holocene faulting in southern and southeastern Alaska and of subduction of the Pacific plate beneath southern Alaska; others simply encompass areas of apparently homogeneous seismicity and (or) distinctive geologic structure. Upper-bound magnitudes range from 7.3 for lesser seismic zones to 8.5 for zones representing major interactions between the Pacific and North American plates. The smaller earthquakes ($M<6.4$) were modeled as point sources, and, where single faults comprise seismic-source zones, the larger earthquakes were modeled as line sources, with length appropriate to magnitude. Within each zone, earthquakes were assumed to occur randomly over time. The Schnabel and Seed (1973) peak-acceleration-attenuation relations for rock sites were employed, and no term was included to allow for stochastic scatter in acceleration.

Woodward-Clyde Consultants (1978) analyzed an area of the Gulf of Alaska from Yakutat Bay to west of Kayak Island (fig. 36B) in their Offshore Alaska Seismic Exposure Study prepared for the 21 oil company members of the Alaska Subarctic Offshore Committee (see summary by Patwardhan and others, 1981). They derived more detailed sources for the subduction zone and shallow fault structures, and represented each earthquake as a rupture on a planar surface. Earthquakes of $M<7.5$ were assumed to occur randomly over time. In contrast, larger shocks within the subduction zone were modeled by a nonrandom probability of occurrence, consistent with the identification of a seismic gap within the study region (fig. 24). Probabilistic estimates corresponding to a 100-year return period were computed for an exposure time of 40 years, beginning at the time of the study. Two peak-acceleration- attentuation relations were

---

[3]The concept of return period applies to a process in which events occur randomly over time. The return period is the average time interval between events. Here, the event of interest is the occurrence of shaking exceeding some threshold value. Return period R is related to the probability p that the threshold value will be exceeded over an exposure time T through the equation $1-p=\exp(-T/R)$, where T and R are measured in terms of the same unit. If T is much smaller than R, then $p \sim T/R$.

[4]The actual return period is 95 years, corresponding to a 10-percent probability of exceedence over 10 years.

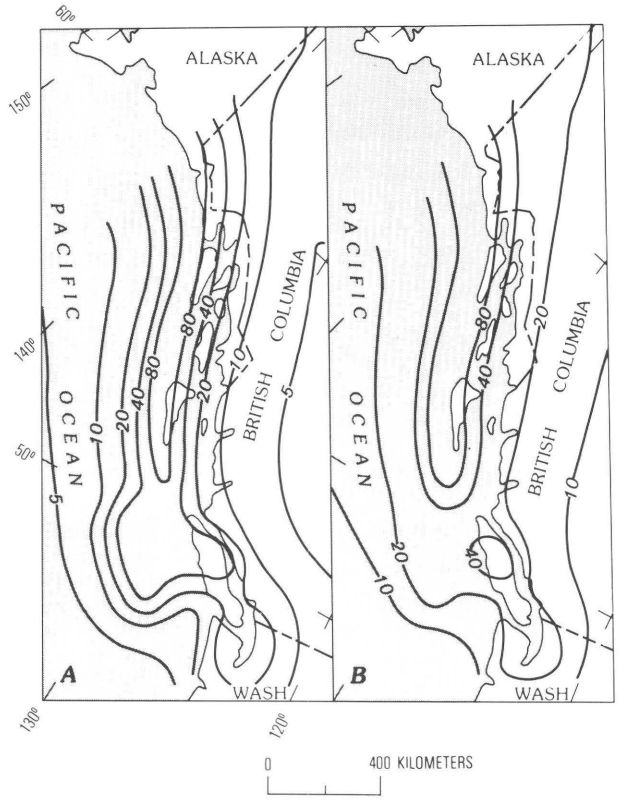

Figure 35. Probabilistic maps of peak horizontal acceleration and velocity in western British Columbia and adjacent offshore region at a 10-percent probability of exceedence in 50 years, or a return period of about 500 years (from Weichert and Hyndman, 1982, fig. 5). A, Acceleration (contours in percent of gravity). B, Velocity (contours in centimeters per second).

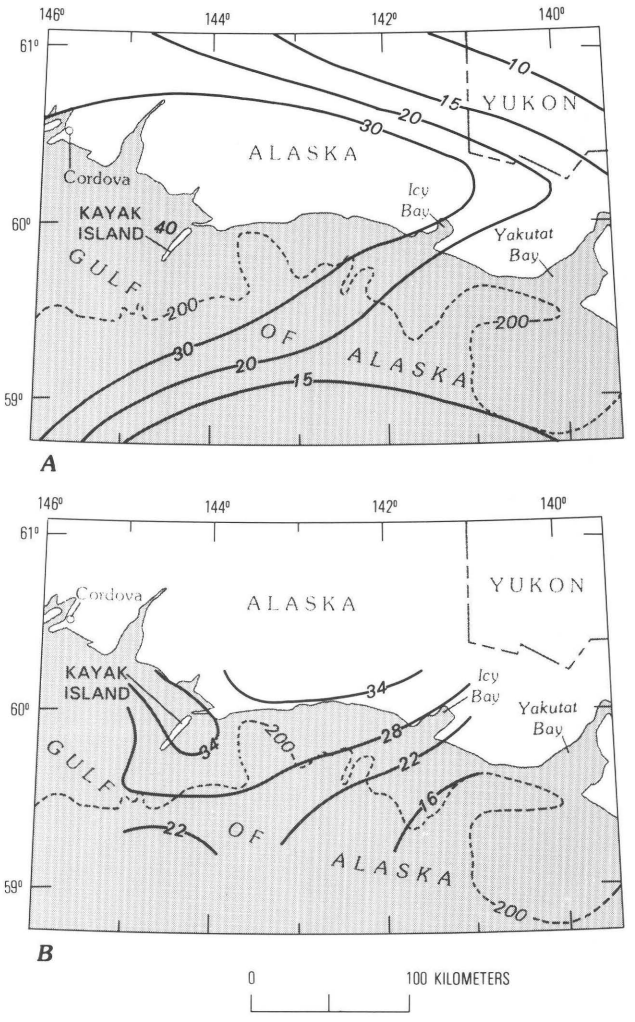

Figure 36. Probabilistic maps of peak horizontal acceleration (in percent of gravity) for northeastern Gulf of Alaska region at a return period of about 100 years. Dashed line represents 200-m isobath, approximate edge of the Continental Shelf. A, Rock sites, 10-percent exceedence probability over 10 years (modified from Thenhaus and others, 1985, fig. 5). B, Sites on shallow stiff soil, 33-percent exceedence probability over 40 years (modified from Patwardhan and others, 1981, fig. 7).

employed, one for earthquakes shallower than 20 km, and another for deeper events; both relations are for sites with less than about 45 m of stiff clay, sand, or gravel overlying rock. The relation for the deeper events predicts peak accelerations at a given distance from the rupture surface as much as 2 to 3 times larger than those predicted by the relation for shallow events. The scatter about the mean relations was assumed to be log-normally distributed. The Schnabel and Seed (1973) relations used by Thenhaus and others (1985) predict peak accelerations approximately intermediate between those given by the two Woodward-Clyde relations.

The results from these two studies are displayed in figure 36 as contours of peak acceleration, with a common annual probability of exceedence of about 0.01. Analysis of the several factors in the two studies that may contribute to differences in the results is beyond the scope of this report. Given the differences in the various components of the analyses, the results are notably similar in predicting a range in peak acceleration from about 0.15 to 0.35 or 0.40 g on rock or stiff-soil sites along the Continental Shelf from Yakutat Bay to Kayak Island.

American Petroleum Institute guidelines

The American Petroleum Institute (1982), in its guidelines for the planning, design, and construction of fixed offshore platforms, presented another example of ground-shaking maps for the Continental Shelf of the United States. The shelf is divided into six zones (0-5) in terms of earthquake potential and related ground motion (fig. 37). Each zone is assigned an effective horizontal ground acceleration, ranging from 0.0 g in zone 0 to 0.4 g in zone 5, to be used for design of major steel-frame structures in the absence of site-specific data. The effective accelerations are used to

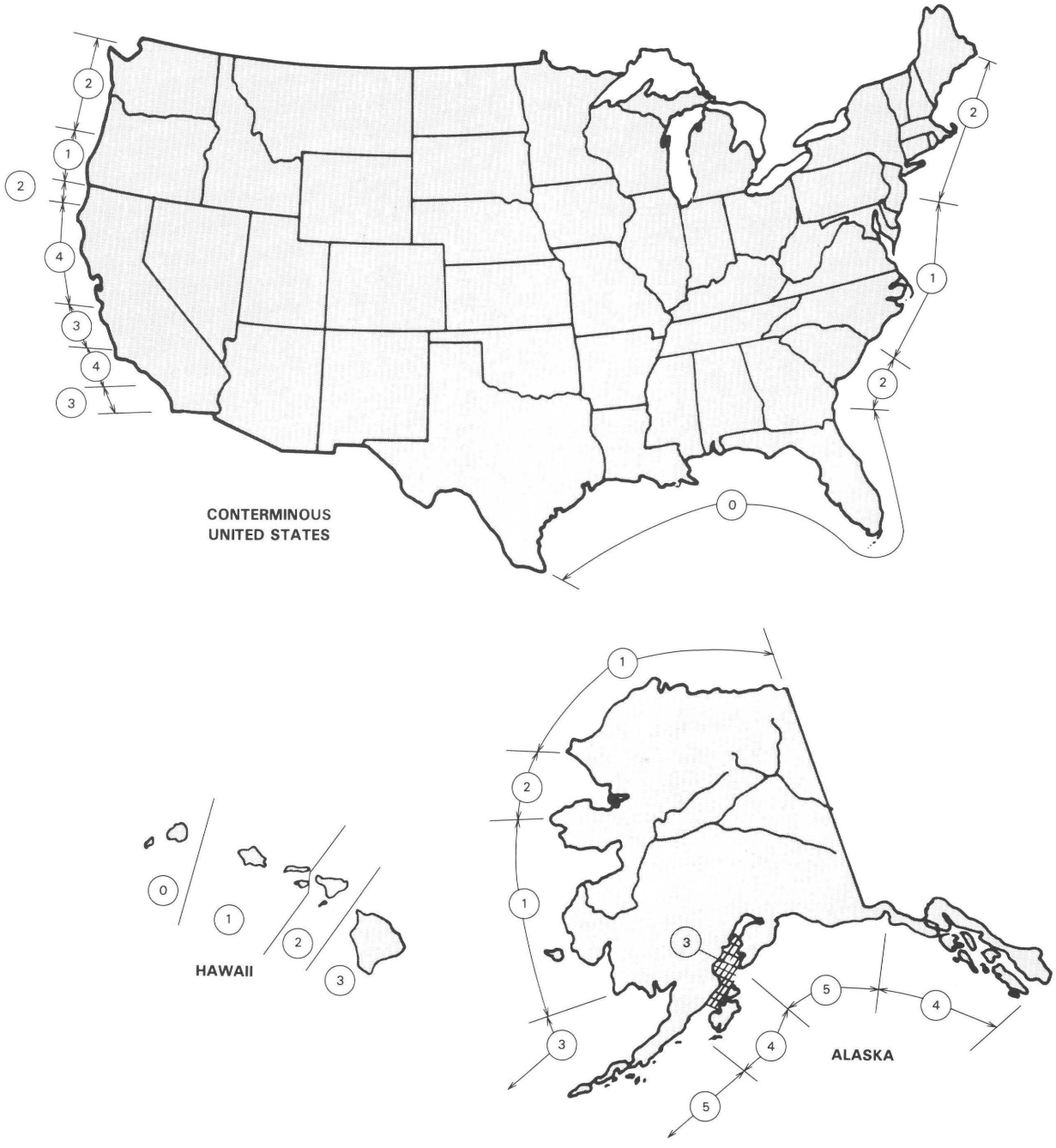

Figure 37. Earthquake-risk zones used in American Petroleum Institute's guidelines for the design of fixed offshore platforms in United States coastal waters (from American Petroleum Institute, 1982, fig. 2.3.6-1). Effective horizontal accelerations for scaling of design response spectra are 0, 0.05, 0.10, 0.20, 0.25, and 0.40 g for zones 0 through 5, respectively.

scale normalized response spectra, which are referenced to three types of foundation conditions: rock, shallow strong alluvium, and deep strong alluvium. The guidelines recommend that platforms located on significant accumulations of soft clay, loose sand, and silt deserve special analytical studies to determine the appropriate input ground motion.

The guidelines state that for areas of low seismicity (zones 0, 1, and 2), environmental factors other than earthquakes normally control platform design. They further state that for zone 0 no earthquake analysis is required but that for zones 1 and 2 sufficient calculations are required to confirm that earthquake loading does not exceed half the strength requirements imposed by other environmental conditions. For more seismically active areas (zones 3, 4, and 5), the guidelines recommend that the design ground motions should be determined by a site-specific study, but allow the

design motions to be taken from figure 37 in the absence of detailed seismic data and site-specific studies.

In reference to these guidelines, we recommend that for zones 3, 4, and 5 the corresponding effective horizontal ground accelerations of 0.20, 0.25, and 0.40 g be used only for preliminary design considerations and that final strength requirements for earthquake loading of offshore platforms be based on site-specific studies utilizing state-of-the-art techniques to model expectable ground motion. Such modeling can provide better information on the relative levels of input ground motion within the period range of platform resonances.

Sea-floor failures

Avoidance and accommodation are both important strategies for mitigating the potential hazards associated with sea-floor failures (Garrison and Bea, 1977). The strategy of avoidance, which involves the selective siting of a structure to avoid potentially hazardous areas, recognizes that failure of surficial geologic deposits is geographically limited. Although strong ground shaking, which is the triggering mechanism for earthquake-related failures, is a pervasive earthquake effect, the extent of sea-floor failure is limited by the distribution of materials that are susceptible to failure. The strategy of accommodation is founded on the assumption that a structure can be designed to withstand threats to its integrity and performance arising from sea-floor failures.

Avoidance is generally the preferred strategy where seismic shaking might trigger large permanent displacements within geologic foundation materials, because such displacements can impose catastrophic loads on the structure. For example, the hurricane-induced soil movement that toppled South Pass 70 Platform B in the Gulf of Mexico (Sterling and Strohbeck, 1973) displaced the base of the platform about 25 m in a downslope direction and caused buckling failure in the piles on which the platform was supported. Comparison of shear strength-depth profiles for soil borings obtained before and after the hurricane suggests that significant movements occurred to depths of at least 20 m. Measurable changes in bottom topography extended over an area greater than 15 km^2, and the maximum change in water depth exceeded 10 m. Slides of comparable or greater size, which at least in part are attributable to seismic shaking and which in some places are probably the result of several episodes of shaking, are visible in bottom and subbottom reflection profiles obtained in seismically active zones off California (Edwards and others, 1980; Lee and others, 1981), British Columbia (Yorath, 1980), and Alaska (Hampton and Bouma, 1977; Molnia and others, 1977; Carlson, 1978). For example, seismic profiles in the Kayak Trough in the northern Gulf of Alaska (fig. 38) reveal a massive submarine slide above the inferred rupture zone of the great 1964 earthquake.

The strategy of accommodation, however, may be practicable for sea-floor failures in which a temporary loss of strength in geologic materials occurs, but little permanent displacement. Without significant displacement of the geologic foundation materials, a structure is not subjected to extreme external loads, as occur in sliding. Thus, the detrimental effects of liquefaction in shallow sediment can be countered by anchoring the foundation of a structure below the depth to which liquefaction occurs, such as for a pile-supported structure, or by designing a buried structure to be neutrally buoyant with respect to the liquefied sediment, such as for a pipeline. Implementation of either mitigation strategy requires the ability to identify areas subject to seismically induced failures. The strategy of accommodation further demands the capability to predict the probable characteristics of potential failures, particularly the depth and areal extent of failure and the amount and pattern of resulting displacements.

This section focuses on failures in sedimentary deposits. Although submarine rock slopes may fail in response to strong seismic shaking, failure of sedimentary deposits is the dominant problem confronting coastal and offshore structures because of the wide-

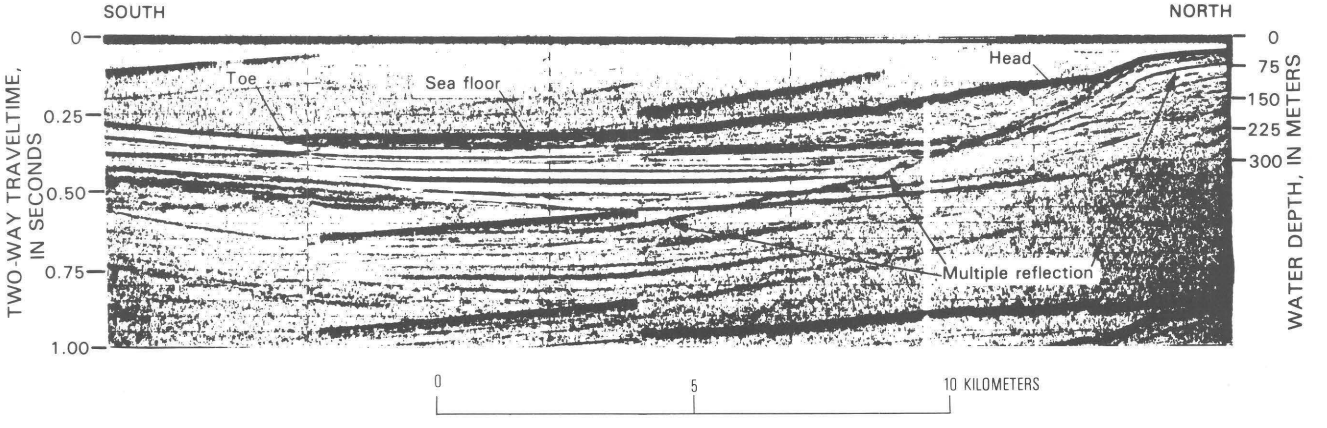

Figure 38. High-resolution seismic profile (vertical section) approximately along axis of an 18-km-long submarine slide in the Kayak Trough, northern Gulf of Alaska (from Carlson and Molnia, 1977, fig. 12). Multiple reflection arises from energy reflected twice between sea surface and sea floor. Thickness of disturbed zone decreases from about 120 m south of scarp at head of slide to about 20 m near toe.

spread presence of sediment and its greater susceptibility to failure.

Few incidents of seismically induced sea-floor failure have been documented, and none has been thoroughly investigated to determine the specific geotechnical and seismic conditions under which it occurred. Accordingly, evaluation of the physical mechanisms and the seismic, geologic, hydrologic, and geotechnical conditions that contribute to sea-floor failures relies heavily on experience with subaerial failures and laboratory investigations of failure mechanisms. A descriptive summary of subaerial failures associated with historical earthquakes in northern California was compiled by Youd and Hoose (1978). Detailed field investigations and engineering analyses of individual ground failures since 1964 have significantly increased our understanding of the mechanism of and conditions for failure. Particularly relevant to the problem of sea-floor failures are studies of failures in sedimentary deposits on gentle slopes and level ground (for example, Seed and Idriss, 1967; Seed and Wilson, 1967; Youd, 1973). The importance of pore-fluid-pressure changes and the cyclicity of seismic loading in the failure of sedimentary deposits have been demonstrated in laboratory studies (Seed and Chan, 1966; Lee and Seed, 1967; Peacock and Seed, 1968).

The occurrence of earthquake-induced failures in sea-floor sediment depends on the character of seismic shaking and the susceptibility of the sediment to failure. Two important characteristics of shaking are its amplitude and duration. The importance of duration is documented both in case studies of failures in sedimentary deposits on land (Lemke, 1967; Seed and Wilson, 1967) and in laboratory investigations of failure processes (Lee and Seed, 1967). For example, the extensive lateral sliding at Turnagain Heights in Anchorage during the great 1964 Alaska earthquake began some 1-1/2 to 2 minutes after the shaking began, and the area of sliding expanded as shaking continued (Seed and Wilson, 1967). Significant sliding occurred only after many cycles of shaking had weakened the underlying soils.

Both amplitude and duration of shaking increase with earthquake magnitude. Thus, sea-floor failures must be expected to be more numerous and to occur at greater distances from the source of seismic shaking in larger earthquakes. Such behavior has been documented for liquefaction failures on land (Youd and Perkins, 1978). For earthquakes of $\underline{M}<5$, significant liquefaction effects on land have not been observed; for shocks of $\underline{M}=5.0$–5.9, potentially damaging liquefaction failures have been observed to distances of about 10 km; and for shocks in the range $\underline{M}=6.0$–6.9, the maximum distance is about 50 km. In the 1964 Alaska $\underline{M}=9.2$ earthquake, liquefaction-induced ground displacements capable of causing significant damage—differential horizontal or vertical ground displacements of more than 10 cm—occurred out to distances of 130 km (Youd and Perkins, 1978). Because liquefiable sediment is more likely to be present on the sea floor, this onshore experience should be regarded as an uncertain minimum guide to the liquefaction potential in the offshore environment.

The susceptibility of marine sediment to failure during earthquakes is governed by the dynamic strength of the sediment and by the slope of the sea floor. In some places, the inertial forces caused by seismic shaking may alone be sufficient to overcome the frictional resistance to downslope movement. This failure mechanism is probably more important in the offshore environment than on land because of the low shear strength of much marine sediment in its natural condition of saturation. In other places, seismic shaking may sharply reduce the shear strength of sedimentary formations, and lead to loss of bearing capacity in geologic foundation materials or to lateral or downslope mass movements. An important mechanism for seismic weakening of saturated sediment is the increase of pore-fluid pressures accompanying cyclic deformation of the soil during the passage of seismic waves (fig. 39). Such an increase of pore pressure results from local densification of the sediment as shaking causes particles to pack more tightly. This increase in pressure reduces the shear strength of the sediment. In extreme cases, the strength can drop to zero, so that the sediment will deform as a liquid, that is, liquefy.

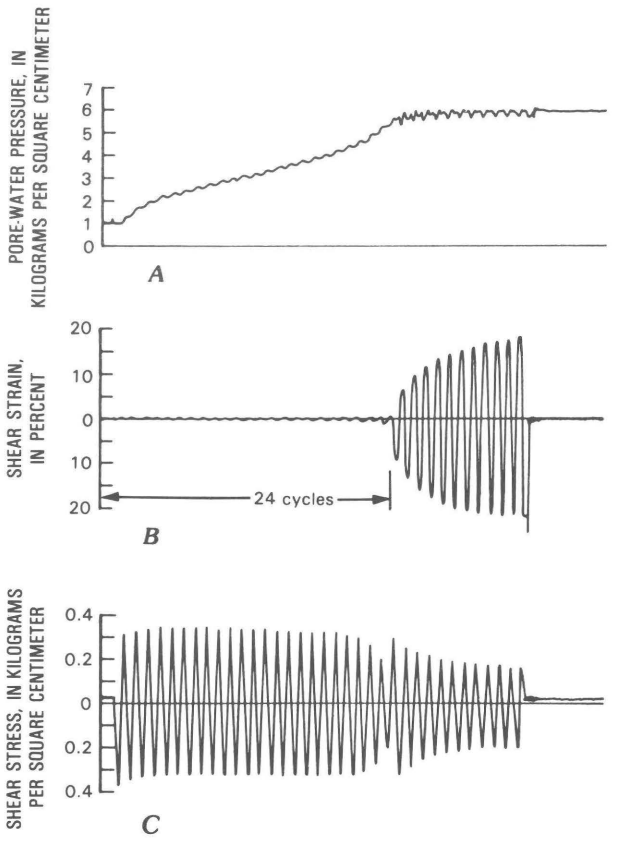

Figure 39. Records from undrained cyclic-shear test on loose sand (from Seed and Idriss, 1982, fig. 42). Gradual increase in pore-water pressure (A) and ensuing abrupt decrease in shear strength—seen as an increase in shear strain (B)—is caused by repetitive cyclic shearing of sample (C). Significant strain occurred after 24 cycles of shear, only when increase in pore pressure practically balanced initial confining pressure acting on the sample.

The seismic stability of marine sediment is determined by the environment in which it is deposited and by its postdepositional history. Submarine failures are most common in areas of rapid deposition, where sedimentation outpacing consolidation results in underconsolidated deposits with naturally high pore pressures. Thus, submarine slumps and slides are particularly likely in the vicinity of active deltas (see Coleman and Garrison, 1977, for a discussion of the geologic aspects of marine slope stability in a deltaic regimen). Grain size and degree of sorting are important factors influencing seismic stability. Loosely packed well-sorted fine sand and coarse silt are particularly prone to liquefaction. The strength of a particular sediment increases with both consolidation and cementation, and because both processes are time dependent, stability generally increases with the age of a sediment. Thus, failures are more common in Holocene sediment than in Pleistocene deposits, and more common in Pleistocene units than in earlier Cenozoic formations.

Because of the low strength of much marine sediment, submarine slope failures generally are larger and occur on flatter slopes than do subaerial failures (Hampton and others, 1978). Dimensions, slope, and relative importance of various instability factors (table 1) are compiled for several submarine slope failures attributable at least in part to strong seismic shaking. It is evident that failures on slopes of 1^{o} and less are not uncommon, may involve large areas, and can extend to sufficient depths to cause severe foundation problems.

Areal evaluation

Methods have been developed for evaluating the potential of earthquake-induced failures on both areal and site-specific bases. Areal evaluations typically express the relative likelihood of failure throughout a region, possibly with dimensions of tens or hundreds of kilometers. Though qualitative and broad in scope, areal assessments are particularly valuable early in the development of an offshore area, for example, in identifying areas where sea-floor failures are particularly likely and in establishing minimum technical stipulations for the siting and design of offshore facilities. Areal evaluations, however, are insufficiently detailed and precise to determine the final siting and design of an important offshore structure. For that purpose, a site-specific evaluation is needed that will provide more specific, quantitative information regarding the probability of sea-floor failure during the lifetime of the structure and the probability and extent of resulting sea-floor deformation.

Areal assessments of slope stability have been prepared for several earthquake-prone regions, both onshore (for example, Nilsen and others, 1979) and offshore (for example, Self and Mahmood, 1977). The variation in relative slope stability for part of the Kodiak shelf off Alaska is shown in fig. 40, using a fivefold classification of relative stability (table 2; Self and Mahmood, 1977). Classification of stability is based on three considerations: soil type, steepness of slope, and evidence of past slope failure. Soil types are differentiated both by stratigraphy—that is, geologic age and sediment type—and by engineering properties that could lead to varying foundation behavior. Soil types were mapped in a program of geophysical profiling, sea-floor sampling, and standard soil testing. The map provides a qualitative assessment of the variation in slope stability and identifies areas where slope-failure problems are likely to be either most acute or least severe. No information is provided, however, on the probability that slope failure will occur within a given exposure time. To date, areal evaluations of slope failure in seismic zones have not focused specifically on seismically induced slope failures but have considered all slope failures regardless of their origin. Nonetheless, recent research into the occurrence and mechanisms of earthquake-triggered slope failures is leading to areal assessments that specifically address seismically induced failures (for example, Wieczorek and others, 1985).

A method for probabilistic mapping of liquefaction potential on land (Youd and Perkins, 1978; Youd and others, 1978a) has been developed that incorporates information on the likelihood that a triggering level of ground shaking will occur within some future time interval. A liquefaction-potential map is prepared by combining two constituent maps: a liquefaction-opportunity map that depicts how often a level of ground shaking sufficient to cause liquefaction is likely to occur, and a liquefaction-susceptibility map that shows the distribution of sedimentary units and the relative ease with which the various units can liquefy during strong shaking. The resulting liquefaction-potential map delineates areas where liquefaction is most likely to occur over a given time interval, and is a useful guide to where additional site-specific investigations may be needed before specific siting and engineering decisions.

Site-specific evaluation

The degree of hazard that sea-floor failures can pose to offshore and coastal facilities justifies detailed multidisciplinary investigations to evaluate the stability of the sea floor at and surrounding the site (Garrison and Bea, 1977). An early step in site investigations should be a search for evidence of past failures that might indicate the possibility of future failures. The seismic-reflection techniques used in the identification of surface faults (see subsection above entitled "Geologic Record") are also applicable to the problem of detecting and mapping failures involving substantial deformation (figs. 13, 38). Other investigations needed to assess the seismic stability of the sea floor include detailed bathymetric surveys to determine slopes, geologic mapping and sampling to identify what materials are present and to recognize active geologic processes, seismologic studies to evaluate exposure to seismic shaking (see subsection above entitled "Seismic Shaking"), and geotechnical studies to determine the engineering properties of geologic materials.

Several methods are available for assessing the seismic liquefaction potential of saturated sediment (see reviews by Seed, 1979b, and Seed and Idriss, 1982). The existing methods may be categorized as

Table 1. Submarine slope failures attributed at least in part to seismic shaking

[Length of disturbed area is measured in the downslope direction. Individual failure dimensions: L, length; W, width. Importance of instability factors: E, earthquake shaking; W, wave loading; O, oversteepening; S, rapid sedimentation; G, free gas. Importance: H, high; M, moderate; L, low; N, negligible]

Region	Location	Physiographic setting	Water depth (m)	Slope (°)	Disturbed area			Individual failure dimensions (km)	Sedimentation rate ($m/10^3$ yr)	Importance of instability factors E W O S G	Reference
					Length (km)	Width (km)	Thickness (km)				
Southern California Borderland.	Off San Mateo Point.	Lower continental slope.	600-750	3-4	4.5 3.5	3 3	50 50	---	0.05-0.1	H N - N N	Edwards and others (1980).
Northern California Borderland.	Off Humboldt Bay.	Lower slope between continental shelf and marginal plateau.	460-580	1	6.5	15	30-85?	.35-0.60(W)	---	H N - - -	Lee and others (1981).
Do	Off the Klamath River.	Continental shelf-----	60-65	.25	.6-1.4	20	5	---	---	H - N - -	Field and others (1982)
Gulf of Alaska--------	Off Icy Bay------	do----------	48-200	.5	10-20	90	15-40	.5-1.0(L), .2(W)	68-80	M M N H N	Carlson (1978), Hampton and others (1978).
Do----------	Kayak Trough-----	do----------	42-227	1	18	15	20-120	---	7.5-15	H M L H M	Molnia and others (1977), Hampton and others (1978).
Do----------	Copper River prodelta.	do----------	40-125	.5	8	100	20-40	.3-1.0(L)	10-15	M M N H M	Hampton and others (1978).
Do----------	Off Portlock Bank.	Upper continental slope.	760-1,200	1.2	6.5	---	200	---	---	H N M N N	Do.
Do----------	Off Middle Albatross Bank.	do----------	690-1,300	3.4	5.3	12	300	---	---	H N H N N	Do.

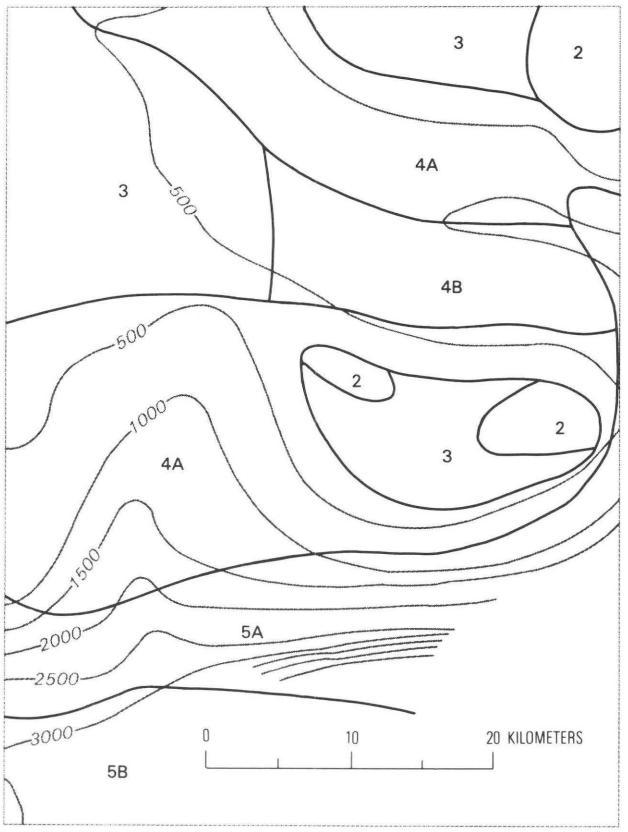

Figure 40. Relative-slope-stability map of part of the Continental Shelf south of Kodiak Island, Alaska, at approximately lat 56° N., long 154° W. (modified from Self and Mahmood, 1977, fig. 9). Heavy lines define areas of varying slope stability; numbers refer to classification scheme in table 2. Light lines are bathymetric contours (in feet).

either empirical or analytic. Empirical methods are based on field observations of liquefaction during previous earthquakes. The potential is evaluated by comparing the characteristics of the sediment and the expected earthquake shaking at the study site with those at sites where the presence or absence of liquefaction during earlier shocks has already been documented. Standard penetration resistance is the sediment characteristic most commonly used as the index of liquefaction susceptibility. Analytic methods are based on the behavior of saturated sediment during cyclic shearing as determined in laboratory investigations. Analytic methods featuring nonlinear-effective-stress analyses of the dynamic response of saturated sediment permit direct evaluation of cyclic mobility or liquefaction potential (Finn and others, 1977; Liou and others, 1977; Martin and Seed, 1979). Though new and relatively unproven, such methods promise to be highly useful in offshore applications. The application of both empirical and analytic methods was illustrated by Nataraja and others (1978) in a case study for a proposed waste-water outfall pipe extending about 800 m offshore from Puerto Rico.

The reliability and accuracy of empirical methods are limited by the sparseness of available field data on liquefaction and by the difficulties in reliably measuring sediment properties that are sensitive indicators of liquefaction susceptibility. Thus, empirical methods are most useful for preliminary evaluations of liquefaction potential. Where empirical methods do not indicate a large factor of safety, the evaluation should be supplemented by analytic methods (Seed, 1979b). Both empirical and analytic methods have been incorporated into probabilistic schemes for the site evaluation of liquefaction potential (for example, Yegian and Whitman, 1978; Haldar and Tang, 1979; Davis and Berrill, 1982).

Available methods for evaluating slope stability fall into two categories based on the failure criteria used in the analyses (Morgenstern and Sangrey, 1978). The first category includes limit-equilibrium methods, in which the stresses necessary to cause displacement along some postulated failure surface are compared with the available shear strength of the materials along this surface. Failure is considered to occur when stresses tending to cause displacement exceed the mobilized shear resistance of the material. The second category includes deformation methods, in which failure criteria are based on the deformation of a slope calculated from stress-strain analysis. Because it is the amount of deformation rather than the internal stresses in the material that poses a problem to the engineer, deformation methods of analysis are potentially more useful. Deformation methods, however, require knowledge of the stress-strain characteristics of the material, which is not needed in limit-equilibrium analyses, and also more sophisticated computations.

In limit-equilibrium methods, the inertial forces arising from seismic shaking are modeled as static forces that are resisted by the undrained shear strength mobilized along the potential failure surface at the time of failure (Morgenstern, 1967). Both horizontal and vertical components of seismic shaking can be accommodated (Hampton and others, 1978). Psuedostatic analyses of seismic slope stability by limit-equilibrium methods have been used to estimate the sensitivity of submarine slopes to seismic shaking (Morgenstern, 1967) and to evaluate the possible effect of shaking on slope stability on the continental slope off Israel (Almagor and Wiseman, 1977) and on the Continental Shelf and upper continental slope in the Gulf of Alaska (Hampton and others, 1978). There are difficulties with such pseudostatic methods, in regard both to the gross simplification of a complex dynamic process as an equivalent static process and to the selection of appropriate static-force coefficients to represent cyclic seismic forces (Seed, 1967).

In deformation methods of slope-stability analysis, the cyclicity of seismic shaking is explicitly accounted for in calculating the cumulative deformation of a slope. Newmark (1965) proposed a procedure for evaluating potential slope deformations for rigid-plastic stress-strain behavior, on the basis of a simple model of a block resting on an inclined plane that is subjected to seismic accelerations. In this model, when the seismic acceleration exceeds some critical threshold, the inertial forces acting on the block overcome the yield resistance, and the block slips. The history of downslope movement is calculated by twice integrating over time the effective acceleration

Table 2. Classification of relative slope stability, Kodiak shelf area, Alaska

[From Self and Mahmood (1977, table 1). Rock types: Ki, indurated metamorphic Cretaceous rock; Td, very dense and hard Tertiary sediment; Ti, indurated Tertiary rock. Soil types (all of Quaternary age): Qc, soft to stiff clays; Qg, glacial till; Qls, loose to firm sand and silt; Qsl, slide deposits; Qsw, migrating sand waves.]

Map unit (fig. 37)	Relative slope stability	Rock and soil types	Steepness of slope	Condition of slope
1	Highest----	Ti, Ki	Nearly flat to moderate-----	No evidence of mass movement or large-scale erosion.
2	High-------	Td	Nearly flat to moderately gentle.	Do.
3	Moderate---	Qg, Qc, Qls, Qsw.	do----------	No evidence of mass movement; some scour apparent.
4A	Low--------	Qg, Qc, Qls, Qsw, Td, Ti.	Moderate to very steep------	Evidence of creep or presence of tension cracks.
4B	Low--------	Qc, Qls	Nearly flat to steep--------	Lies at base of potentially unstable slope; may be covered by debris from future slides.
5A	Lowest-----	Qsl, Qc, Qls, Td, Ti.	Moderate to precipitous-----	Strong evidence of incipient or recent rotational, translatatory, or flow slides; probably unstable.
5B	Lowest-----	Qc, Qls	Nearly flat to steep--------	Lies at base of unstable (5A) slopes.

causing the block to slip. Using actual recordings of ground motion, Wilson and Keefer (1983) evaluated the procedure for a subaerial slope failure triggered by a moderate-size earthquake. The Newmark method has been extended in subsequent work to account explicitly for the buildup of pore pressures during earthquake shaking (Sarma, 1975) and to accommodate elasto-plastic stress-strain behavior (Makdisi and Seed, 1978). These deformation methods assume that the shear strength in the material along the failure surface is constant once failure begins. H.B. Seed and coworkers, employing finite-element-modeling techniques and dynamic testing of sediment and engineered soils in the laboratory, have developed more sophisticated methods of deformation analysis that allow for changes in the strengths of materials that occur during the course of an earthquake (Seed and others, 1975; Seed, 1979a). To date, these methods have been applied primarily to embankment dams, although they could also be extended to the evaluation of submarine slope stability. A limitation to the application of such sophisticated finite-element analyses is the difficulty in determining the dynamic strain-dependent strength properties of sediment. Although improvements in methods of soil testing are helping to reduce this obstacle, a serious unsolved problem is the recovery of samples of marine sediment that are sufficiently undisturbed to be suitable for laboratory testing to deduce their onsite engineering properties and dynamic behavior.

Turbidity currents

Because turbidity currents derive from subaqueous slope failures, evaluation of slope stability is an important aspect of assessing the likelihood and possible effects of turbidity currents. Additional factors to be investigated are the conditions under which a submarine slump or slide is transformed into turbulent flow, the offshore location at which these conditions exist, and the characteristics of turbidity currents that would pose hazards to offshore facilities. The strategy of hazard mitigation would then be one of avoidance or accommodation. If avoidance is impossible for facilities downslope from a potential slump area, design features will be required to mitigate the potential hazards from sediment scour and hydrodynamic-current loads, which may result from turbidity currents.

The first question to be addressed in any hazards assessment is whether the phenomenon can occur. It may be most useful to look first for evidence of past occurrence; circumstantial evidence can be sought both upslope and downslope from the site or project area. Upslope, bathymetry and shallow geologic structure can be examined for evidence of slope failures. Downslope, the fabric, sorting and composition of sediment can be examined where a turbidity current would be expected to dissipate and deposit its load. If the evidence for past currents is inconclusive, we must rely simply on evaluating the geologic and bathymetric conditions upslope from the site or project area. The methods discussed in the preceding subsection can be used to identify potentially unstable sedimentary slopes. In addition, consideration must be given to whether the sea-floor grade downslope from an area of potential instability is sufficiently steep for the slump or slide to attain the critical velocity for transformation into a turbidity current.

Although the conditions under which a submarine slump or slide is transformed into a turbidity current

are not well understood, steep slopes are clearly an important factor in the generation of turbidity currents. Thus, the potential for turbidity currents is greater on the continental slope, where petroleum exploration has not yet been vigorously pursued, than on the shelf. In particular, turbidity currents are recognized as an important sediment-transport process in submarine canyons on the continental slope; however, this does not imply that sufficient conditions of unstable sediment and steep slopes are absent on the Continental Shelf.

Tsunamis

Although tsunami wave heights are not great enough to be of concern in the design of offshore facilities in water depths of tens of meters, they can pose serious hazards to ancillary coastal facilities, such as loading terminals, storage tanks, and pipelines. All three mitigation strategies—selective siting, appropriate design, and early warning and preparedness—are to some degree effective in minimizing the losses from tsunamis, depending on whether the tsunami is of local or distant origin.

Evaluation of the potential occurrence and effects of locally generated tsunamis must follow an assessment of coastal and nearshore submarine slides (see subsection above entitled "Sea-Floor Failures"). Sites that are hazardous from the standpoint of coastal slumping are also subject to inundation from local slide-induced waves, as evidenced in Seward during the 1964 Alaska earthquake (fig. 16). The 1964 shock, however, also demonstrated that wave runup on shores adjacent to the area of coastal sliding is commonly smaller than on opposite-facing shores of bays and fiords (von Huene and Cox, 1972). To reliably evaluate potential local tsunami waves, knowledge is required of the history of local tsunamis and their generation mechanisms, the earthquake potential of the region, the seismic stability of coastal geologic units, and the hydrodynamics of the local coast, basin, or estuary. Typically, not all possible sources of local tsunamis can be identified, and so a design strategy to accommodate wave heights and runup greater than the largest known occurrences is important in coastal regions with high earthquake potential.

For tsunamis from distant sources, the hazard-mitigation strategy may involve not only prediction of tsunami effects as the basis for selective siting and appropriate design, but also early warning. Any site on a coast exposed to the open sea, or within a bay or inlet that is so exposed at its mouth, has some degree of tsunami exposure. The frequency of tsunami occurrence, however, varies significantly among the coastal regions of the world. Because approximately 80 percent of global earthquakes border the Pacific Ocean, the Pacific has a much higher frequency of tsunamis than other oceans; from 1900 to 1973, 200 tsunamis were observed or recorded in the Pacific (Spaeth, 1975). Though less frequent, tsunamis have also occurred in the Atlantic and Caribbean Oceans and in the Mediterranean and Black Seas. Compilations of historical occurrences are available for most coastal regions (Murty, 1977).

The characteristics of distant tsunami waves depend on the generation mechanism and other influences of the source region, modifications during oceanic propagation, and coastal modifications in the vicinity of the site in question (Murty, 1977). Because records are not commonly available on the open ocean, the oceanic characteristics can be estimated only qualitatively from what is known of the generation mechanism and from observed properties of the waves at coastal sites. As a tsunami approaches a coast, the tsunami is modified extensively. The continental slope tends to reflect energy back to sea; the continental shelf tends to trap energy at wavelengths on the order of the shelf width; the coastal zone acts as a filter with characteristics determined by the coastal configuration and bathymetry (Cox, 1972); and, finally, the topography of the coastline influences wave runup on shore.

To mitigate potential coastal hazards, either through selective siting to minimize exposure or through design to accommodate effects, tsunami wave heights and runup distances must be predicted on the basis of the historical record and numerical modeling (Houston, 1979; Camfield, 1980). If the historical record is adequate to establish the frequency of tsunamis of various sizes, then the probability that a tsunami wave will exceed a given height over some future time interval can be calculated. A probabilistic tsunami map for the contiguous United States and Alaska (fig. 41) shows the tsunami hazard to be greater on the Pacific coast than on the Atlantic, Gulf, or Arctic coasts, and greatest along the Gulf of Alaska. Detailed hazard maps for California, Oregon, Washington, and Hawaii were presented by Houston (1979, figs. 3-11).

For a site at which significant tsunamis are expected, the last line of defense is shutdown and evacuation after early warning of an impending tsunami. The Pacific region is served by the Pacific Tsunami Warning Center in Honolulu (Spaeth, 1975), which issues two basic types of bulletins. "Watch" bulletins are issued when an earthquake has been detected that is of sufficient magnitude and in such a location that generation of a tsunami is possible. "Warnings" are issued when the Center has received positive evidence, from tide-gage stations in the source region, that a tsunami has been generated; such warnings contain the estimated times of arrival of the principal wave at the participating stations. Major offshore petroleum operations in the coastal Pacific would be linked to this warning system, either directly or through a local participating agency.

Regional tsunami-warning systems are also in operation in areas with a history of damaging tsunamis; the most highly developed such systems are in Alaska (Butler, 1971; Sokolowski and others, 1984) and Japan (Ichikawa and Watanabe, 1983). These systems have data from regional seismograph and tide-gage stations telemetered to a central location. Nearby, potentially tsunamigenic earthquakes are located rapidly, generally within 15 minutes, and a warning is issued to the local area. Because these warnings are based on seismic data alone, they are commonly issued when tsunamis have not actually been generated. Confirmation of tsunami generation, however, is soon obtained, and so inconveniences due

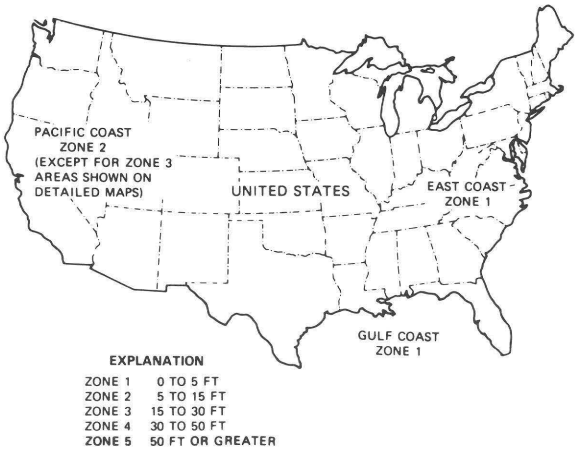

Figure 41. Probabilistic map of tsunami elevation for the contiguous United States and Alaska at a 10-percent probability of exceedence in 50 years, or a return period of about 500 years (from Houston, 1979, fig. 2).

to false warnings are minimal, given the high level of protection provided by the system.

CONCLUSION

This report has provided a general overview of the subject of earthquakes and their effects at offshore sites. For examples, we have drawn on our experience and some of the pertinent literature pertaining to earthquakes in Canada and the United States and their adjacent offshore areas. A glance at a global-seismicity map reveals that similar seismic conditions prevail in numerous areas worldwide where an offshore petroleum potential exists in geologic environments similar to those of North America. The techniques for assessment of earthquake potential and the evaluation and mitigation of earthquake hazards discussed here pertain equally to these areas.

The subjects discussed here are an inexact science. The earthquake potential of a given region, such as the Gulf of Alaska, may be obvious to anyone working in the Earth sciences. However, the effects that these earthquakes will have in areas of exploitable petroleum resources are not so obvious, even to the specialist. The offshore environment is a frontier not only for petroleum development but also for the evaluation of earthquake effects and their attendant hazards to marine facilities. Mitigation of potential hazards requires state-of-the-art investigations and good measures of scientific, engineering, and socioeconomic judgment.

Potential earthquake hazards are not restricted to tectonically active continental margins that have undergone numerous historical earthquakes. Significant parts of this report have dealt with the passive margins of eastern North America, where evaluation and mitigation are made more difficult by our inability to explain the earthquakes there in simple global tectonic terms.

REFERENCES CITED

Abe, Katsuyuki, and Kanamori, Hiroo, 1980, Magnitudes of great shallow earthquakes from 1953 to 1977: Tectonophysics, v. 62, no. 3-4, p. 191-203.

Aki, Keiiti, 1982, Strong motion prediction using mathematical modeling techniques: Seismological Society of America Bulletin, v. 72, no. 6, pt. B, p. S29-S41.

Algermissen, S.T., Perkins, D.M., Thenhaus, P.C., Hanson, S.L., and Bender, B.L., 1982, Probabilistic estimates of maximum acceleration and velocity in rock in the contiguous United States: U.S. Geological Survey Open-File Report 82-1033, 77 p.

Allen, C.R., 1975, Geological criteria for evaluating seismicity: Geological Society of America Bulletin, v. 86, no. 8, p. 1041-1057.

Allen, C.R., Hanks, T.C., and Whitcomb, J.H., 1975, Seismological studies of the San Fernando earthquake and their tectonic implications, in Oakeshott, G.B., ed., San Fernando, California, earthquake of 9 February 1971: California Division of Mines and Geology Bulletin 196, p. 257-262.

Almagor, Gideon, and Wiseman, Gdalyah, 1977, Analysis of submarine slumping in the continental slope of the southern coast of Israel: Marine Geotechnology, v. 2 (Marine Slope Stability Volume), p. 349-388.

American Petroleum Institute, 1982, Recommended practice for planning, designing, and constructing fixed offshore platforms (13th ed.): Publication API RP 2A, 96 p.

Anderson, J.G., 1979, Estimating the seismicity from geological structure for seismic-risk studies: Seismological Society of America Bulletin, v. 69, no. 1, p. 135-158.

Ando, Masataka, 1977, Slip rates and recurrence times from analysis of major earthquakes on Pacific-North American plate boundary in western North

America [abs.]: Eos (American Geophysical Union Transactions), v. 58, no. 6, p. 438.

Applied Technology Council, 1978, Tentative provisions for the development of seismic regulations for buildings: U.S. National Bureau of Standards Special Publication 510, 514 p.

Ariman, Teoman, and Muleski, G.E., 1981, A review of the response of buried pipelines under seismic excitations: Earthquake Engineering and Structural Dynamics, v. 9, no. 2, p. 133-151.

Arno, N.L., and McKinney, L.F., 1973, Harbor and waterfront facilities, in The great Alaska earthquake of 1964: Engineering: Washington, U.S. National Academy of Sciences, p. 526-643.

Ayres, J.M., and Sun, T.-Y., 1973, Nonstructural damage, in Benfer, N.A., and Coffman, J.L., eds., San Fernando, California, earthquake of February 9, 1971: Washington, U.S. Department of Commerce, National Oceanic and Atmospheric Administration, Environmental Research Laboratories, v. 1, pt. B, p. 735-776.

Ayres, J.M., Sun, T.-Y., and Brown, F.R., 1973, Nonstructural damage to buildings, in The great Alaska earthquake of 1964: Engineering: Washington, U.S. National Academy of Sciences, p. 346-456.

Basham, P.W., and Adams, John, 1982, Earthquake hazards to offshore development on the eastern Canadian continental shelves: Canadian Conference on Marine Geotechnical Engineering, 2d, Dartmouth, Nova Scotia, Canada, 1982, Proceedings, 6 p.

Basham, P.W., Adams, John, and Anglin, F.M., 1983, Earthquake source models for estimating seismic risk on the eastern Canadian continental margin: Canadian Conference on Earthquake Engineering, 4th, Vancouver, British Columbia, Canada, 1983, Proceedings, p. 495-508.

Basham, P.W., Weichert, D.H., Anglin, F.M., and Berry, M.J., 1982, New probabilistic strong seismic ground motion maps of Canada: A compilation of earthquake source zones, methods and results: Ottawa, Ontario, Canadian Department of Energy, Mines and Resources, Earth Physics Branch Open-File Report 82-33, 205 p.

-----1984, New probabilistic strong seismic ground motion maps of Canada: Seismological Society of America Bulletin, v. 75, no.2, p. 563-595.

Bea, R.G., 1979, Earthquake and wave design criteria for offshore platforms: American Society of Civil Engineers Proceedings, Structural Division Journal, v. 105, no. ST2, p. 401-419.

Bea, R.G., Audibert, J.M.E., and Akky, M.R., 1979, Earthquake response of offshore platforms: American Society of Civil Engineers Proceedings, Structural Division Journal, v. 105, no. ST2, p. 377-400.

Benfer, N.A., and Coffman, J.L., eds., 1973, Utilities, transportation, and sociological aspects, v. 2 of San Fernando, California, earthquake of February 9, 1971: Washington, U.S. Department of Commerce, National Oceanic and Atmospheric Administration, Environmental Research Laboratories, 325 p.

Berg, Eduard, Cox, D.C., Furumoto, A.S., Kajiura, K., Kawasumi, H., and Shima, E., 1972, Source of major tsunami, in The great Alaska earthquake of 1964: Oceanography and coastal engineering: Washington, U.S. National Academy of Sciences, p. 122-139.

Bolt, B.A., 1978, The local magnitude M_L of the Kern County earthquake of July 21, 1952: Seismological Society of America Bulletin, v. 68, no. 2, p. 513-515.

Bonilla, M.G., 1970, Surface faulting and related effects, in Wiegel, R.L., ed., Earthquake engineering: Englewood Cliffs, N.J., Prentice-Hall, p. 47-74.

-----1973, Trench exposures across surface fault ruptures associated with San Fernando earthquake, in Benfer, N.A., Coffman, J.L., and Bernick, J.R., eds., San Fernando, California, earthquake of February 9, 1971: Washington, U.S. Department of Commerce, National Oceanic and Atmospheric Administration, Environmental Research Laboratories, v. 3, p. 173-182.

Bonilla, M.G., Mark, R.K., and Lienkaemper, J.J., 1984, Statistical relations among earthquake magnitude, surface rupture length, and surface fault displacement: Seismological Society of America Bulletin, v. 74, no. 6, p. 2379-2411.

Boore, D.M., 1977, The motion of the ground in earthquakes: Scientific American, v. 237, no. 6, p. 68-78.

-----1983, Strong-motion seismology--1979 through 1980: Reviews of Geophysics and Space Physics, v. 21, no. 6, p. 1308-1318.

Boore, D.M., and Joyner, W.B., 1982, The empirical prediction of ground motion: Seismological Society of America Bulletin, v. 72, no. 6, pt. B, p. S43-S60.

Bouchon, Michel, and Aki, Keiiti, 1980, Simulation of long-period, near-field motion for the great California earthquake of 1857: Seismological Society of America Bulletin, v. 70, no. 5, p. 1669-1682.

Brune, J.N., 1970, Tectonic stress and the spectra of seismic shear waves from earthquakes: Journal of Geophysical Research, v. 75, no. 26, p. 4997-5009.

Buchanan-Banks, J.M., Pampeyan, E.H., Wagner, H.C., and McCulloch, D.S., 1978, Preliminary map showing recency of faulting in coastal south-central California: U.S. Geological Survey Miscellaneous Field Studies Map MF-910, 11 p., scale 1:250,000, 3 sheets.

Burford, R.O., and Harsh, P.W., 1980, Slip on the San Andreas fault in central California from alinement array surveys: Seismological Society of America Bulletin, v. 70, no. 4, p. 1233-1261.

Burford, R.O., Nason, R.D., and Harsh, P.W., 1978, Studies of fault creep in central California: U.S. Geological Survey Earthquake Information Bulletin, v. 10, no. 5, p. 174-181.

Butler, H.M., 1971, Palmer Seismological Observatory: Earthquake Notes, v. 42, no. 1, p. 15-36.

Camfield, F.E., 1980, Tsunami engineering: Fort

Belvoir, Va., U.S. Army Corps of Engineers, Coastal Engineering Research Center Special Report 6, 222 p.

Campbell, K.W., 1981, Near-source attenuation of peak horizontal acceleration: Seismological Society of America Bulletin, v. 71, no. 6, p. 2039-2070.

Carlson, P.R., 1978, Holocene slump on continental shelf off Malaspina Glacier, Gulf of Alaska: American Association of Petroleum Geologists Bulletin, v. 62, no. 12, p. 2412-2426.

Carlson, P.R., and Molnia, B.F., 1977, Submarine faults and slides on the continental shelf, northern Gulf of Alaska: Marine Geotechnology, v. 2 (Marine Slope Stability Volume), p. 275-290.

Carlson, P.R., Plafker, George, and Bruns, T.R., 1985, Selected seismic profiles and map of the seaward extension of the Fairweather fault, eastern Gulf of Alaska: U.S. Geological Survey Miscellaneous Field Studies Map, scale 1:500,000, 2 sheets in press .

Chavez, Dave, Gonzalez, Javier, Reyes, Alfonso, Medina, Mauru, Duarte, Carlos, Brune, J.N., Vernon, F.L., III, Simons, Richard, Hutton, L.K., German, P.T., and Johnson, C. E., 1982, Mainshock location and magnitude determination using combined U.S. and Mexican data, in The Imperial Valley, California, earthquake of October 15, 1979: U.S. Geological Survey Professional Paper 1254, p. 51-54.

Chung, D.H., and Bernreuter, D.L., 1981, Regional relationships among earthquake magnitude scales: Reviews of Geophysics and Space Physics, v. 19, no. 4, p. 649-663.

Clifford, P.J., Germain, F.R., and Cason, R.L., 1979, A totally new approach to seafloor mapping: Offshore Technology Conference, 11th, Houston, Tex., Proceedings, v. 3, p. 1681-1689.

Coleman, J.M., and Garrison, L.E., 1977, Geological aspects of marine slope stability, northwestern Gulf of Mexico: Marine Geotechnology, v. 2 (Marine Slope Stability Volume), p. 9-44.

Cornell, C.A., 1968, Engineering seismic risk analysis: Seismological Society of America Bulletin, v. 58, no. 5, p. 1583-1606.

Coulter, H.W., and Migliaccio, R.P., 1966, Effects of the earthquake of March 27, 1964, at Valdez, Alaska: U.S. Geological Survey Professional Paper 542-C, p. C1-C36.

Cox, D.C., 1972, Review of the tsunami, in The great Alaska earthquake of 1964: Oceanography and coastal engineering: Washington, U.S. National Academy of Sciences, p. 354-360.

Crouse, C.B., Hileman, J.A., Turner, B.E., and Martin, G.R., 1980, Compilation, assessment and expansion of the strong earthquake ground motion data base: U.S. Nuclear Regulatory Commission Report NUREG/CR-1660, 135 p.

Davis, R.O., and Berrill, J.B., 1982, Energy dissipation and seismic liquefaction in sands: Earthquake Engineering and Structural Dynamics, v. 10, no. 1, p. 59-68.

Delflache, M.L., Glasscock, M.S., Hayes, D.A., Ruez, W.J., and Wildenstein, A.W., 1977, Design of the Hondo Platform for 850-feet water depth in the Santa Barbara Channel: Offshore Technology Conference, 9th, Houston, Tex., 1977, Proceedings, v. 4, p. 17-26.

Dewey, J.W., 1979, A consumer's guide to instrumental methods for determination of hypocenters, in Hatheway, A.W., and McClure, C.R., Jr., eds., Geology in the siting of nuclear power plants: Geological Society of America Reviews in Engineering Geology, v. 4, p. 109-117.

Doxsee, W.W., 1948, The Grand Banks Newfoundland earthquake of November 18, 1929: Ottawa, Ontario, Canada, Dominion Observatory Publications, v. 7, no. 7, p. 323-335.

Eckel, E.B., 1967, Effects of the earthquake of March 27, 1964, on air and water transport, communications, and utilities systems in south-central Alaska: U.S. Geological Survey Professional Paper 545-B, p. B1-B27.

Edwards, B.D., Field, M.E., and Clukey, E.C., 1980, Geological and geochemical analysis of a submarine slump, California borderland: Offshore Technology Conference, 12th, Houston, Tex., 1980, Proceedings, v. 1, p. 399-410.

Engdahl, E.R., Dewey, J.W., and Fujita, Kazuya, 1982, Earthquake location in island arcs: Physics of the Earth and Planetary Interiors, v. 30, no. 2, p. 145-156.

Engdahl, E.R., and Lee, W.H.K., 1976, Relocation of local earthquakes by seismic ray tracing: Journal of Geophysical Research, v. 81, no. 23, p. 4400-4406.

Field, M.E., Gardner, J.V., Jennings, A.E., and Edwards, B.D., 1982, Earthquake-induced sediment failure on a 0.25° slope, Klamath River delta, California: Geology, v. 10, no. 10, p. 542-546.

Finn, W.D.L., Lee, K.W., and Martin, G.R., 1977, An effective stress model for liquefaction: American Society of Civil Engineers Proceedings, Geotechnical Engineering Division Journal, v. 103, no. GT6, p. 517-533.

Fletcher, J.B., and Sykes, L.R., 1977, Earthquakes related to hydraulic mining and natural seismic activity in western New York State: Journal of Geophysical Research, v. 82, no. 26, p. 3767-3780.

Fuis, G.S., 1982, Displacement along the Superstition Hills fault triggered by the earthquake, in The Imperial Valley, California, earthquake of October 15, 1979: U.S. Geological Survey Professional Paper 1254, p. 145-154.

Fukao, Yoshio, 1973, Thrust faulting at a lithospheric plate boundary: The Portugal earthquake of 1969: Earth and Planetary Science Letters, v. 18, no. 2, p. 205-216.

Garrison, L.E., and Bea, R.G., 1977, Bottom stability as a factor in platform siting and design: Offshore Technology Conference, 9th, Houston, Tex., 1977, Proceedings, v. 3, p. 127-133.

Gawthrop, William, 1975, Seismicity of the central California coastal region: U.S. Geological Survey Open-File Report 75-134, 87 p.

-----1978, The 1927 Lompoc, California, earthquake: Seismological Society of America Bulletin, v. 68, no. 6, p. 1705-1716.

Gohn, G.S., ed., 1983, Studies related to the Charleston, South Carolina, earthquake of 1886--tectonics and seismicity: U.S. Geological Survey Professional Paper 1313.

Greene, H.G., Lee, W.H.K., McCulloch, D.S., and Brabb, E.E., 1973, Faults and earthquakes in the Monterey Bay region, California: U.S. Geological Survey Miscellaneous Field Studies Map MF-518, scale 1:250,000, 4 sheets.

Gutenberg, Beno, and Richter, C.F., 1954, Seismicity of the Earth and associated phenomena (2d ed.): Princeton, N.J., Princeton University Press, 310 p.

Haldar, Achintya, and Tang, W.H., 1979, Probabilistic evaluation of liquefaction potential: American Society of Civil Engineers Proceedings, Geotechnical Engineering Division Journal, v. 105, no. GT2, p. 145-163.

Hampton, M.A., 1972, The role of subaqueous debris flow in generating turbidity currents: Journal of Sedimentary Petrology, v. 42, no. 4, p. 775-793.

Hampton, M.A., and Bouma, A.H., 1977, Slope instability near the shelf break, western Gulf of Alaska: Marine Geotechnology, v. 2 (Marine Slope Stability Volume), p. 309-331.

Hampton, M.A., Bouma, A.H., Carlson, P.R., Molnia, B.F., Clukey, E.C., and Sangrey, D.A., 1978, Quantitative study of slope instability in the Gulf of Alaska: Offshore Technology Conference, 10th, Houston, Tex., 1978, Proceedings, v. 4, p. 2307-2318.

Hanks, T.C., 1976, Observations and estimation of long-period strong ground motion in the Los Angeles Basin: Earthquake Engineering and Structural Dynamics, v. 4, no. 5, p. 473-488.

----1979a, $\underline{b}$ values and $\omega^{-\gamma}$ seismic source models: Implications for tectonic stress variations along active crustal fault zones and the estimation of high-frequency strong ground motion: Journal of Geophysical Research, v. 84, no. B5, p. 2235-2242.

---1979b, The Lompoc, California, earthquake (November 4, 1927; $\underline{M}$ = 7.3) and its aftershocks: Seismological Society of America Bulletin, v. 69, no. 2, p. 451-462.

Hanks, T.C., Hileman, J.A., and Thatcher, Wayne, 1975, Seismic movements of the larger earthquakes of the southern California region: Geological Society of America Bulletin, v. 86, no. 8, p. 1131-1139.

Hanks, T.C., and Kanamori, Hiroo, 1979, A moment magnitude scale: Journal of Geophysical Research, v. 84, no. B5, p. 2348-2350.

Hanson, R.D., 1973, Behavior of liquid-storage tanks, in The great Alaska earthquake of 1964: Engineering: Washington, U.S. National Academy of Sciences, p. 331-339.

Hasegawa, H.S., Basham, P.W., and Berry, M.J., 1981, Attenuation relations for strong seismic ground motion in Canada: Seismological Society of America Bulletin, v. 71, no. 6, p. 1943-1962.

Hasegawa, H.S., Chou, C.W., and Basham, P.W., 1979, Seismotectonics of the Beaufort Sea: Canadian Journal of Earth Sciences, v. 16, no. 4, p. 816-830.

Hasegawa, H.S., Lahr, J.C., and Stephens, C.D., 1980, Fault parameters of the St. Elias, Alaska, earthquake of February 28, 1979: Seismological Society of America Bulletin, v. 70, no. 5, p. 1651-1660.

Hastie, L.M., and Savage, J.C., 1970, A dislocation model for the 1964 Alaska earthquake: Seismological Society of America Bulletin, v. 60, no. 4, p. 1389-1392.

Hays, W.W., 1980, Procedures for estimating earthquake ground motions: U.S. Geological Survey Professional Paper 1114, 77 p.

Hays, W.W., ed., 1983, A workshop on "The 1886 Charleston earthquake and its implications for today": Proceedings of Conference XX: U.S. Geological Survey Open-File Report 83-843, 502 p.

Healy, J.H., Rubey, W.W., Griggs, D.T., and Raleigh, C.B., 1968, The Denver earthquakes: Science, v. 161, no. 3848, p. 1301-1310.

Heaton, T.H., and Kanamori, Hiroo, 1984, Seismic potential associated with subduction in the northwestern United States: Seismological Society of America Bulletin, v. 74, no. 3, p. 933-941.

Heezen, B.C., and Drake, C.L., 1964, Grand Banks slump: American Association of Petroleum Geologists Bulletin, v. 48, no. 2, p. 221-225.

Heezen, B.C., Ericson, D.B., and Ewing, Maurice, 1954, Further evidence for a turbidity current following the 1929 Grand Banks Newfoundland earthquake: Deep-Sea Research, v. 1, no. 4, p. 193-202.

Heezen, B.C., and Ewing, Maurice, 1952, Turbidity currents and submarine slumps, and the 1929 Grand Banks Newfoundland earthquake: American Journal of Science, v. 250, no. 12, p. 849-873.

---1955, Orleansville Algeria earthquake and turbidity currents: American Association of Petroleum Geologists Bulletin, v. 39, no. 12, p. 2505-2514.

Heidebrecht, A.C., Basham, P.W., Rainer, J.H., and Berry, M.J., 1984, Engineering applications of new probabilistic seismic ground motion maps of Canada: Canadian Journal of Civil Engineering, v. 10, no. 4, p. 670-680.

Henyey, T.L., Teng, T.-I., McRaney, J.K., and Manov, D.V., 1979, A sea-floor seismic monitoring network around an offshore oilfield platform and recording of the August 13, 1978, Santa Barbara earthquake: Offshore Technology Conference, 11th, Houston, Tex., 1979, Proceedings v. 5, p. 2219-2223.

Hermann, R.B., Park, S.-K., and Wang, C.-Y., 1981, The Denver earthquakes of 1967-1968: Seismological Society of America Bulletin, v. 71, no. 3, p. 731-745.

Houston, J.R., 1979, Tsunamis, seiches and landslide-induced water waves: Vicksburg, Miss., U.S. Army Engineer Waterways Experiment Station Miscellaneous Paper S-73-1, Report 15, 88 p.

Hove, K., Selnes, P.B., and Burngum, Hilomar, 1982, Seaquakes: A potential threat to offshore structures: Oslo, Norwegian Geotechnical Institute Publication 143, 9 p.

Hove, K., 1983, Seaquakes, an hazard to offshore platforms?, in Ritsema, A.R., and Gürpinar, Aybars, eds., in Seismicity and seismic risk in the offshore North Sea area: Dordrecht, Holland, Reidel, p. 149-150.

Hsieh, P.A., and Bredehoeft, J.D., 1981, A reservoir analysis of the Denver earthquakes: A case of induced seismicity: Journal of Geophysical Research, v. 86, no. B2, p. 903-920.

Hyndman, R.D., and Ellis, R.M., 1981, Queen Charlotte fault zone: Microearthquakes from a temporary array of land stations and ocean bottom seismographs: Canadian Journal of Earth Sciences, v. 18, no. 4, p. 776-788.

Hyndman, R.D., Riddihough, R.P., and Herzer, R., 1979, The Nootka fault zone--a new plate boundary off western Canada: Royal Astronomical Society Geophysical Journal, v. 58, no. 3, p. 667-683.

Hyndman, R.D., and Rogers, G.C., 1981, Seismicity surveys with ocean bottom seismographs off western Canada: Journal of Geophysical Research, v. 86, no. B5, p. 3867-3880.

Hyndman, R.D., Rogers, G.C., Bone, M.N., Lister, C.R.B., Wade, U.S., Barrett, D.L., Davis, E.E., Lewis, T., Lynch, S., and Seeman, D., 1978, Geophysical measurements in the region of the Explorer ridge off western Canada: Canadian Journal of Earth Sciences, v. 15, no. 9, p. 1508-1525.

Ichikawa, Masaji, and Watanabe, Hideo, 1983, A new system for tsunami warning in the Japan Meteorological Agency, in Iida, K., and Iwasaki, T., eds., Tsunamis: Their science and engineering: Tokyo, Terra Scientific Publishing, p. 51-60.

Idriss, I.M., 1978, Characteristics of earthquake ground motions, in Earthquake engineering and soil dynamics: American Society of Civil Engineers, Geotechnical Engineering Division Specialty Conference, Pasadena, Calif., 1978, Proceedings, v. 3, p. 1151-1265.

Jennings, C.W., 1975, Fault map of California with locations of volcanoes, thermal springs and thermal wells: California Division of Mines and Geology Geologic Data Map 1, scale 1:750,000.

Johnson, J.A., and Traubenik, M.L., 1978, Magnitude-dependent near-source ground motion spectra, in Earthquake engineering and soil dynamics: American Society of Civil Engineers, Geotechnical Engineering Division Specialty Conference, Pasadena, Calif., 1978, Proceedings, v. 1, p. 530-539.

Johnson, L.R., and Silva, Walt, 1981, The effects of unconsolidated sediments upon the ground motion during local earthquakes: Seismological Society of America Bulletin, v. 71, no. 1, p. 127-142.

Johnson, S.H., and Jones, P.R., 1978, Microearthquakes located on the Blanco fracture zone with sonobuoy arrays: Journal of Geophysical Research, v. 83, no. B1, p. 255-261.

Jones, P.R., and Johnson, S.H., 1978, Sonobuoy array measurements of active faulting on the Gorda Ridge: Journal of Geophysical Research, v. 83, no. B7, p. 3435-3440.

Joyner, W.B., and Boore, D.M., 1981, Peak horizontal acceleration and velocity from strong-motion records including records from the 1979 Imperial Valley, California, earthquake: Seismological Society of America Bulletin, v. 71, no. 6, p. 2011-2038.

Joyner, W.B., and Chen, A.T.F., 1975, Calculation of nonlinear ground response in earthquakes: Seismological Society of America Bulletin, v. 65, no. 5, p. 1315-1336.

Joyner, W.B., Warrick, R.E., and Oliver, A.A., III, 1976, Analysis of seismograms from a downhole array in sediments near San Francisco Bay: Seismological Society of America Bulletin, v. 66, no. 3, p. 937-958.

Jungels, P.H., and Frazier, G.A., 1973, Finite element analysis of the residual displacements for an earthquake rupture: Source parameters for the San Fernando California earthquake: Journal of Geophysical Research, v. 78, no. 23, p. 5062-5083.

Kachadoorian, Reuben, 1965, Effects of the earthquake of March 27, 1964, at Whittier, Alaska: U.S. Geological Survey Professional Paper 542-B, p. B1-B21.

Kanamori, Hiroo, 1977, The energy release in great earthquakes: Journal of Geophysical Research, v. 82, no. 20, p. 2981-2987.

-----1979, A semi-empirical approach to prediction of long-period ground motions from great earthquakes: Seismological Society of America Bulletin, v. 69, no. 6, p. 1645-1670.

Kanamori, Hiroo, and Anderson, D.L., 1975, Theoretical basis of some empirical relations in seismology: Seismological Society of America Bulletin, v. 65, no. 5, p. 1073-1095.

Kanamori, Hiroo, and Jennings, P.C., 1978, Determination of local magnitudes, M_L, from strong-motion accelerograms: Seismological Society of America Bulletin, v. 68, no. 2, p. 471-485.

Kanamori, Hiroo, and Regan, Janice, 1982, Long-period surface waves, in The Imperial Valley, California, earthquake of October 15, 1979: U.S. Geological Survey Professional Paper 1254, p. 55-58.

Keen, C.E., and Hyndman, R.D., 1979, Geophysical review of the continental margins of eastern and western Canada: Canadian Journal of Earth Sciences, v. 16, no. 3, pt. 2, p. 712-747.

Kennedy, R.P., Darrow, A.C., and Short, S.A., 1977, General considerations for seismic design of oil pipeline systems, in The current state of knowledge of lifeline earthquake engineering: American Society of Civil Engineers, Technical Council of Lifeline Earthquake Engineering Specialty Conference, Los Angeles, 1977, Proceedings, p. 2-17.

King, L.H., 1980, Aspects of regional surficial geology related to site investigation requirements--eastern Canadian shelf, in Ardus, D.A., ed., Offshore site investigation: London, Graham and Trotman, p. 37-57.

King, L.H., and MacLean, Brian, 1970, Continuous seismic-reflection study of Orpheus gravity anomaly: American Association of Petroleum Geologists Bulletin, v. 54, no. 11, p. 2007-2031.

Kost, Garrison, and Sharpe, R.L., 1977, Seismic-resistant design of piping, equipment and appurtenances for offshore-structures: Offshore Technology Conference, 9th, Houston, Tex., 1977, Proceedings, v. 1, p. 203-214.

Krause, D.C., White, W.C., Piper, D.J.W., and Heezen, B.C., 1970, Turbidity currents and cable breaks in the western New Britain Trench: Geological Society of America Bulletin, v. 81, no. 7, p. 2153-2160.

Kuenen, P.H., 1952, Estimated size of the Grand Banks turbidity current: American Journal of Science, v. 250, no. 12, p. 874-884.

Lahr, J.C., and Plafker, George, 1980, Holocene Pacific-North America plate interaction in southern Alaska: Implications for the Yakataga seismic gap: Geology, v. 8, no. 10, p. 483-486.

Lahr, J.C., Stephens, C.D., Hasegawa, H.S., and Boatwright, John, 1980, Alaska seismic gap only partially filled by 28 February 1979 earthquake: Science, v. 207, no. 4437, p. 1351-1353.

Lajoie, K.R., Sarna-Wojcicki, A.M., and Yerkes, R.F., 1982, Quaternary chronology and rates of crustal deformation in the Ventura area, California, in Cooper, J.D., compiler, Neotectonics in southern California: Geological Society of America Guidebook for Field Trips, 1982, p. 43-51.

Lawson, A.C., chairman, 1908, The California earthquake of April 18, 1906: Report of the State Earthquake Investigation Commission: Carnegie Institution of Washington Publication 87, 451 p.

Lay, Thorne, Given, J.W., and Kanamori, Hiroo, 1982, Long-period mechanism of the 8 November 1980, Eureka, California, earthquake: Seismological Society of America Bulletin, v. 72, no. 2, p. 439-456.

Lee, H.J., Edwards, B.D., and Field, M.E., 1981, Geotechnical analysis of a submarine slump, Eureka, California: Offshore Technology Conference, 13th, Houston, Tex., 1981, Proceedings, v. 4, p. 53-65.

Lee, K.L., and Seed, H.B., 1967, Cyclic stress conditions causing liquefaction of sand: American Society of Civil Engineers Proceedings, Soil Mechanics and Foundations Division Journal, v. 93, no. SM1, p. 47-70.

Lee, W.H.K., Johnson, C.E., Henyey, T.L., and Yerkes, R.F., 1978, A preliminary study of the Santa Barbara, California, earthquake of August 13, 1978, and its major aftershocks: U.S. Geological Survey Circular 797, 14 p.

Lee, W.H.K., and Stewart, S.W., 1981, Principles and applications of microearthquake networks (Advances in Geophysics, supp. 2): New York, Academic Press, 293 p.

Lee, W.H.K., Yerkes, R.F., and Simirenko, M., 1979, Recent earthquake activity and focal mechanisms in the western Transverse Ranges, California: U.S. Geological Survey Circular 799-A, 26 p.

Lefort, J.P., and Haworth, R.T., 1978, Geophysical study of basement fractures on the western European and eastern Canadian shelves: Transatlantic correlations and late Hercynian movements: Canadian Journal of Earth Sciences, v. 15, no. 3, p. 397-404.

Lemke, R.W., 1967, Effects of the earthquake of March 27, 1964, at Seaward, Alaska: U.S. Geological Survey Professional Paper 542-E, p. E1-E43.

Liou, C.P., Streeter, V.L., and Richart, F.E., 1977, Numerical model for liquefaction: American Society of Civil Engineers Proceedings, Geotechnical Engineering Division Journal, v. 103, no. GT6, p. 589-606.

Machette, M.N., 1978, Dating Quaternary faults in the southwestern United States by using buried calcic paleosols: U.S. Geological Survey Journal of Research, v. 6, no. 3, p. 369-381.

Makdisi, F.I., and Seed, H.B., 1978, Simplified procedure for estimating dam and embankment earthquake-induced deformation: American Society of Civil Engineers Proceedings, Geotechnical Engineering Division Journal, v. 104, no. GT7, p. 849-867.

Malloy, R.J., and Merrill, G.F., 1969, Vertical crustal movement of the sea floor associated with the Prince William Sound, Alaska, earthquake, in Leipold, L.E., ed., The Prince William Sound, Alaska, earthquake of 1964 and aftershocks: U.S. Department of Commerce, Coast and Geodetic Survey Publication 10-3, v. 2, pt. C, p. 327-338.

Martin, G.R., Lam, I.P., Tsai, C.F., and Anderson, D.G., 1979, Seismic response of soft offshore soils--a parametric study: U.S. National Conference on Earthquake Engineering, 2d, Stanford, Calif., 1979, Proceedings: Berkeley, Calif., Earthquake Engineering Research Institute, p. 583-592.

Martin, P.P., and Seed, H.B., 1979, Simplified procedure for effective stress analysis of ground response: American Society of Civil Engineers Proceedings, Geotechnical Engineering Division Journal, v. 105, no. GT6, p. 739-758.

McCann, W.R., Perez, O.J., and Sykes, L.R., 1980, Yakataga gap, Alaska: Seismic history and earthquake potential: Science, v. 207, no. 4437, p. 1309-1314.

McCrossan, R.G., and Porter, J.W., 1973, The geology and petroleum potential of the Canadian sedimentary basins--a synthesis, in McCrossan, R.G., ed., The future petroleum provinces of Canada--their geology and potential: Calgary, Alberta, Canadian Society of Petroleum Geologists Memoir 1, p. 589-720.

McGavin, G.L., 1981, Earthquake protection of essential building equipment: New York, Wiley, 464 p.

McGuire, R.K., 1976, FORTRAN computer program for seismic risk analysis: U.S. Geological Survey Open-File Report 76-67, 90 p.

-----1978, FRISK: Computer program for seismic risk analysis using faults as earthquake sources: U.S. Geological Survey Open-File Report 78-1007, 71 p.

McGuire, R.K., and Hanks, T.C., 1980, RMS accelerations and spectral amplitudes of strong ground motion during the San Fernando, California earthquake: Seismological Society of America

Bulletin, v. 70, no. 5, 1907-1919.
Meteorological Research Institute, 1980, Permanent ocean-bottom seismograph observation system: Tokyo, Japan, Technical Report 4, 233 p. [in Japanese, with English summary].
Miles, R.W., 1977, Practical design of earthquake resistant steel reservoirs, in The current state of knowledge of lifeline earthquake engineering: American Society of Civil Engineers, Technical Council on Lifeline Earthquake Engineering Specialty Conference, Los Angeles, 1977, Proceedings, p. 168-182.
Miller, R.K., and Felszeghy, S.F., 1978, Engineering features of the Santa Barbara earthquake of August 13, 1978: Berkeley, Calif., Earthquake Engineering Research Institute, 140 p.
Milne, W.G., 1970, The Snipe Lake, Alberta earthquake of March 8, 1970: Canadian Journal of Earth Sciences, v. 7, no. 6, p. 1564-1567.
Molnia, B.F., Carlson, P.R., and Bruns, T.R., 1977, Large submarine slide in Kayak Trough, Gulf of Alaska, in Coates, D.R., ed., Landslides: Geological Society of America Reviews in Engineering Geology, v. 3, p. 137-148.
Morgenstern, N.R., 1967, Submarine slumping and the initiation of turbidity currents, in Richards, A. F., ed., Marine geotechnique: International Research Conference on Marine Geotechnique, Monticello, Ill., 1966, Proceedings: Urbana, University of Illinois Press, p. 189-220.
Morgenstern, N.R., and Sangrey, D.A., 1978, Methods of stability analysis, chap. 7 of Schuster, R.L., and Krizek, R.J., eds., Landslides: Analysis and control: Washington, U.S. National Academy of Sciences, Transportation Research Board Special Report 176, p. 155-171.
Moriwaki, Y., and Doyle, E.H., 1978, Site effects on microzonation at offshore areas: International Conference on Microzonation, 2d, San Francisco, 1978, Proceedings, v. 3, p. 1433-1445.
Murty, T.S., 1977, Seismic sea waves--tsunamis: Ottawa, Ontario, Canada, Fisheries Research Board Bulletin 198, 337 p.
Nair, V.V.D., 1978, Aseismic design of offshore platforms, in Earthquake engineering and soil dynamics: American Society of Civil Engineers, Geotechnical Engineering Division Specialty Conference, Pasadena, Calif., 1978, Proceedings, v. 2, p. 660-684.
Nason, R.D., 1973, Fault creep and earthquakes on the San Andreas fault, in Kovach, R.L., and Nur, Amos, eds., Proceedings of the conference on tectonic problems of the San Andreas fault system: Stanford University Publications in the Geological Sciences, v. 13, p. 275-285.
Nataraja, M.S., Wong, I.H., and Toto, J.V., 1978, Liquefaction potential at an ocean outfall in Puerto Rico, in Earthquake engineering and soil dynamics: American Society of Civil Engineers, Geotechnical Engineering Division Specialty Conference, Pasadena, Calif., 1978, Proceedings, v. 2, p. 685-703.
Newmark, N.M., 1965, Effects of earthquakes on dams and embankments: Géotechnique, v. 15, no. 2, p. 139-160.
Newmark, N.M., Blume, J.A., and Kapur, K.K., 1973, Seismic design spectra for nuclear power plants: American Society of Civil Engineers Proceedings, Power Division Journal, v. 99, no. PO2, p. 287-303.
Newmark, N.M., and Hall, W.J., 1969, Seismic design criteria for nuclear reactor facilities: World Conference of Earthquake Engineering, 4th, Santiago, Chile, 1969, Proceedings, v. 2, sess. B4, p. 37-50.
Nilsen, T.H., Wright, R.H., Vlasic, T.C., and Spangle, W.E., 1979, Relative slope stability and land-use planning in the San Francisco Bay region, California: U.S. Geological Survey Professional Paper 944, 96 p.
Nowroozi, A.A., 1973, Seismicity of the Mendocino escarpment and the aftershock sequence of June 26, 1968: Ocean bottom seismic measurements: Seismological Society of America Bulletin, v. 63, no. 2, p. 441-456.
Nuttli, O.W., 1973, Seismic wave attenuation and magnitude relations for eastern North America: Journal of Geophysical Research, v. 78, no. 5, p. 876-885.
-----1979, The relation of sustained maximum ground acceleration and velocity to earthquake intensity and magnitude: Vicksburg, Miss., U.S. Army Engineer Waterways Experiment Station Miscellaneous Paper S-76-1, Report 16, 74 p.
-----1983, Average seismic source-paramter relations for mid-plate earthquakes: Seismological Society of America Bulletin, v. 73, no. 2, p. 519-535.
Nuttli, O.W., Bollinger, G.A., and Griffiths, D.W., 1979, On the relation between modified Mercalli intensity and body-wave magnitude: Seismological Society of America Bulletin, v. 69, no. 3, p. 893-909.
Patwardhan, A.S., 1978, Factors influencing seismic exposure evaluation for offshore areas: International Conference on Microzonation, 2d, San Francisco, 1978, Proceedings, v. 3, p. 1291-1305.
Patwardhan, A.S., Idriss, I.M., Hobgood, J.M., Kulkarni, R.B., and Sadigh, K., 1981, Characterization of earthquake sources in the Gulf of Alaska: Marine Geotechnology, v. 4, no. 3, p. 243-267.
Peacock, W.M., and Seed, H.B., 1968, Sand liquefaction under cyclic loading simple shear conditions: American Society of Civil Engineers Proceedings, Soil Mechanics and Foundations Division Journal, v. 94, no. SM3, p. 689-708.
Pelton, J.R., Meissner, C.W., and Smith, K.D., 1984, Eyewitness account of normal surface faulting: Seismological Society of America Bulletin, v. 74, no. 3, p. 1083-1089.
Perez, O.J., and Jacob, K.H., 1980, Tectonic model and seismic potential of the eastern Gulf of Alaska and Yakataga seismic gap: Journal of Geophysical Research, v. 85, no. B12, p. 7132-7150.
Perkins, D.M., Thenhaus, P.C., Hanson, S.L., Ziony, J.I., and Algermissen, S.T., 1980, Probabilistic estimates of maximum seismic horizontal ground

motion on rock in the Pacific Northwest and the adjacent outer continental shelf: U.S. Geological Survey Open-File Report 80-471, 39 p.

Perkins, D.M., Wharton, M.K., Thenhaus, P.C., Diment, W.H., Wentworth, C.M., Hanson, S.L., and Algermissen, S.T., 1979, Probabilistic estimates of maximum seismic acceleration in rock on the East Coast and the adjacent outer continental shelf: U.S. Geological Survey interagency report to U.S. Bureau of Land Management, 22 p.

Piper, D.J.W., and Normark, W.R., 1982, Effects of the 1929 Grand Banks earthquake on the continental slope off eastern Canada, in Current research, part B: Geological Survey of Canada Paper 82-13, p. 147-151.

Plafker, George, 1965, Tectonic deformation associated with the 1964 Alaska earthquake: Science, v. 148, no. 3678, p. 1675-1687.

-----1967, Surface faults on Montague Island associated with the 1964 Alaska earthquake: U.S. Geological Survey Professional Paper 543-G, p. G1-G42.

-----1969, Tectonics of the March 27, 1964, Alaska earthquake: U.S. Geological Survey Professional Paper 543-I, p. I1-I74.

Plafker, George, and Kachadoorian, Reuben, 1966, Geologic effects of the March 1964 earthquake and associated seismic sea waves on Kodiak and nearby islands, Alaska: U.S. Geological Survey Professional Paper 543-D, p. D1-D46.

Plafker, George, and Rubin, Meyer, 1978, Uplift history and earthquake recurrence as deduced from marine terraces on Middleton Island, Alaska, in Proceedings of Conference VI: Methodology for identifying seismic gaps and soon-to-break gaps: U.S. Geological Survey Open-File Report 78-943, p. 687-721.

Plapp, J.E., and Mitchell, J.P., 1960, A hydrodynamic theory of turbidity currents: Journal of Geophysical Research, v. 65, no. 3, p. 983-992.

Ploessel, M.R., 1978, High-resolution geophysical surveys, a technique for microzonation of the continental shelf: International Conference on Microzonation for Safer Construction, 2d, San Francisco, 1978, Proceedings, v. 2, p. 647-655.

Porcella, R.L., ed., 1979, Seismic engineering program report, May-August 1978: U.S. Geological Survey Circular 785-B, 18 p.

Porter, L.D., Ragsdale, J.T., and McJunkin, R.D., 1979, Processed data from the strong-motion records of the Santa Barbara earthquake of 13 August 1978: California Division of Mines and Geology Special Report 144, 3 v.

Prothero, W.A., 1984, Ocean bottom seismometer technology: Eos (American Geophysical Union Transactions), v. 65, no. 13, p. 113-116.

Raleigh, C.B., Healy, J.H., and Bredehoeft, J.D., 1976, An experiment in earthquake control at Rangely, Colorado: Science, v. 191, no. 4233, p. 1230-1237.

Reece, E.W., Reyerson, D.E., and McNeill, R.L., 1981, Long-term measurements of ground motions offshore: International Conference on Recent Advances in Geotechnical Earthquake Engineering and Soil Dynamics, Rolla, Mo., 1981, Proceedings, v. 1, p. 377-380.

Reimnitz, Erk, 1972, Effects in the Copper River Delta, in The great Alaska earthquake of 1964: Oceanography and coastal engineering: Washington, U.S. National Academy of Sciences, p. 290-302.

Richardson, R.M., Solomon, S.C., and Sleep, N.H., 1979, Tectonic stress in the plates: Reviews of Geophysics and Space Physics, v. 17, no. 5, p. 981-1019.

Richter, C.F., 1935, An instrumental earthquake magnitude scale: Seismological Society of America Bulletin, v. 25, no. 1, p. 1-32.

-----1958, Elementary seismology: San Francisco, W.H. Freeman, 768 p.

Rinne, J.E., 1967, Oil storage tanks, in Wood, F. J., ed., The Prince William Sound, Alaska, earthquake of 1964 and aftershocks: U.S. Department of Commerce, Coast and Geodetic Survey Publication 10-3, v. 2, pt. A, p. 245-252.

Ritsema, A. R., and Gürpinar, Aybars, eds., 1983, Seismicity and saismic risk in the offshore North Sea area: Dordrecht, Holland, Reidel, 420 p.

Rogers, A.M., and Malkiel, A., 1979, A study of earthquakes in the Permian Basin of Texas-New Mexico: Seismological Society of America Bulletin, v. 69, no. 3, p. 843-865.

Rogers, G.C., 1980, Juan de Fuca plate map JFP-4, Seismicity: Ottawa, Ontario, Canadian Department of Energy, Mines and Resources, Earth Physics Branch Open-File Report 80-3, scale 1:2,000,000.

Ryan, W.B.F., and Heezen, B.C., 1965, Ionian Sea submarine canyons and the 1908 Messina turbidity current: Geological Society of America Bulletin, v. 76, no. 8, p. 915-932.

Sarma, S.K., 1975, Seismic stability of earth dams and embankments: Géotechnique, v. 25, no. 4, p. 743-761.

Savage, J.C., Burford, R.O., and Kinoshita, W.T., 1975, Earth movements from geodetic measurements, in Oakeshott, G.B., ed., San Fernando, California, earthquake of 9 February 1981: California Division of Mines and Geology Bulletin 196, p. 175-186.

Savage, J.C., and Hastie, L.M., 1966, Surface deformation associated with dip-slip faulting: Journal of Geophysical Research, v. 71, no. 20, p. 4897-4904.

Schnabel, P.B., and Seed, H.B., 1973, Accelerations in rock for earthquakes in the western United States: Seismological Society of America Bulletin, v. 63, no. 2, p. 501-516.

Seeber, Leonardo, and Armbruster, J.G., 1981, The 1886 Charleston, South Carolina earthquake and the Appalachian detachment: Journal of Geophysical Research, v. 86, no. B9, p. 7874-7894.

Seed, H.B., 1967, Slope stability during earthquakes: American Society of Civil Engineers Proceedings, Soil Mechanics and Foundations Division Journal, v. 93, no. SM4, p. 299-323.

-----1979a, Considerations in the earthquake-resistant design of earth and rockfill dams: Géotechnique, v. 29, no. 3, p. 215-263.

-----1979b, Soil liquefaction and cyclic mobility evaluation for level ground during earthquakes: American Society of Civil Engineers Proceedings, Geotechnical Engineering Division Journal, v. 105, no. GT2, p. 201-254.

Seed, H.B., and Chan, C.K., 1966, Clay strength under earthquake loading conditions: American Society of Civil Engineers Proceedings, Soil Mechanics and Foundations Division Journal, v. 92, no. SM2, p. 53-78.

Seed, H.B., and Idriss, I.M., 1967, Analysis of soil liquefaction: Niigata Japan earthquake: American Society of Civil Engineers Proceedings, Soil Mechanics and Foundations Division Journal, v. 93, no. SM3, p. 83-108.

-----1982, Ground motions and soil liquefaction during earthquakes: Berkeley, Calif., Earthquake Engineering Research Institute, 134 p.

Seed, H.B., Idriss, I.M., Lee, K.L., and Makdisi, F.I., 1975, Dynamic analysis of the slide in the Lower San Fernando Dam during the earthquake of February 9, 1971: American Society of Civil Engineers Proceedings, Geotechnical Engineering Division Journal, v. 101, no. GT9, p. 889-911.

Seed, H.B., and Wilson, S.D., 1967, The Turnagain Heights landslide, Anchorage Alaska: American Society of Civil Engineers Proceedings, Soil Mechanics and Foundations Division Journal, v. 93, no. SM4, p. 325-353.

Self, G.W., and Mahmood, Arshud, 1977, Assessment of relative slope stability of Kodiak Shelf, Alaska, using high-resolution acoustic profiling data: Marine Geotechnology, v. 2 (Marine Slope Stability Volume), p. 333-347.

Sharp, R.V., 1981, Variable rates of late Quaternary strike slip on the San Jacinto fault zone, southern California: Journal of Geophysical Research, v. 86, no. B3, p. 1754-1762.

-----1982, Comparison of 1979 surface faulting to earlier displacements in central Imperial Valley, in The Imperial Valley, California, earthquake of October 15, 1979: U.S. Geological Survey Professional Paper 1254, p. 213-221.

Sharp, R.V., Lienkemper, J.J., Bonilla, M.G., Burke, D.B., Cox, B.F., Herd, D.G., Miller, D.M., Morton, D.M., Ponti, D.J., Rymer, M.J., Tinsley, J.C., Yount, J.C., Kahle, J.E., Hart, E.W., and Sieh, K.E., 1982, Surface faulting in the central Imperial Valley, in The Imperial Valley, California, earthquake of October 15, 1979: U.S. Geological Survey Professional Paper 1254, p. 119-143.

Sherard, J.L., Cluff, L.S., and Allen, C.R., 1974, Potentially active faults in dam foundations: Géotechnique, v. 24, no. 3, p. 367-428.

Sieck, H.C., and Self, G.W., 1977, Analysis of high resolution seismic data, in Payton, C.E., ed., Seismic stratigraphy--applications to hydrocarbon exploration: American Association of Petroleum Geologists Memoir 26, p. 353-385.

Sieh, K.E., 1978a, Prehistoric large earthquakes produced by slip on the San Andreas fault at Pallett Creek, California: Journal of Geophysical Research, v. 83, no. B8, p. 3907-3939.

-----1978b, Slip along the San Andreas fault associated with the great 1857 earthquake: Seismological Society of America Bulletin, v. 68, no. 5, 1421-1448.

-----1982, Slip along the San Andreas fault associated with the earthquake, in The Imperial Valley, California, earthquake of October 15, 1979: U.S. Geological Survey Professional Paper 1254, p. 155-159.

Sieh, K.E., and Jahns, R.H., 1984, Holocene activity on the San Andreas fault at Wallace Creek, California: Geological Society of America Bulletin, v. 95, no. 8, p. 883-896.

Silver, E.A., 1971, Transitional tectonics and late Cenozoic structure of the continental margin of northernmost California: Geological Society of America Bulletin, v. 82, no. 1, p. 1-22.

Singh, S.K., Bazan, E., and Esteva, L., 1980, Expected earthquake magnitude from a fault: Seismological Society of America Bulletin, v. 70, no. 3, p. 903-914.

Slemmons, D.B., 1977, Faults and earthquake magnitude: Vicksburg, Miss., U.S. Army Engineer Waterways Experiment Station Miscellaneous Paper S-73-1, Report G, 166 p.

Smith, S.W., and Knapp, J.S., 1980, The northern termination of the San Andreas fault, in Streitz, R., and Sherburne, R., eds., Studies of the San Andreas fault zone in northern California: California Division of Mines and Geology Special Report 140, p. 153-164.

Smith, S.W., and Wyss, Max, 1968, Displacement on the San Andreas fault subsequent to the 1966 Parkfield earthquake: Seismological Society of America Bulletin, v. 58, no. 6, p. 1955-1973.

Smith, W.E.T., 1962, Earthquakes of eastern Canada and adjacent areas, 1534-1927: Ottawa, Ontario, Canada, Dominion Observatory Publications, v. 26, p. 271-301.

Sokolowski, T.J., Fuller, G.W., Blackford, M.E., and Jorgensen, W.J., 1984, The Alaska Tsunami Warning Center's automatic earthquake processing system, in Tsunami Symposium, Hamburg, 1983, Proceedings: Washington, U.S. Department of Commerce, National Oceanic and Atmospheric Administration, Environmental Research Laboratories, p. 131-147.

Southern California Gas Co., 1973, Earthquake effects on Southern California Gas Company facilities, in Benfer, N.A., and Coffman, J.L., eds., San Fernando, California, earthquake of February 9, 1971: U.S. Department of Commerce, National Oceanic and Atmospheric Administration, Environmental Research Laboratories, v. 2, p. 59-63.

Spaeth, M.G., 1975, Communications plan for tsunami warning system (8th ed.): Washington, U.S. Department of Commerce, National Oceanic and Atmospheric Administration, 207 p.

Spaeth, M.G., and Berkman, S.C., 1972, The tsunami as recorded at tide stations and the seismic sea wave warning system, in The great Alaska earthquake of 1964: Oceanography and coastal engineering: Washington, U.S. National Academy of Sciences, p. 38-110.

Spudich, Paul, and Orcutt, John, 1982, Estimation of earthquake ground motions relevant to the triggering of marine mass movements, in Saxov, Svend, and Nieuwenkuis, J.K., eds., Marine slides and other mass movements: New York, Plenum, p. 219-231.

Stein, Seth, Sleep, N.H., Geller, R.J., Wang, S.-C., and Kroeger, G.C., 1979, Earthquakes along the passive margin of eastern Canada: Geophysical Research Letters, v. 6, no. 7, p. 537-540.

Steinmetz, R.L., Murff, J.D., Latham, G., Roberts, A., Donoho, P., Babb, L., and Eichel, T., 1981, Seismic instrumentation of the Kodiak Shelf: Marine Geotechnology, v. 4, no. 3, p. 193-221.

Sterling, G.H., and Strohbeck, E.E., 1973, The failure of the South Pass 70 "B" Platform in Hurricane Camille: Offshore Technology Conference, 5th, Houston, Tex., 1973, Preprints, v. 2, p. 719-730.

Stewart, G.S., and Helmberger, D.V., 1981, The Bermuda earthquake of March 24, 1978: A significant oceanic intraplate event: Journal of Geophysical Research, v. 86, no. B8, 7027-7036.

Street, R.L., and Lacroix, A., 1979, An empirical study of New England seismicity: 1727-1977: Seismological Society of America Bulletin, v. 69, no. 1, p. 159-175.

Street, R.L., and Turcotte, F.T., 1977, A study of northeastern North American spectral moments, magnitudes, and intensities: Seismological Society of America Bulletin, v. 67, no. 3, p. 599-614.

Sutton, G.M., McDonald, W.G., Prentiss, O.D., and Thanos, S.N., 1965, Ocean-bottom seismic observations: Institute of Electrical and Electronics Engineers Proceedings, v. 53, no. 12, p. 1909-1921.

Swan, F.H., Schwartz, D.P., and Cluff, L.S., 1980, Recurrence of moderate-to-large magnitude earthquakes produced by surface faulting on the Wasatch fault zone, Utah: Seismological Society of America Bulletin, v. 70, no. 5, p. 1431-1462.

Swanger, H.J., and Boore, D.M., 1978a, Simulation of strong-motion displacements using surface-wave modal superposition: Seismological Society of America Bulletin, v. 68, no. 4, p. 907-922.

-----1978b, Importance of surface waves in strong ground motion in the period range of 1 to 10 seconds: International Conference on Microzonation, 2d, San Francisco, 1978, Proceedings, v. 3, p. 1447-1457.

Sweeney, J.F., Irving, E., and Geuer, J.W., 1978, Evolution of the Arctic Basin, in Sweeney, J.F., ed., Arctic geophysical review: Ottawa, Ontario, Canadian Department of Energy, Mines and Resources, Earth Physics Branch Publications, v. 45, no. 4, p. 91-100.

Sykes, L.R., 1971, Aftershock zones of great earthquakes, seismicity gaps, and earthquake prediction for Alaska and the Aleutians: Journal of Geophysical Research, v. 76, no. 32, p. 8021-8041.

-----1978, Intraplate seismicity, reactivation of preexisting zones of weakness, alkaline magmatism, and other tectonism postdating continental fragmentation: Reviews of Geophysics and Space Physics, v. 16, no. 4, p. 621-688.

Thatcher, Wayne, and Plafker, George, 1977, The 1899 Yakutat Bay, Alaska earthquakes: Seismograms and crustal deformation [abs.]: Geological Society of America Abstracts with Programs, v. 9, no. 4, p. 515.

Thenhaus, P.C., ed., 1983, Summary of workshops concerning regional seismic source zones of parts of the conterminous United States convened by the U.S. Geological Survey, 1979-1980, Golden, Colorado: U.S. Geological Survey Circular 898, 36 p.

Thenhaus, P.C., Perkins, D.M., Ziony, J.I., and Algermissen, S.T., 1980, Probabilistic estimates of maximum seismic horizontal ground motions on rock in coastal California and the adjacent outer continental shelf: U.S. Geological Survey Open-File Report 80-924, 69 p.

Thenhaus, P.C., Ziony, J.I., Diment, W.H., Hopper, M.G., Perkins, D.M., Hanson, S.L., and Algermissen, S.T., 1985, Probabilistic estimates of maximum horizontal ground acceleration on rock in Alaska and the adjacent outer continental shelf: Earthquake Spectra, v. 1, no. 2, p. 285-306.

Turbitt, T., Browitt, C.W.A., Morgan, S.N., Newmark, R., and Petrie, D.L., 1983, Instrumentation for North Sea seismic data acquisition, in Retsema, A.R., and Gürpinar, Aybars, eds., Seismicity and seismic risk in the offshore North Sea area: Dordrecht, Holland, Reidel, p. 155-171.

Tyler, R.G., and Beck, J.L., 1983, An earthquake alarm system for the Maui A offshore platform, New Zealand: Seismological Society of America Bulletin, v. 73, no. 1, p. 297-305.

U.S. Geological Survey staff, 1971, Surface faulting, in The San Fernando, California, earthquake of February 9, 1971: U.S. Geological Survey Professional Paper 733, p. 55-76.

Van Dorn, W.G., 1972, Source mechanism of the major tsunami, in The great Alaska earthquake of 1964: Oceanography and coastal engineering: Washington, U.S. National Academy of Sciences, p. 111-121.

Van Dorn, W.G., and Cox, D.C., 1972, Oceanic character, propagation, and coastal modification of the major tsunami, in The great Alaska earthquake of 1964: Oceanography and coastal engineering: Washington, U.S. National Academy of Sciences, p. 147-157.

von Huene, Roland, and Cox, D.C., 1972, Locally generated tsunamis and other local waves, in The great Alaska earthquake of 1964: Oceanography and coastal engineering: Washington, U.S. National Academy of Sciences, p. 211-221.

Vrana, R.S., 1971, Seismic activity near the eastern end of the Murray fracture zone: Geological Society of America Bulletin, v. 82, no. 3, p. 789-791.

Wallace, R.E., 1968, Notes on stream channels offset by the San Andreas fault, southern Coast Ranges, California, in Dickinson, W.R., and Grantz, Arthur, eds., Proceedings of conference on geologic problems of the San Andreas fault

system: Stanford University Publications in the Geological Sciences, v. 11, p. 6-21.
-----1970, Earthquake recurrence intervals on the San Andreas fault: Geological Society of America Bulletin, v. 81, no. 10, p. 2875-2890.
-----1984, Eyewitness account of surface faulting during the earthquake of 28 October 1983, Borah Peak, Idaho: Seismological Society of America Bulletin, v. 74, no. 3, p. 1091-1094.
Wallace, T.C., Helmberger, D.V., and Ebel, J.E., 1981, A broad-band study of the 13 August 1978, Santa Barbara earthquake: Seismological Society of America Bulletin, v. 71, no. 6, p. 1701-1718.
Watt, B.J., Boaz, I.B., and Dowrick, D.J., 1978, Response of concrete gravity platforms to earthquake excitations: Journal of Petroleum Technology, v. 30, no. 3, p. 318-324.
Weaver, C.S., and Smith, S.W., 1983, Regional tectonic and earthquake hazard implications of a crustal fault zone in southwestern Washington: Journal of Geophysical Research,v. 88, no. B12, p. 10371-10383.
Weichert, D.H., 1980, Estimation of the earthquake recurrence parameters for unequal observation periods for different magnitudes: Seismological Society of America Bulletin, v. 70, no. 4, p. 1337-1346.
Weichert, D.H., and Hyndman, R.D., 1982, Microzonation of the Queen Charlotte Islands and adjacent areas: International Conference on Microzonation, 3d, Seattle, 1982, Proceedings, v. 3, p. 1489-1500.
-----1983, A comparison of the rate of seismic activity and several estimates of deformation in the Puget Sound area, in Yount, J.C., and Crosson, R.S., eds., Earthquake hazards of the Puget Sound region, Washington: U.S. Geological Survey Open-File Report 83-19, p. 105-130.
Weichert, D.H., and Milne, W.G., 1979, On Canadian methodologies of probabilistic seismic risk estimation: Seismological Society of America Bulletin, v. 69, no. 5, p. 1549-1566.
-----1980, Canadian strong motion records: Ottawa, Ontario, Canadian Department of Energy, Mines and Resources, Earth Physics Branch, Open-File Report 80-1, 22 p.
Weichert, D.H., Pomeroy, P.W., Munro, P.S., and Mork, P.N., 1982, Strong motion records from Miramichi, New Brunswick, 1982 aftershocks: Ottawa, Ontario, Canadian Department of Energy, Mines and Resources, Earth Physics Branch Open-File Report 82-31, 12 p.
Weller, J.M., 1972, Human response to tsunami warnings, in The great Alaska earthquake of 1964: Oceanography and coastal engineering: Washington, U.S. National Academy of Sciences, p. 222-228.
Wentworth, C.M., and Mergner-Keefer, Marcia, 1981, Reverse faulting along the eastern seaboard and the potential for large earthquakes, in Beavers, J.E., ed., Earthquakes and earthquake engineering: The eastern United States: Ann Arbor, Mich., Ann Arbor Science Publishers, v. 1, p. 109-128.
Wesson, R.L., Helley, E.J., Lajoie, K.R., and Wentworth, C.M., 1975, Faults and future earthquakes, in Borcherdt, R.D., ed., Studies for seismic zonation of the San Francisco Bay Region: U.S. Geological Survey Professional Paper 941-A, p. A1-A30.
Wetmiller, R.J., 1985, Earthquakes near Rocky Mountain House, Alberta and their relationship to gas production facilities [abs.]: Earthquake Notes, v. 55, no. 1, p. 18.
Whitcomb, J.H., and Hutton, L.K., 1978, On the magnitude of the August 13, 1978, Santa Barbara, California, earthquake [abs.]: Eos (American Geophysical Union Transactions), v. 59, no. 12, p. 1130.
White, W.R.H., 1966, The Alaska earthquake—its effect in Canada: Canadian Geographical Journal, v. 72, no. 6, p. 210-219.
Wieczorek, G.F., Wilson, R.C., and Harp, E.L., 1985, Seismic slope stability map of San Mateo County, California: U.S. Geological Survey Miscellaneous Investigations Series Map I-1257-E, scale 1:62,500 in press .
Wiegel, R.L., 1970, Tsunamis, in Wiegel, R.L., ed., Earthquake engineering: Englewood Cliffs, N.J., Prentice-Hall, p. 253-306.
Wilson, B.W., and Torum, A., 1972a, Effects of the tsunami: An engineering study, in The great Alaska earthquake of 1964: Oceanography and coastal engineering: Washington, U.S. National Academy of Sciences, p. 361-523.
-----1972b, Runup heights of the major tsunami on North American coasts, in The great Alaska earthquake of 1964: Oceanography and coastal engineering: Washington, U.S. National Academy of Sciences, p. 158-180.
Wilson, R.C., and Keefer, D.K., 1983, Dynamic analysis of a slope failure from the 6 August 1979 Coyote Lake, California, earthquake: Seismological Society of America Bulletin, v. 73, no. 3, p. 863-877.
Woodward-Clyde Consultants, 1978, Offshore Alaska seismic exposure study: San Francisco, report prepared for Alaska Subarctic Offshore Committee, 6 v.
Wu, F.T., 1968, Parkfield earthquake of June 28, 1966: Magnitude and source mechanism: Seismological Society of America Bulletin, v. 58, no. 2, p. 689-709.
Wyss, Max, 1979, Estimating maximum expectable magnitude of earthquakes from fault dimensions: Geology, v. 7, no. 7, p. 336-340.
Yegian, M.K., and Whitman, R.V., 1978, Risk analysis for ground failure by liquefaction: American Society of Civil Engineers Proceedings, Geotechnical Engineering Division Journal, v. 104, no. GT7, p. 921-938.
Yerkes, R.F., and Lee, W.H.K., 1979a, Late Quaternary deformation in the western Transverse Ranges, California: U.S. Geological Survey Circular 799-B, p. 27-37.
-----1979b, Maps showing faults and fault activity, and epicenters, focal depths, and focal mechanisms for 1970-1975 earthquakes, western Transverse Ranges, California: U.S. Geological Survey Miscellaneous Field Studies Map MF-

1032, scale 1:250,000, 2 sheets.
Yorath, C.J., 1980, The Apollo structure in Tofino Basin, Canadian Pacific continental shelf: Canadian Journal of Earth Sciences, v. 17, no. 6, p. 758-775.
Youd, T.L., 1973, Ground movements in Van Norman Lake vicinity during San Fernando earthquake, in Benfer, N.A., Coffman, J.L., and Bernick, J.R., eds., San Fernando, California, earthquake of February 9, 1971: U.S. Department of Commerce, National Oceanic and Atmospheric Administration, Environmental Research Laboratories, v. 3, p. 197-206.
Youd, T.L., and Hoose, S.N., 1978, Historic ground failures in northern California associated with earthquakes: U.S. Geological Survey Professional Paper 993, 177 pp.
Youd, T.L., and Perkins, D.M., 1978, Mapping liquefaction-induced ground failure potential: American Society of Civil Engineers Proceedings, Geotechnical Engineering Division Journal, v. 104, no. GT4, p. 433-446.
Youd, T.L., Tinsley, J.C., Perkins, D.M., King, E.J., and Preston, R.F., 1978a, Liquefaction potential map of San Fernando Valley, California: International Conference on Microzonation for Safer Construction, 2d, San Francisco, 1978, Proceedings, v. 1, p. 267-278.
Youd, T.L., Yerkes, R.F., and Clark, M.M., 1978b, San Fernando faulting damage and its effect on land use, in Earthquake engineering and soil dynamics: American Society of Civil Engineers, Geotechnical Engineering Division Specialty Conference, Pasadena, Calif., 1978, Proceedings, v. 2, p. 1111-1125.
Ziony, J.I., Wentworth, C.M., Buchanan-Banks, J.M., and Wagner, H.C., 1974, Preliminary map showing recency of faulting in coastal southern California: U.S. Geological Survey Miscellaneous Field Studies Map MF-585, 15 p., scale 1:250,000, 3 sheets.
Zoback, M.D., and Zoback, M.L., 1981, State of stress and intraplate earthquakes in the United States: Science, v. 213, no. 4503, p. 96-104.

INTENSITY, MAGNITUDE, AND SEISMIC MOMENT

Before the existence of instruments to record seismic waves, earthquakes were ranked by size in terms of the severity of the effects they caused. Early seismologists introduced the parameter of intensity as a qualitative measure of the effects of an earthquake upon people, structures, and natural features. Several descriptive scales were adopted, defining levels of intensity in terms of various earthquake effects. The intensity scale most widely used today in the United States and Canada is the modified Mercalli scale (Richter, 1958, p. 137-138), which has 12 levels of intensity ranging from imperceptible shaking to catastrophic damage. Although intensity is a qualitative measure, it is expressed numerically, generally by Roman numerals; the larger numbers correspond to the more severe effects. The severity of effects varies with location, primarily as a function of distance from the earthquake source; higher intensities generally occur closer to the source. Thus, maximum observed intensity can serve as an indicator of the relative strength of an earthquake, except in those events for which no observations have been obtained close to the source because the earthquake is either shallow but distant, or close but deep. To overcome these limitations and the subjectivity involved in assigning intensities, an instrumental scale of earthquake size was introduced by C.F. Richter in 1935.

The instrumental-magnitude scale is based on the principle that the amplitude of recorded seismic waves reflects the strength of the earthquake at its source. If two earthquakes of different size occur in the same place and are recorded by the same seismograph, the larger shock will cause larger amplitudes on the seismograms. Richter (1935) defined earthquake magnitude as the common logarithm of the maximum amplitude recorded by a standard seismograph, corrected to a fixed reference distance to compensate for the attenuation of ground motion with distance from the source. By definition, a shock of $M=3$ would generate a maximum trace amplitude of 1 mm on a standard horizontal seismograph (magnification, 2,800; free period, 0.8 s; damping coefficient, 0.8) at a distance of 100 km from the epicenter. Richter's initial magnitude scale was derived for shocks recorded to distances of 600 km in southern California, where earthquakes are less than 15 km deep. This scale is commonly referred to as the Richter or local-magnitude scale, and values derived from it are commonly designated M_L. Subsequently, other magnitude scales were defined for application to more distant and deeper earthquakes, and to earthquakes in regions where the efficiency of seismic-wave transmission differs from that in southern California.

The seismic waves generated by an earthquake can be grouped approximately into two types: body waves, which penetrate deep within the Earth, and surface waves, which propagate near the surface. Long-period surface waves, which attenuate more slowly with distance than do body waves, are a dominant feature of seismograms from distant shallow-focus earthquakes. Accordingly, a surface-wave-magnitude scale was derived on the basis of surface waves with periods of about 20 s recorded at distances beyond 2,000 km; these magnitudes are designated M_s. Earthquakes deeper than several tens of kilometers do not excite large 20-s surface waves, and so a magnitude scale based on the amplitude of body waves was derived for application to both deep and shallow earthquakes. In current practice, body-wave magnitudes, m_b, are based on the amplitude of compressional (P) waves of about 1-s period, recorded to distances as great as several thousand kilometers. Short-period P-waves undergo abnormal attenuation in the upper mantle in the depth interval 75-200 km beneath the Western United States, and so the m_b values calculated for Western United States earthquakes are diminished relative to Central or Eastern United States shocks. Nuttli (1973) developed a short-period-magnitude scale based on the amplitude of higher mode surface waves. Because higher mode

surface waves do not penetrate into the upper mantle, their amplitudes are unaffected by variations in the attenuation properties of the upper mantle. Magnitudes derived from this scale are designated m_{bLg}, where the subscript b indicates that the measured waves are of 1-s period and Lg designates the type of surface waves used.

When magnitude scales were first introduced, seismologists hoped that all such scales would give the same number for a given earthquake. However, such agreement between scales is impossible because the spectral content of earthquakes varies with earthquake size and different scales measure the amplitudes, or energy, in different spectral bands. M_L, m_b, and M_S measure spectral amplitudes at periods of 0.2-1, 1, and 20 s, respectively. Because the ratio of long- to short-period amplitudes increases with earthquake size, the ratio of M_S to m_b, for example, increases with earthquake size. Thus, for a given earthquake, different magnitude scales generally yield different values. In describing the size of an earthquake, not only the magnitude but also the scale to which it pertains must be specified. As a corollary, it must be recognized that no single magnitude can adequately describe the size of an earthquake, in the sense of defining the spectrum of seismic motion at the source.

The magnitude scales discussed above are observed empirically to saturate at larger magnitudes; above some saturation threshold, earthquakes do not yield larger magnitude values as they increase in size. The m_b scale saturates near 7, and the M_S scale near 8.5. Earthquakes substantially larger than m_b=7, for example, register about m_b=7 regardless of their actual size, because the amplitude of 1-s waves fails to increase with the increasing size of the earthquake. This saturation arises from the fact that the wavelength for a 1-s-period P-wave is several kilometers, typically 5 to 8 km, whereas the length of fault rupture for an earthquake larger than m_b=7 may be a few to many times larger. Thus, waves of 1-s period cannot reflect the gross faulting characteristics of the entire earthquake but, instead, those of only a fraction of the entire rupture. In contrast, at wavelengths longer than the rupture length, the earthquake source appears to be a point; the rupture process appears to be relatively coherent, and the amplitudes of the long-period waves truly reflect the size of the earthquake.

Seismic moment, M_0, is another measure of earthquake size, whose values can be determined from the spectral amplitude of long-period body or surface waves—periods longer than the time required for the rupture to propagate to the end of the fault. Seismic moment can be viewed as a measure of the spectral amplitude of the earthquake source at zero frequency. Seismic moment is a more fundamental measure of the size of an earthquake than is magnitude because seismic moment relates size to the physical attributes of the faulting episode generating the earthquake. In terms of faulting parameters, seismic moment equals the product μAD, where μ is the modulus of rigidity of the rock containing the fault, A is the area of the fault rupture, and D is the average displacement over the rupture. Thus, seismic moment relates the static properties of fault rupture to the long-period level of radiated seismic waves. Seismic moment permits an estimation of the average slip on a buried fault from seismograms of an earthquake if the area of the rupture can be determined independently, for example, either from the spatial distribution of aftershocks or from the radiation properties of long-period seismic waves. Conversely, for historical earthquakes that occurred before seismographs were operating, the long-period level of shaking can be inferred from observations of the length of surface faulting and the amount of fault slip, assuming a value for the width or depth of faulting.

Kanamori (1977) and Hanks and Kanamori (1979) defined a magnitude scale based on seismic moment, where the moment magnitude M is defined by the relation $M=(2/3)\log M_0-10.7$. The moment-magnitude scale has the desirable features that it does not saturate for large shocks and that it provides a means for determining earthquake magnitude from geologic observations of surface faulting or from geodetic measurements of crustal deformation. For these reasons and because of the fundamental physical significance of seismic moment, the moment magnitude scale is increasingly used as a simple index of earthquake size in preference to other scales. M_L and m_b, however, remain appropriate scales for estimating strong ground motion close to the earthquake source for the design of structures, because these scales directly measure the amplitude of ground motion at periods near 1 s, close to the resonant periods of many important structures.

Table 3 lists magnitudes and seismic moments for the earthquakes specifically discussed in this report. Where available, different magnitudes are included to illustrate the differences in values obtained with different scales. The moment magnitudes were computed from the listed seismic moments, except for four midplate earthquakes for which they were computed from m_b or M_S magnitudes using the empirical relations of Nuttli (1983). The magnitudes cited in the body of this report are moment magnitudes.

For shocks that occurred before 1899, no instrumental recordings are available from which magnitudes can be calculated; however, m_{bLg} magnitudes for Central and Eastern United States events have been estimated on the basis of the observed patterns of intensities in relation to patterns for more recent shocks for which instrumental magnitudes are available; these estimates are listed in parentheses. The uncertainity in a given magnitude derived from the amplitudes of seismic waves recorded at several stations over a wide range of azimuths is generally less than 0.3. The saturation of magnitude scales is clearly seen in comparing the M_S and M values for the 1957 and 1964 earthquakes and the m_b, M_S, and M values for the 1965 shock; all these events were large Alaskan shocks associated with subduction along the Aleutian Island arc.

The values of seismic moment were determined from many types of data. For many events, the listed magnitude is the average of several values based on different data sets. The moment for the 1811 shock was estimated from the area within which damage occurred (modified Mercalli intensity of VI or

Table 3. Magnitudes and moments for earthquakes discussed in this report

[Magnitudes in parenthesis are estimated from intensity patterns. Bases for determining moment: A, area of aftershock zone; C, crustal deformation; F, surface faulting; I, area subjected to modified Mercalli intensity of at least VI; S, seismograms. 1 N·m=10^7 dyne·cm. Numbers in brackets are references]

Date	Location	M_L	m_{bLg}	m_b	M_S	M	Moment (10^{18} N·m)	Basis
Nov. 18, 1755	Off Cape Anne, Maine	(5.8-6.0) [1]				5.8-6.1		
Jan. 9, 1857	Fort Tejon, Calif					7.8-7.9 [2]	530-880 [3]	F
Aug. 31, 1886	Charleston, S.C	(6.6-6.9) [4]				6.9-7.3		
Sept. 4, 1899	Yakutat Bay, Alaska				8.5 [5]	8.1	1,500 [6]	S
Sept. 10, 1899	do				8.4 [5]	8.1	1,000 [6]	S
Apr. 18, 1906	San Francisco, Calif				8-1/4 [7]	7.7 [2]	350-430 [3]	F
Nov. 16, 1920	Off Banks Island, Beaufort Sea.				6-1/2 [7]	6.2		
Nov. 4, 1927	Off Lompoc, Calif				7.3 [7]	7.3 [2]	100 [8]	S, I
Nov. 18, 1929	Grand Banks off Newfoundland.				7.2 [7]	6.5	6 [9]	S
Nov. 20, 1933	Baffin Bay				7.3 [7]	6.7		
Nov. 10, 1938	Alaska Peninsula, Alaska				8.3 [7]	8.2 [10]	2,800 [10]	S, A
Aug. 22, 1949	Queen Charlotte Islands, British Columbia, Canada.				8.1 [7]	8.1 [10]	1,500 [10]	---
July 21, 1952	Kern County, Calif	7.2 [11]			7.7 [7]	7.5 [2]	200 [8]	S, I
Mar. 9, 1957	Andreanof Islands, Alaska				8.1 [12]	9.1 [10]	58,500 [10]	A
July 10, 1958	Southeastern Alaska, Alaska.				7.9 [12]	7.7 [12]	400 [13]	S
						8.2 [10]	2,900 [10]	A
Mar. 28, 1964	Prince William Sound, Alaska.				8.4 [12]	9.2 [10]	82,000 [14]	S, C
June 18, 1964	Niigata, Japan			6.2 [15]	7.4 [14]	7.6	290 [14]	S
Feb. 4, 1965	Rat Islands, Alaska			6.1 [15]	8.2 [12]	8.7 [10]	12,500 [14]	S
June 28, 1966	Parkfield, Calif	5.6 [16]	---	5.0 [15]	6.4 [17]	6.2	2.6 [14]	S, C
Aug. 9, 1967	Denver, Colo			5.0 [15]	4.4 [4]	4.8	.021 [18]	S
Feb. 28, 1969	West of Gibraltar, Atlantic Ocean.			6.5 [15]	7.8 [12]	7.8 [10]	600 [19]	S
Feb. 9, 1971	San Fernando, Calif	6.4 [20]	---	6.2 [15]	6.6 [14]	6.6 [2]	12 [14]	S, C
Aug. 13, 1978	Santa Barbara, Calif	5.1 [21]	---	5.4 [15]	5.7 [15]	6.0	1.1 [22]	---
Feb. 28, 1979	Saint Elias, Alaska			6.2 [15]	7.1 [15]	7.6 [23]	250 [24]	S
Oct. 15, 1979	Imperial Valley, Calif	6.6 [25]	---	5.6 [15]	6.9 [15]	6.5	7 [26]	S
Nov. 8, 1980	Eureka, Calif			6.2 [27]	7.2 [27]	7.4	130 [28]	S
Oct. 28, 1983	Borah Peak, Idaho			6.2 [27]	7.3 [27]	6.9	25 [27]	S

References:
1. Street and Lacroix (1979, p. 164).
2. Hanks and Kanamori (1979, p. 2349).
3. Sieh (1978b, p. 1447).
4. Nuttli and others (1979, p. 898, 907).
5. Thatcher and Plafker (1977).
6. Wayne Thatcher (oral commun., 1983).
7. Gutenberg and Richter (1954).
8. Hanks and others (1975, p. 1132).
9. Street and Turcotte (1977, p. 601).
10. Kanamori (1977, p. 2982).
11. Bolt (1978, p. 514).
12. Abe and Kanamori (1980, p. 195).
13. Ando (1977, p. 438).
14. Kanamori and Anderson (1975, p. 1078).
15. International Seismological Centre, Monthly Bulletins.
16. Kanamori and Jennings (1978, p. 484).
17. Wu (1968, p. 691).
18. Herrmann and others (1981, p. 736).
19. Fukao (1973, p. 210).
20. Allen and others (1975, p. 260).
21. Whitcomb and Hutton (1978).
22. Wallace and others (1981, p. 1710).
23. Joyner and Boore (1981, p. 2017).
24. Hasegawa and others (1980, p. 1655).
25. Chavez and others (1982, p. 53).
26. Kanamori and Regan (1982, p. 57).
27. U.S. Geological Survey, Monthly Listings, Preliminary Determination of Epicenters.
28. Lay and others (1982, p. 439).

greater). For the 1857 and 1906 shocks on the San Andreas fault in California, moments were calculated from the length of surface faulting and the observed fault offset. For the 1949, 1957, and 1958 earthquakes, moments were derived from an empirical correlation between moment and rupture area, in which the area was inferred from the spatial distribution of aftershock hypocenters. The moment based on the aftershock area for the 1958 shock is about 7 times greater than that calculated directly from long-period surface waves. This discrepancy indicates the difficulty of determining reliable moment estimates by means of indirect techniques. Experience with many well-studied earthquakes indicates that moment estimates from seismograms and from static fault parameters generally agree within a factor of 2.

For further information about magnitude scales and the relations between scales and about earthquake-source mechanics and magnitude scales, the reader is referred to Chung and Bernreuter (1981) and Boore (1977), respectively.

GPO 587-044/45001